Université catholique de Louvain

École polytechnique de Louvain (EPL)

Fast ultra thin temperature silicon sensor

Dissertation presented by
Mathilde Bontemps

for obtaining the Master's degree in
Electrical Engineering

Supervisor(s)
Denis Flandre, Laurent Francis

Reader(s)
Nicolas André, Marc Bekemans

Academic year 2016-2017

Abstract

In this work a fast temperature sensor is studied for the application of aerospace field. The sensor has to detect, with a fast time response, in the order of the ms, the temperature rise of a MOSFET on to which it is placed, to avoid damaging the power circuit. The studied device is composed of an ultra-thin SOI thermodiode placed on a membrane and coupled to a micro-heater. The response time of the diode is measured while heating with an embedded micro-heater or with a power MOSFET on which the device is glued. It is found to be 20 ms when using the micro-heater and 106 s when using the power MOSFET. Numerical simulations were used to understand the device behaviour and the computed response time varies from 3.45 ms to 170 ms with the heater and 1.29 s with the power MOSFET. The difference with experimental measurements can be explained by the influence of the thermal model of the power MOSFET and the metal package.

Acknowledgements

I would like to express my gratitude to my supervisors Denis Flandre and Laurent Francis for the useful comments and remarks about my work through the learning of my master thesis.
I would also like to thank Nicolas André and Thibault Delhaye for their precious help during the work. Without their passionate participation, my master thesis could not have been successfully conducted.
I would also like to thank Marc Bekemans, from Thales Alenia Space Belgium, for being my reader and taking the time to explain me in details the working principle of power components.
I would also like to acknowledge all the people who were involved in my master thesis and who always answer to my questions and help me when it was needed.
Finally, I would like to thank my family and my friends for their support during the realisation of my master thesis.

Contents

List of symbols

Symbol	Meaning	Units
λ	Wavelength	[m]
$\Delta\lambda$	Resonant wavelength	[m]
T	Temperature	[K] or [°C]
n_{eff}	Effective index	/
n_g	Group index of the guided mode	/
α_W	Thermal expansion coefficient	[°C^{-1}]
σ_T	Change of the refractive index with the temperature	[°C^{-1}]
$\Delta\lambda_L$	Thermal expansion effect	[m]
$\Delta\lambda_T$	Thermo-optic effect	[m]
λ_B	Bragg wavelength	[nm]
$\Delta\lambda_B$	Shift of Bragg wavelength	[nm]
α_{sub}	Thermal expansion coefficient of substrate material	[°C^{-1}]
ξ	Thermo-optic coefficient	[°C^{-1}]
P_e	Elastic-optic coefficient	/
K_T	Sensitivity of optical sensor	[pm/°C]
α_R	Temperature coefficient of resistance	[Ω/Ω/°C]
R_0	Nominal temperature sensor resistance	[Ω]
R_C	Resistance of series connections	[Ω]
α	First temperature coefficient	[K^{-1}]
β	Second temperature coefficient	[K^{-2}]
T_0	Room temperature	[K or °C]
d	Diode coefficient	[V/°C]
$J_{n(p)}$	Electron (hole) current density	[A/m^2]
$D_{n(p)}$	Diffusivity of the electrons (holes)	[m^2/s]
$L_{n(p)}$	Diffusion length for electrons (holes)	[m]
n_p	Electrons concentration in p-type semiconducting layer	[cm^{-3}]
p_n	Holes concentration in n-type semiconducting layer	[cm^{-3}]
A	Junction or cross-section area	[m^2]
q	Electric charge of the electron	[C]
k	Boltzmann's constant	[J/K]
I_S	Saturation current	[A]
N_A	Acceptor concentration	[cm^{-3}]
N_D	Donor concentration	[cm^{-3}]
n_i	Intrinsic carrier concentration	[cm^{-3}]
V_g	Extrapolated voltage at zero temperature	[V]
η	Process dependent parameter	/
τ_L	Time life of carrier	[s]
ϵ_s	Dielectric permittivity	[pF/cm]

Φ_0	Junction voltage	[V]
μ	Mobility of the carriers	$[cm^2/(V.s)]$
α_μ	Coefficient	1.2-2
n	Non ideal factor	/
k	Thermal conductivity	[W/(m.K)]
c_p	Heat capacity	[J/(kg.K)]
ρ	Density	[kg/m^3]
h	Convection coefficient	[W/($m^2.K$)]
τ	Response time	[s]

Introduction

Today, satellites and rockets contain many power circuits which heat up and can reach temperatures higher than 150 °C. If the temperature of power circuits is too high, these devices can be damaged, for example in the worst case, we could imagine that the circuit explodes. The aim of this work is to design a fast temperature sensor which will be glued on the power circuit, to detect its temperature. If the detected temperature is higher than 150 °C, the power circuit will be shut down to have time for cooling down and then it will be put again in operation. The main specification of the sensor is its speed to detect the variation of temperature. We would like to have a time response in the order of ms, allowing system to react before damages.

Many temperature sensors can be used but the studied one is based on a thermodiode, because they are reported to have a fast time response, in the order of ms, which is the expected response time. Moreover, when they are built with the SOI (Silicon-On-Insulator) technology, they can reach temperature up to 650 °C, even if the maximum temperature reached by a power circuit is around 175 °C. Furthermore, the area of a sensor based on a diode is in the order of mm^2 which is lower than the area of a power transistor which is about 100 mm^2.

Four parameters have influence on response time of diode-based sensor: the first one is the choice of the design. The second one is the choice of materials for the different layers constituting the sensor. The third one is the planar area of the sensor and the last one is the substrate.
In a first time, the diode is coupled with a micro-heater, the heating element, and then the sensor will be glued on a power circuit with the power circuit as heating part.Static measurements, current-voltage, will be made to recover the I-V curve of the diode. Pulsed measurements will be done to obtain the variation of the temperature in the diode in function of the temperature of the micro-heater or in function of the power circuit temperature. In the same time, simulations will be made with LTSpice to study a simplified thermal model and with Comsol ® in order to study the heat transfer through the device.

The first chapter of this work, *State of art*, is a literature review which compares the existing temperature sensors in order to justify the choice of the diode based sensor. The second chapter, *Heat transfer in the sensor* presents the thermal response of the sensor to a step of temperature. In this chapter, simulations will be made to analyse the heat transfer through the die. The third chapter, *Power circuit* will be dedicated to the study of the power circuit and its thermal model. The fourth chapter, *Thin film and transfer on a PCB*, will explain how to thin down a die and how to transfer it on a final substrate to be able to measure correctly the temperature. Finally, the last chapter, *Results and discussion*, is the experimental part of the work, where the time response of the die is studied among other things like the step of temperature, the sensitivity of the die to temperature and so on.

Chapter 1

State of art

The goal of this chapter is to find the best temperature sensor suitable for the final application. Different kinds of sensors based on different concepts and technologies will be presented along with their main specifications, advantages and drawbacks. The sensors can be divided into two main categories, the first one is about optical temperature sensor and the second one gathers the electrical temperature sensor.

1.1 Optical temperature sensors

The main interests for optical temperature sensor are their immunity against electromagnetic interference, their robustness and their isolated sensing [1, 2]. The studied optical temperature sensors are the ring resonator and the Fiber Bragg Grating.

1.1.1 Ring resonator

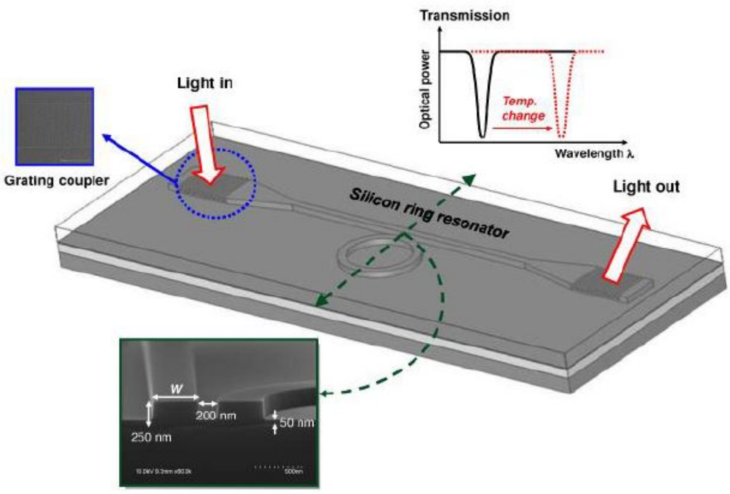

Figure 1.1: Temperature sensor based on a silicon ring resonator [1]

On figure 1.1, we can see the temperature sensor based on a ring resonator. The ring resonator is linked to a grating coupler and when the temperature varies, the value of the refractive index changes because of the thermo-optic effects and the circumference of the ring is also changed with the temperature. Therefore, the variation of the wavelength, λ, in function of the temperature is given by the following equation:

$$\Delta\lambda = \Delta\lambda_L + \Delta\lambda_T = \alpha_W \frac{n_{eff}}{ng} \lambda \Delta T + \frac{\sigma_T}{n_g} \lambda \Delta T$$

Where:

- $\Delta\lambda$ is the resonant wavelength
- $\Delta\lambda_L$ is the thermal expansion effect
- $\Delta\lambda_T$ is the thermo-optic effect
- α_W is the coefficient of thermal expansion
- n_{eff} is the effective index
- n_g is the group index of the guided mode
- ΔT is the variation of temperature
- $\sigma_T \equiv \frac{\partial n_{eff}}{\partial T}$ is the change of the refractive index with the temperature

As we can see on figure 1.1, according to [1], the silicon ring is placed in the center of the device. Two grating coupler, one for the input light and the other one for the output light, are at both ends of the device. A bus connects the ring to the grating couplers.
These sensors are reported to have a fast response about 6 μs, which is faster than the specification, the desired response time is in the order if ms. They have a small size, a few μm and they should work under high temperature until 300 °C [1]. The sensor is manufactured by using a 0.18 μm standard CMOS process and according to [1], the size of the different parts of the device are the following:

- Height of the waveguide equal to 250nm
- Slab thickness is 50nm
- The radius of the ring is 4μm
- The ring-to-bus gap is 200nm
- The width of the waveguide (W) is around 500nm

These different sizes can be seen of the zoom of figure 1.1.

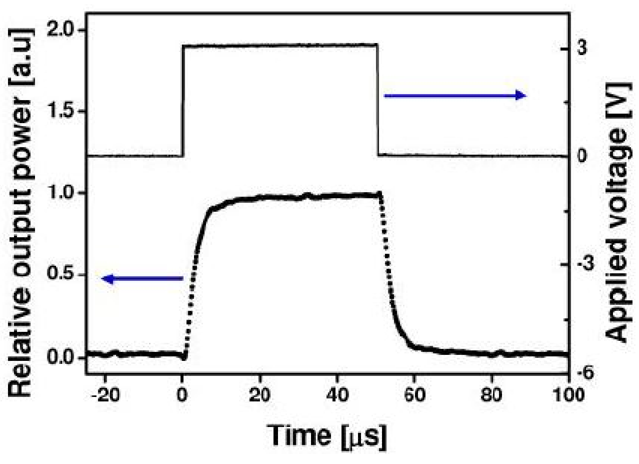

Figure 1.2: Relative output power when a pulse of voltage is applied on a heating electrode [1]

The interesting part of this sensor is the ultra fast response time, about 6μ s, as it can be seen on figure 1.2 and it should work for temperature until 300°C. The way used to apply a step of temperature on the sensor is by heating an electrode. To do this, a pulse of voltage is applied in order to generate a heating flux and therefore an increase of temperature. The sensitivity of the device is also studied by [1], they show that it is dependent of the width of the waveguide. They conclude that the best sensitivity is 83 pm/°C for a waveguide width of 500 nm. By decreasing or increasing the width of the waveguide, the sensitivity is reduced by a 10 pm/°C (pico-meter per degree Celsius).
The main issue with this kind of sensor is that we need to convert a shift of an optical wavelength into an electrical signal. It means that we need a matched filter or an arrayed waveguide grating for example.

1.1.2 Temperature sensor based on fiber Bragg grating

Fiber Bragg Grating (FBG) reflects a wavelength light whose value shifts in function of the temperature and/or strain. As a consequence, it is needed to make a distinction between both phenomena. For example, if we are interested in the influence of the temperature, we have to use packaged FGB temperature sensor in order to be sure that the fiber Bragg grating in the package does not have any bending, tension, compression or other strain effects [3]. When a single tube to protect the grating, there is a compromised to do between the resistance of the fiber and the time response. Indeed, if the coating layer is bigger, the resistance of the fiber is improved but the time response increases. On the other hand, if the coating layer is thinner, the strength of the sensor is reduced but the time response decreases [2].
The relationship between the wavelength and the temperature is given by the following equation [2]:

$$\Delta\lambda_B = \lambda_B(\alpha_W + \xi + (1 - P_e)(\alpha_{sub} - \alpha_W))\Delta T \tag{1.1}$$

- $\Delta\lambda_B$ is the shift of the Bragg wavelength expressed in nm
- λ_B is the Bragg wavelength expressed in nm
- α_W is the thermal expansion coefficient of FBG expressed in °C^{-1}
- ξ is thermo-optic coefficient which do not change of value with the encapsulation expressed in °C^{-1}
- P_e is valid elastic-optic constant do not have units
- α_{sub} is the thermal expansion coefficient of substrate material expressed in °C^{-1}
- ΔT is the variation of temperature expressed in °C

By using equation (1.1), we can compute the sensitivity, K_T:

$$K_T = \frac{\Delta\lambda_B}{\Delta T} = \lambda_B(\alpha_W + \xi + (1 - P_e)(\alpha_{sub} - \alpha_W))$$

By looking on given units, we can see that the sensitivity is expressed in nm/°C.

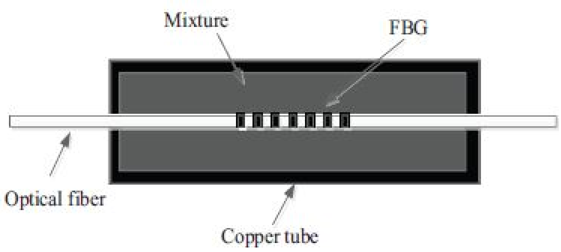

Figure 1.3: Encapsulation of the fiber [2]

On figure 1.3, we can see the tubular encapsulation chosen in [2] which is chosen especially for the fast heat conduction. In [2], the metal tube is filled with a special mixture, whose exact composition is not described, instead of the air to achieve a high sensitivity and a response time in the order of ms. It is assumed that the response time is divided into two parts. The first one corresponds to the time for which the heat transfers from the outside to the metal tube and the second one is the time for which the heat transfers from the special mixture to the grating of the fiber.

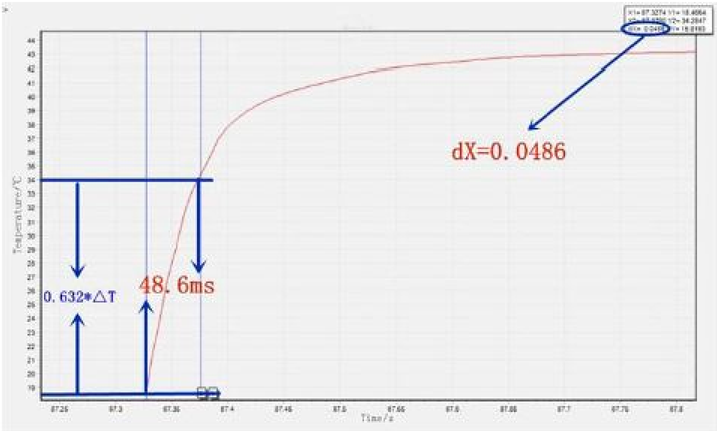

Figure 1.4: Temperature response curve for tubular encapsulation of a fiber Bragg grating. The step of temperature is applied on the external environment [2]

As we can see on figure 1.4, the measured time response is 48.6 ms. The experimental sensitivity is 27.6 pm/°C. The drawback of this particular temperature sensor is that it is designed for applications in the oceans. Therefore, even if the time response is in the order of ms, the maximum temperature which is reached is 45 °C which is much lower than the expected step of temperature, 150 °C.

1.2 Electrical temperature sensors

There are different kinds of studied electrical temperature sensors. The first one is based on a resistance whose value changes according the temperature and the others are based either on a diode or a transistor combined with a micro-hot-plate.

1.2.1 Resistive temperature sensor

A Resistance Temperature Sensor (RTD) is a passive circuit element for which the value of resistance increases with the temperature. In order to measure the resistance, it is necessary to convert it into a voltage which will drive a differential amplifier. The use of the amplifier will remove the common mode noise and increases the sensitivity of the device [4].
Two possible ways to measure this resistance, the first one is to connect the the RTD in one leg of a Wheatstone bridge which is excited by a constant reference voltage or we can use a reference current and measure the corresponding voltage drop over the RTD [4].

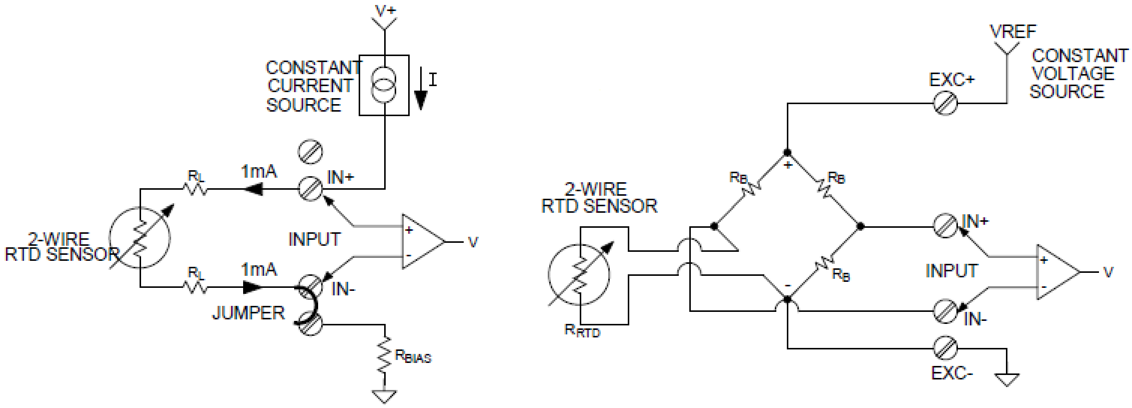

Figure 1.5: Measurement of the RTD signal, using a reference current on the left figure and using a Wheatstone bridge on the right figure [4]

On figure 1.5, we can see both ways to measure the voltage drop on a resistance temperature sensor. The schematic on the left is limited to short distances between the sensor and the measuring instrument because there is no lead-wire compensation. On the right schematic of figure 1.5, there is a lead-wire compensation but the the resistance of the Wheatstone bridge has to match to the base resistance of the sensor [4].
An important parameter for the Resistance Temperature Detector (RTD) is the Temperature Coefficient of Resistance (TCR) also called the α_R coefficient, expressed in [Ω/Ω/°C]. This coefficient represents the change in the resistance per one degree of the change in temperature and it can be used to compute the sensitivity of the device. The resistance change is proportional to the alpha coefficient multiplied by the change in the temperature. Consequently, we can write the following equation:

$$\Delta R = \alpha_R R_0 \Delta T \tag{1.2}$$

Where R_0 is the nominal sensor temperature resistance. Therefore, to calculate the value of the resistance at any temperature T, we can use:

$$R_T = [R_0 + (\alpha_R R_0 \Delta T)] \tag{1.3}$$

The sensitivity is computed by multiplying the alpha coefficient with the value of the resistance at the reference temperature (R_0) as follows:

$$K_{RTD} = R_0 \times \alpha_R \tag{1.4}$$

The value of the sensitivity is directly proportional to the value of the temperature coefficient of resistance. A sensor having a high sensitivity does not necessarily means the sensor will be more accurate but it means that if the produced signal is larger, then it will be less sensitive to the lead-wire effects and electrical noise because the signal-to-noise ratio is often increased at the sensor interface [4]. If a larger resistance is used instead of a higher sensitivity, the output voltage will be the same but with less excitation current which helps to reduce the self-heating effect.

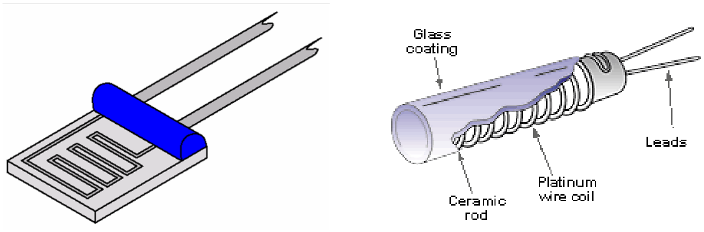

(a) Thin-film element [5] (b) Traditional RTD [6]

Figure 1.6: Both ways to build a Resistance temperature detector

On figure 1.6, we can see both ways to construct the resistance temperature detector. On figure 1.6.(a), the RTD is built by using a thin film of platinum or nickel-iron deposited on a ceramic substrate, then it is etched by a laser to the desired reference resistance [4]. The advantages of this technique is that the thin-film elements can have higher resistance with less metal over small area. Moreover their time response is faster than the one for the technique consisting in a coil of metal wound to an accurate value of resistance around a ceramic or a bobbin of glass [4]. The design of this RTD can be seen on figure 1.6.(b).
The different materials that can be used to build a RTD are: platinum, nickel, copper and nickel/iron. The best choice is to take the platinum because it has the wider temperature range (from -260°C to 650°C), moreover it is accurate, predictable, chemically resistant and stable [4].

If the reference value of the resistance platinum used to build the resistance temperature detector is 100 Ω and the value of the temperature coefficient of resistance is $\alpha_R = 0.00385\Omega/\Omega/°C$, by using equation (1.4), the sensitivity of the RTD is $0.385\Omega/°C$.
The response time of a RTD, given at 63 % of the step of temperature, depends on the dimensions of the sensor, the resistance of the thermal contact and the surrounding medium, air or water, [7]. As we would like to use the temperature sensor to detect the rise of temperature in a power circuit, we will assume that the surrounding medium is the air. Therefore, according to [7], the time response can vary from a few seconds to tens of seconds.

1.2.2 Temperature sensor combined with a micro-heater

The other category of electrical temperature sensors is the one where a diode and/or a transistor is combined with a micro-heater.

Temperature calibration of a micro-heater

A first method to calibrate the temperature of the device is to measure the variation of the micro-heater resistance. A second method is computed by the forward voltage drop on the diode at a constant current [8].
For the first method, the dependence of the tungsten resistance in function of the temperature can be given by the following equation:

$$R = (R_0 - R_c).(1 + \alpha(T - T_0) + \beta(T - T_0)^2) + R_C \tag{1.5}$$

In the specific case of *S. Amor et al.* [8], the initial resistance of the tungsten micro-heater is $R_0 = 61.5$ [Ω], the resistance of series connections to the micro-heater is $R_C = 13$ [Ω], the first temperature coefficient of tungsten resistance is $\alpha = 2.05 \times 10^{-3}$ $[K^{-1}]$, the second temperature coefficient of tungsten resistance is $\beta = 0.3 \times 10^{-3}$ $[K^{-2}]$ and $T_0 = 297.15$ $[K]$ is the room temperature. If we take the reciprocal equation, we can find the variation of the temperature in function of the resistance, and the equation is given by:

$$T^2 + T\left(\frac{\alpha}{\beta} - 2T_0\right) - \frac{\alpha}{\beta}T_0 + T_0^2 - \frac{1}{\beta}\left(\frac{R - R_C}{R_0 - R_C} - 1\right) = 0 \tag{1.6}$$

For the second method, at a constant current, the forward voltage drop is given by:

$$V_d = V_0 - d(T - T_0) \tag{1.7}$$

Where V_0 $[V]$ is the initial value of the voltage at room temperature, T_0 [°C] is the room temperature and d [V/°C] is the diode coefficient [8].

Silicon diode temperature sensor

The silicon thermodiode are widely used because they can be integrated on chip with electronic circuit and they have a wide temperature range measurement. Moreover silicon diode can work at a very low current which is an advantage because the power consumption is lower and it reduces the self-heating effect.
The range of temperature for which a thermodiode can operate is limited by the IC processes. When the technology used is bulk silicon, the maximum temperature is approximately limited to 150°C and when the technology used is silicon-on-insulator, the maximum temperature can be up to 250-300 °C [9, 10].
There are two modes of operation for the silicon diode: the first one is based on a constant current, which avoids self-current heating [11] and the second on a constant voltage [9].

Constant current mode [12]
At constant current, the forward voltage is proportional to the temperature as long as the forward driving current is higher than the reverse saturation current [12]. For a pn diode diode, the diffusion current is given by:

$$I = A(J_p + J_n) = qA\left(\frac{D_p}{L_p}p_n + \frac{D_n}{L_n}n_p\right)\left(e^{\frac{qV}{kt}} - 1\right) = I_s(T)\left(e^{\frac{qV}{kt}} - 1\right) \tag{1.8}$$

Typically for a voltage comprised between 0.4 and 0.7 V. In equation (1.8), J_n and J_p are the electron and hole current densities at the physical junction, D_n and D_p are the diffusivity of the electrons and holes respectively, n_p and p_n are the equilibrium electrons and holes concentrations into the p-type and n-type semiconducting layers respectively. L_n and L_p are diffusion lengths for the electrons and holes respectively and A is the junction area [13]. I_s is the saturation current, V is the voltage drop across the diode and k is the Boltzmann's constant. Therefore, the saturation current I_s depends on the temperature through the minority carriers in n-type and p-type, p_n and n_p respectively. Indeed, we have:

$$n_p = \frac{n_i^2}{N_A}, p_n = \frac{n_i^2}{N_D} \tag{1.9}$$

Where n_i is the intrinsic carrier concentration which is proportional to the temperature with the following relationship:

$$n_i^2 \propto T^3 e^{-\frac{qV_g}{kT}} \tag{1.10}$$

The saturation current is given by the following:

$$I_s = CT^{\eta} e^{-\left(\frac{qV_g}{kT}\right)} \tag{1.11}$$

where C is a constant that includes the density of states, effective masses of electrons and holes, carrier mobility, doping density, recombination life time, junction area... [12] η is parameter which depends on

the process, V_g is the extrapolated voltage at zero temperature.
At this point, according to [9], if we consider that $I \gg I_s$, equation 1.8 becomes:

$$I = I_s(T)\left(e^{\frac{qV}{kt}}\right) \tag{1.12}$$

And therefore, by combining this last equation with equation 1.11, we obtain the following equation:

$$V = V_g + \frac{kT}{q}(lnI - lnC - \eta lnT) \tag{1.13}$$

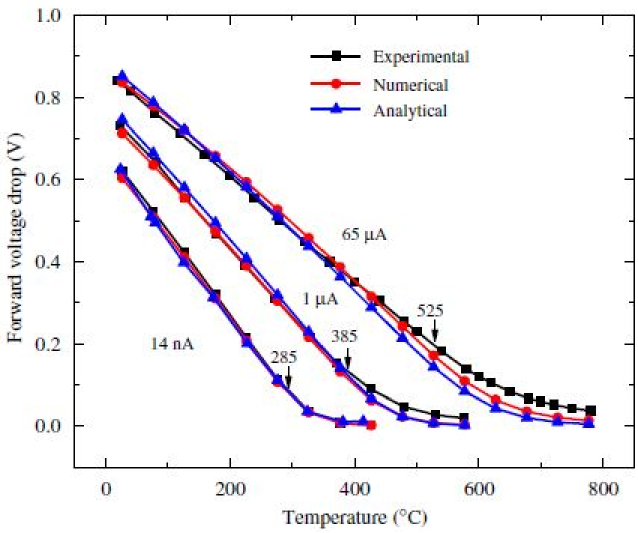

Figure 1.7: Plot of the forward voltage in function of the temperature in a constant current mode, for value of current equal to 14 nA, 1 μA and 65 μA [11]

On figure 1.7, the relationship between the voltage and the temperature is observed and is almost linear at a constant current, by assuming that the driving forward current is much higher than the reverse saturation current.
If we want to explain the nonlinearity that appears at high temperature on figure 1.7, we can not consider anymore that $I \gg I_s$ and therefore, from equation 1.8, we can write the entire expression for the voltage in function of the current [12]:

$$V = \frac{kT}{q}ln\left(\frac{I}{I_s(T)} + 1\right) \tag{1.14}$$

$$= \frac{kT}{q}ln\left(\frac{I}{I_S(T)}\right) + \frac{kT}{q}ln\left(\frac{I_s(T)}{I} + 1\right) \tag{1.15}$$

If we use equations 1.11 and 1.15, we can write:

$$V = V_g - \frac{kT}{q}\eta lnT + \frac{kT}{q}ln\left(\frac{I}{C}\right) + \frac{kT}{q}ln\left(\frac{I_s(T)}{I} + 1\right) \tag{1.16}$$

We assume that we have two temperatures, a working temperature T and the reference temperature T_0 to keep the current constant. The last equation can be written in the following way:

$$V = \left(V_g + \eta\frac{kT_0}{q}\right) - \left(V_g + \eta\frac{kT_0}{q} - V(T_0)\right)\frac{T}{T_0} + \eta\frac{k}{q}\left(T - T_0 - Tln\left(\frac{T}{T_0}\right)\right) + \frac{kT}{q}ln\left(I + \frac{I_s(T)}{I} + I_s(T_0)\right) \tag{1.17}$$

By looking at equation 1.17, we can see the voltage is the sum of a constant term (the first one), a term proportional to the absolute temperature (the second one) and two nonlinear terms [12]. The last term of equation 1.17 becomes important at temperature higher than 550°C. So for lower temperature, we can consider that this term is negligible. The first nonlinear term of equation 1.17 can be cancelled out either by using two different driving currents with a known ratio or by using the same current but for two diodes of different areas and with a known ratio [12, 13]. In consequence, we can conclude that the voltage is proportional to the value of the temperature and almost linear.

Constant voltage mode [9]

In a constant voltage mode, thermodiodes can work in forward or in reverse bias. For the forward bias mode, if we suppose that the forward voltage is higher than 0.1, the forward driving current of the diode is much greater than the reverse saturation current. Therefore, the expression for the current is given by equation 1.12. In consequence, we can re-organise equation 1.13 and we obtain the following equation:

$$lnI = \frac{q(V - V_g)}{kT} + lnC + \eta lnT \tag{1.18}$$

$$= S\frac{1}{T} + lnC + \eta lnT \tag{1.19}$$

Where $S = \frac{q(V-V_g)}{k}$ represents the sensitivity of the temperature. If we neglect the nonlinear terms, we can see that lnI is inversely proportional to the temperature. This mode is more difficult to analyse because the current is proportional to the exponential of the current and therefore we need a logarithmic amplifier.

In reverse bias mode, for a temperature higher than 200°C in case of silicon, the diffusion current through the diode and the saturation current are the same. If we take the logarithm of equation (1.11), we obtain:

$$lnI = lnC + \eta lnT + \frac{-qV_g}{kT} \tag{1.20}$$

Again, if we neglect the nonlinear terms, we obtain:

$$lnI = \frac{-S}{T} \tag{1.21}$$

We can conclude that lnI is inversely proportional to the temperature.

But, for silicon at 300K, the dominant current in reverse junction is the generation-recombination current [14]. The density of this current is given by the following formula:

$$J_{s,r,g} = J_{s,r,g}(e^{qV/2kT} - 1) = \frac{qn_i}{2\tau_L}\sqrt{\frac{2\epsilon_s}{q}(\phi_0 - V)\frac{N_A + N_D}{N_A N_D}} \tag{1.22}$$

Where q is the electric charge of the electron, n_i is the intrinsic concentration, τ_L is the time life of the carriers, ϵ_s is the dielectric permittivity of the material and its value is 1 pF/cm for the silicon, ϕ_0 is the junction voltage, N_A is the acceptor concentration, N_D is the donor concentration [14].

SOI CMOS technology high temperature operation

A first possibility to measure high temperature is to use the Silicon-On-Insulator (SOI) technology which consists in a silicon layer on a silicon dioxide. The use of this technique allows to measure high temperature by isolating the thermodiode from the silicon substrate.

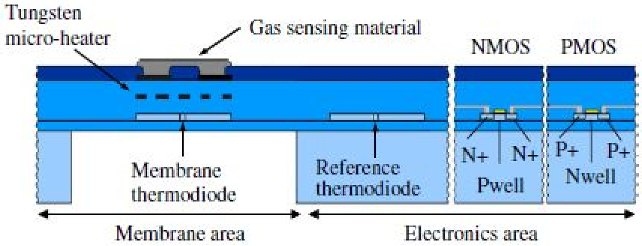

Figure 1.8: Cross section of a SOI micro-hotplate [11]

On figure 1.8, we can observe the cross-section of a temperature sensor implemented in SOI CMOS technology. It can be seen that the design is divided into two parts: *electronic area* which correspond to the standard SOI and the *membrane area*.
This device is mainly composed of a tungsten micro-heater and a membrane thermodiode which allows to monitor the micro-hotplate temperature accurately. The membrane is usually circular to avoid mechanical stress at the edges. Outside of the micro-hotplate, we have another thermodiode which is used to monitor the junction temperature of the IC chip [11].
Often, a micro-heater is composed of three rings: one inner ring and two outer ones. The inner ring has a low resistance and compensates the heat loss caused by convection within the heater. The two outer rings compensate the heat loss coming from the convection outside of the heater area and the conduction [15].
The tungsten is often chosen as the material of the micro-hotplate because it allows to work at temperatures up to 700 °C. Furthermore, this material has good mechanical strength and is more resistant to electro-migration [11, 15]. The choice of material for the micro-hotplate could be the polysilicon or aluminium but the polysilicon has a low long-term stability [16] and the aluminium has a maximum operating temperature lower than the one of the tungsten [17].
In [11], the size of the different elements of the device are the following:

- Diameter of the diode: $\sim 34\mu m$
- Active silicon layer: $0.25\mu m$
- Buried oxyde layer: $1.0\mu m$
- Diameter of the membrane is 300 μm

The use of tungsten for the metallization combined with the thin silicon layer, reduce the depletion region and the value of saturation current is very low, a few fA. Thanks to this low saturation current, we can see on figure 1.7 that the function transfer between the voltage and the temperature is linear until a temperature of 500°C; at this temperature, the driving current is $65\mu A$ [11]. The value of the current influences the slope of the curve. Indeed, if the value of the current is low, for instance a few nA, the nonlinearity appears at lower temperature, like 300°C instead of 550°C for a current of 1 μA [13].
The choice of the value of the forward current is critical. In fact, we need a low value of the current to avoid the self-heating. In the same time, we need a high value of this current to be sure that it is greater than the reverse saturation current [12]. Indeed, if the value of the reverse saturation current is comparable or higher than the value of the forward current, nonlinearities appear at lower temperatures. The advantage with a high current is the reduction of the capacitance while with a low current, the value of the capacitance increases.
The sensitivity of this kind of sensor is about -1.3 [mV/°C] [12] and the response time is about 15 ms [18].

Micro-air-bridge heater: high temperature
Another way to measure high temperature is to use a pn junction diode combined with a micro-air-bridge heater. This sensor operates with a constant voltage mode and therefore, the logarithm of the measured current is inversely proportional to the temperature as it is shown in equation (1.21). As a consequence, the sensitivity is given by the inclination S, which means that more the value of the slope increase, better is the sensitivity [19].

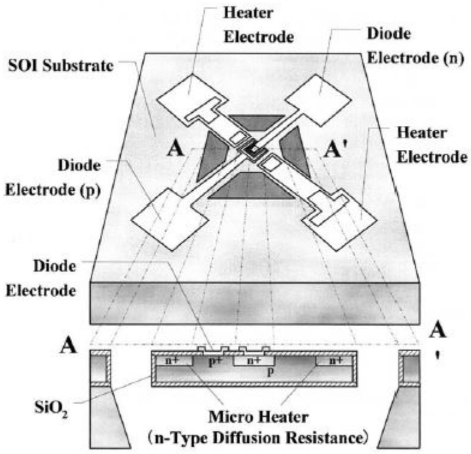

Figure 1.9: Structure of the micro-air-bridge heater [19]

On figure 1.9, we can see an implementation of this kind of temperature sensor. According to [19], the dimensions of the device are the following:

- Diode temperature sensor: 700 $\mu m \times$ 700 μm
- SOI layer: 6 μ thick
- pn junction of the diode: 100 $\mu m \times$ 100 μm
- Length of the micro-air-bridge: 2000 μm

For this particular implementation, The temperature sensor is composed of an operational amplifier in front of the diode in order to apply the appropriate bias-voltage to the pn junction and to control the value of the current which depends on the temperature. Indeed, in order to have a very low resistance, the device has to operate in forward bias at low temperature, from -200 °C to 150 °C, and in reverse bias at high temperature, from 150 °C to 500 °C. This low resistance allows to have a larger signal to noise ratio [19].

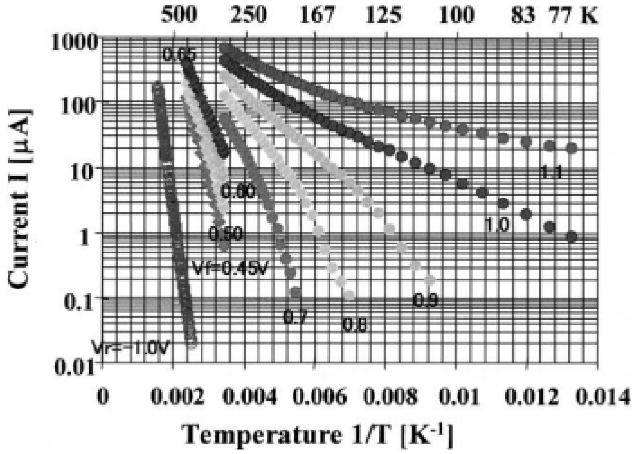

Figure 1.10: Relationship between the current of the pn junction temperature sensor and the temperature for different forward bias voltage and reverse bias voltage [19]

On figure 1.10, we can see the variation of the current in function of the temperature for different voltages. It can be observed that for reverse bias voltage of a value about -1 V, the sensitivity is very high as the slope is very much titled but the exact value is not given. It can also be seen that the maximum value of the current is about 1 mA.

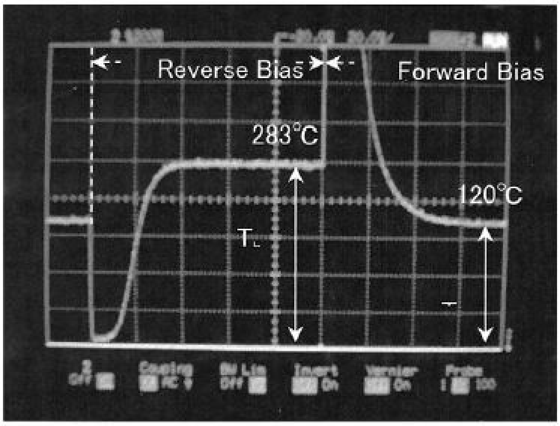

Figure 1.11: Dependence of the voltage with the temperature (20ms per division) [19]

On figure 1.11, we can see a response time of about 20 ms when a step of temperature is applied. We can conclude that the main advantage of the microbridge is that heat can only flow through two or four bridge beams which gives a better thermal isolation. But it is mechanically less stable because it is supported only by fours beams [17].

MOSFET temperature sensor [8]

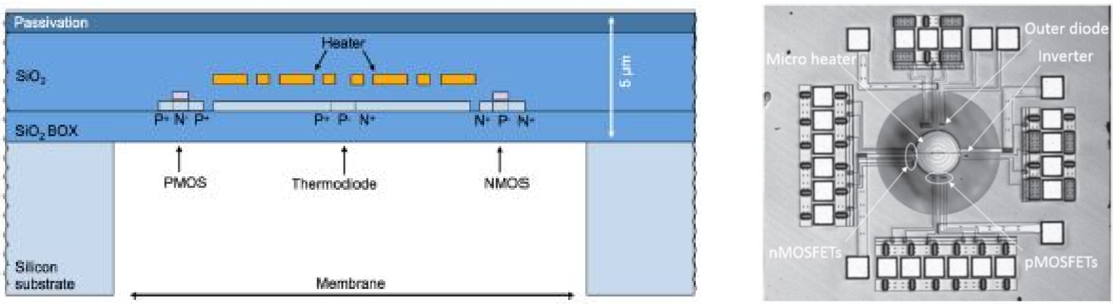

(a) Cross-section of the membrane area

(b) Front view of the chip with location of the components

Figure 1.12: Two different views of the device with MOSFET [8]

On figure 1.12, we can see a cross-section and the chip of device composed with MOS transistors. The diodes are used as temperature sensor but the influence of the temperature can also be seen by studying the characteristics of the MOSFET.

Mobility of the carrier:
The first way to analyse the influence of the temperature is to study the mobility of the carrier. Indeed, the mobility behaviour is given by the following equation [8]:

$$\mu(T) = \mu(T_0)\left(\frac{T}{T_0}\right)^{-\alpha_\mu}$$

Where α_μ is a coefficient with value around 1.2-2, T_0 is the room temperature and T is the final temperature. By looking this equation, we can conclude that the mobility of the carrier is reduced with a rise of the temperature.

Threshold voltage:
The second way to study the influence of temperature is with the shift of the threshold voltage. This variation is mostly induced by the variation of the Fermi level with the intrinsic concentration and the new value is given by the following formula [8]:

$$V_{th} = V_{th0} + K_T\left(\frac{T}{T_0} - 1\right)$$

Where T_0 is the room temperature in K, V_{th0} is the threshold voltage at room temperature expressed in V and K_T is a negative temperature coefficient for nMOSFETs and a positive temperature coefficient for pMOSFETs, this coefficient is expressed in [V/°C], therefore, it is equal to the sensitivity of the transistors.

Subthreshold characteristics:

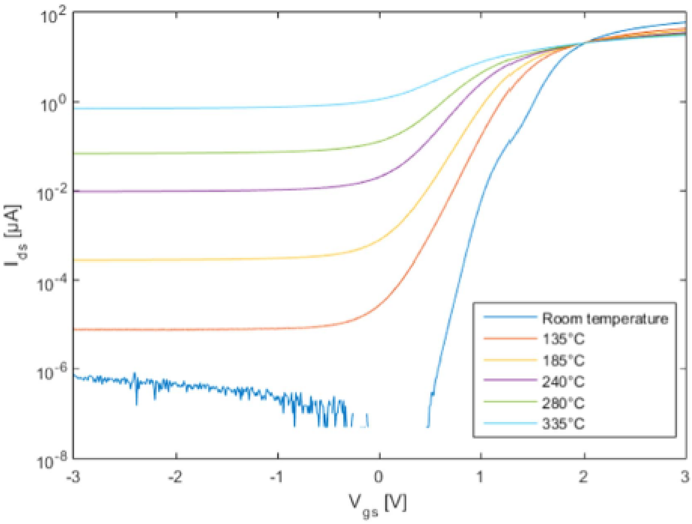

Figure 1.13: Sub-threshold characteristics of a nMOS transistor with a width of 24 μm operating in linear regime with $V_{ds} = 50\ mV$ [8]

On figure 1.13, we can see that when the temperature of the micro-heater increases, the value of the off current increases as well as the value of the sub-threshold slope S. The equation of this slope is given by [8]:

$$S = \frac{\partial(logI_D)}{\partial V_G} = \frac{nkT}{q} ln(10)$$

Where n is the non-ideal factor. When this non-ideal factor is equal to 1, the value of the slope should be around 60 $mV.dec^{-1}$ [8].

The device on figure 1.12.(a) is built in 1 μm partially depleted (PD) silicon on insulator (SOI) technology. The device has a circular membrane with a diameter of 600 um and in its center there is a tungsten micro-heater with a diameter of 200 μm and a thickness of 500 nm. Just beneath the micro-heater, there is a silicon thermodiode with a diameter of 200 μm and a thickness of 250 nm. The MOS transistor, the silicon thermodiode and the tungsten micro-heater are embedded in a 5 μm-thick Si/SiO_2 membrane. All the transistors have a channel length $L = 1\ \mu m$ and the width of nMOS transistor is $W = 6\ \mu m$, the width for the pMOS transistor is 24 μm and the width of the transistor for the CMOS inverter is $W = 4\mu m$ [8]. The approximately total diameter of the device is 2 mm.

In [8], it is found that the sensitivity of the nMOSFET is -3.2 $[mV/]$°C and the one for the pMOSFET is 3.4 [mV/°C] when the width of both transistors is 24 μm.

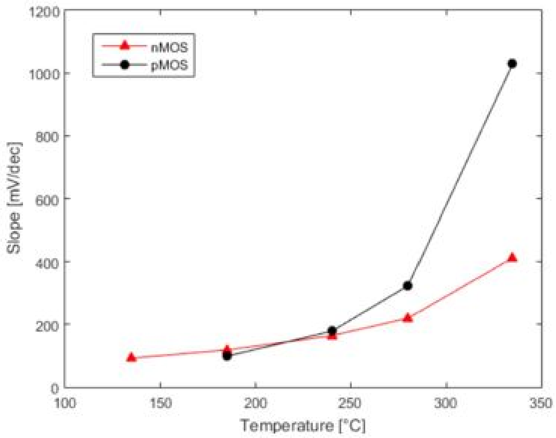

Figure 1.14: Slope of sub-threshold characteristics of the pMOSFET and nMOSFET transistors [8]

On figure 1.14, we can see the slope of the sub-sthreshold characteristics of a nMOS and pMOS transistors. We can see that for a temperature higher than 280 °C, the degradation of the pMOS transistor increases due to a high leakage current for a positve V_{gs} voltage which should come a parasitic channel at the back Si-Box interface [8]. We can also see that the nMOSFET has a breakdown degradation for a temperature higher than 335 °C when the drain voltage is high [8].
The self-heating effect, which introduces errors when measuring high temperature, is less significant in SOI technology than bulk silicon thanks to the low thermal conduction of the SiO_2 buried oxide. Moreover, the air cavity below the membrane increase the barrier for thermal dissipation. The self-heating effect has less influence at high temperature because the mobility of the electron is reduced at very high temperature but in addition to the self-heating, an avalanche effect appears at high V_{ds} for very high temperature as it can be seen on figure 1.15 [8].

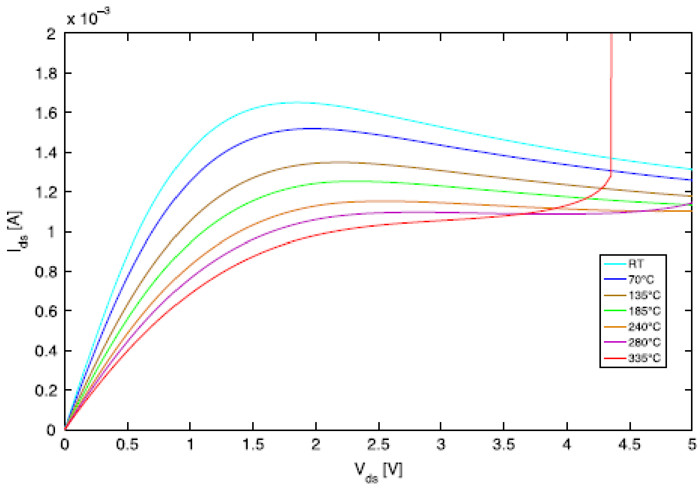

Figure 1.15: Curves $I_{ds} - V_{gs}$, for $V_{gs} = 5\ V$ showing the avalanche effect at high tempetature (>300 °C) for high V_{ds}

1.3 Sensors comparison

Kind of sensor	Silicon ring resonator	Fiber Bragg grating	Silicon diode suspended thermodiode	Silicon diode micro-air-bridge heater	Transistor MOS	Platinum resistor
Technology used	0.18 CMOS process	NA	SOI	SOI	SOI	NA
Temperature range [°C]	up to 300	up to 45	up to 500	-200 to 500	up to 280 for a pMOS and up to 335 for a nMOS	-260 to 650
Time response	6 μs	48.6 ms	15 ms	20 ms	NA	a few seconds to 10 s
Maximum current	NA	NA	65 μA	1 mA	65 μA	NA
Sensitivity	83 [pm/°C]	27.6 [pm/°C]	-1.3 [mV/°C]	high	-3.2 [mV/°C] for nMOS and 3.4 [mV/°C] for pMOS	0.385Ω/°C
Metallization	NA	Copper	Tungsten	NA	Tungsten	Platinum
Mode of operation	/	/	Current constant mode	Voltage constant mode	Constant voltage mode	Reference current or reference voltage
Size of the die	a few μm	15 mm	$4\ mm^2$*	$2\ mm \times 2\ mm$*	$d = 2\ mm$	NA
References	[1]	[2]	[11]	[19]	[8]	[4, 7]

Table 1.1: Comparison between different kinds of temperature sensors

* Estimated value of the chip with the given parameters.
By looking at table 1.1, we can see two temperature sensors are suitable according to the specifications. The first requirement is to have a fast response time, in the order of ms. The second one is that the planar area of the die should be lower than the one of the power MOSFET which is about 100 mm^2; The last one is that the temperature sensor should work at least at a temperature of 150 °C.
The first one is the optical temperature sensor, *Silicon ring resonator*, which has a small size, a few μm, an ultra fast response, 6 μs and can be heated up to 300 °C. The other sensor is an electrical one with a diode and a micro-heater. Indeed, this sensor has a small diameter, 2 μm, a low current, 65 μA, which avoid the self-heating effect and can be heated up to 500 °C. These sensors have comparable advantages but the sensor diode temperature sensor with an integrated micro-heater is chosen due to their availability.

Chapter 2

Heat transfer in the sensor

In this chapter, the heat transfer and the theoretical response of a temperature sensor to a step of temperature will be shown. In chapter 1, we selected a sensor which detects a rise of temperature thanks to a thermodiode. The chosen design is simulated by finite elements with Comsol ® software. The equivalent RC thermal circuit is studied and simulated with LTSpice. A parametric study will be done in order to study the influence of parameters on the dies

2.1 Theoretical heat transfer

The main physical phenomenon present in the sensor is heat transfer which can appear either by conduction, convection or radiation [20].
Conduction: this heat transfer corresponds to an energy exchange by molecular vibrations in solids. The heat flux is proportional to the temperature gradient because it is based on Fourier's law which is given by:

$$q = -k(\nabla T) \tag{2.1}$$

where ∇T is the temperature gradient and k is the thermal conductivity.
Convection: this heat transfer appears at the interface between a solid and a liquid or a gas. It can also take place by the heat transfer inside a liquid or a gas by the movement of the molecules.
Radiation: this heat transfer is made by a transfer of photons. It appears when the transfer by conduction or convection is impossible.

For the design of the sensor, we can consider that the heat propagates only in one direction and by conduction. According to [21], we can consider that the insulation between the membrane and the silicon diode behaves like a resistor R and that the calorific mass of the diode is C. Moreover if we consider that the temperature of the membrane is Θ_e and the temperature of the diode is Θ_C, we can write the following equations:

$$\sum q(t)_{in} - q(t)_{out} = C\frac{d\Theta_C(t)}{dt} \tag{2.2}$$

$$q(t) = \frac{1}{R}(\Theta_e(t) - \Theta_c(t)) \tag{2.3}$$

$$\Rightarrow RC\frac{d\Theta_C(t)}{dt} + \Theta_C(t) = \Theta_e(t) \tag{2.4}$$

If we suppose that $\tau = RC$, the equation becomes:

$$\tau\frac{d\Theta_C(t)}{dt} + \Theta_C(t) = \Theta_e(t) \tag{2.5}$$

The solution is the sum of a transient part, $\Theta_{C1}(t)$ and a stationary one, $\Theta_{C2}(t)$. By solving the equation characteristic $\tau r + 1 = 0$, we have the solution $r = -\frac{1}{\tau}$. Therefore, Θ_{C1} is given by :

$$\Theta_{C1}(t) = Ke^{-\frac{t}{\tau}} \tag{2.6}$$

If a step of temperature with an amplitude T_1 is applied, the stationary solution is $\Theta_{C2}(t) = T_1 u(t)$. The complete solution is:

$$\Theta_C(t) = \Theta_{C1}(t) + \Theta_{C2}(t) = Ke^{-\frac{t}{\tau}} + T_1 \tag{2.7}$$

If we consider that at time $t = 0$, the temperature of the sensor is T_0, we find that $K = T_0 - T_1$ and the general solution is given by:

$$\Theta_C(t) = T_0 e^{-\frac{t}{\tau}} + T_1(1 - e^{-\frac{t}{\tau}}) \Leftrightarrow \Theta_C(t) = T_1 + (T_0 - T_1)e^{-\frac{t}{\tau}} \tag{2.8}$$

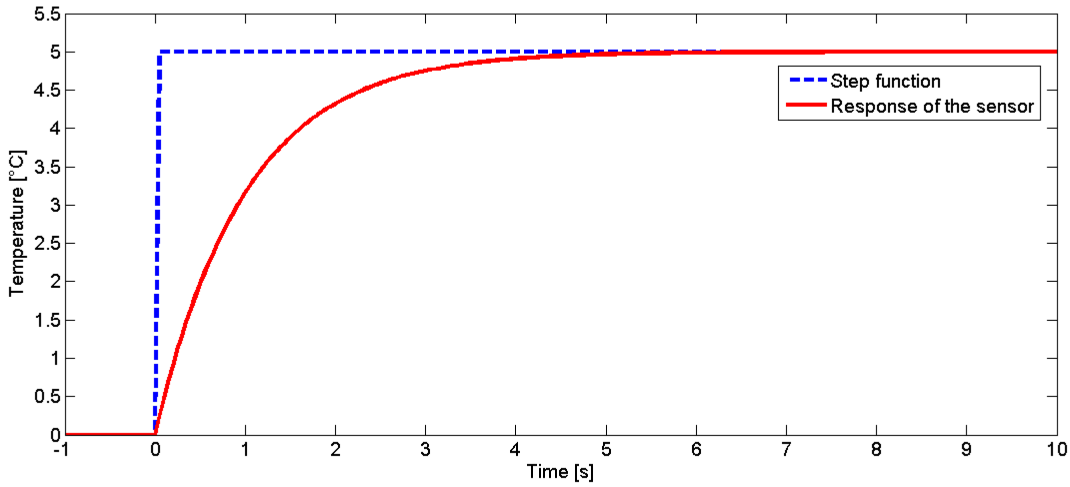

Figure 2.1: Simulation of sensor response to a step of temperature, applied in $t = 0\ s$, according to equation (2.8). For this simulation, $T_0 = 0$°C, $T_1 = 5$°C and the time constant of the system is 20s. Simulation done with Matlab ®.

The time constant is defined as the time needed to reach 63% of the step of temperature. Indeed, equation of the voltage in a RC circuit is given by the following equation:

$$V_{out}(t) = V_{in}(1 - e^{-t/\tau}) \tag{2.9}$$

We want to know the equation for a time t equal to τ, by using equation (2.9), we obtain:

$$V_{out}(t = \tau) = V_{in}(1 - e^{-1}) = V_{in}0.63$$

This why the time response or time constant is defined as being the necessary time to reach 63% of the final value.

2.2 2D representation of the device

The temperature sensor will have a circular shape to avoid mechanical stress at the edges as it was explained in chapter 1. We will focus on the study of two implementations of the device, the first one can be heated either by a power circuit or by the embedded micro-heater. The second one is a thinned die, where the substrate is removed. It is heated by the power circuit. For simulation, we will consider a two dimensional representation which is a cross-section of the device.

2.2.1 Die heated by a micro-heater or a power device

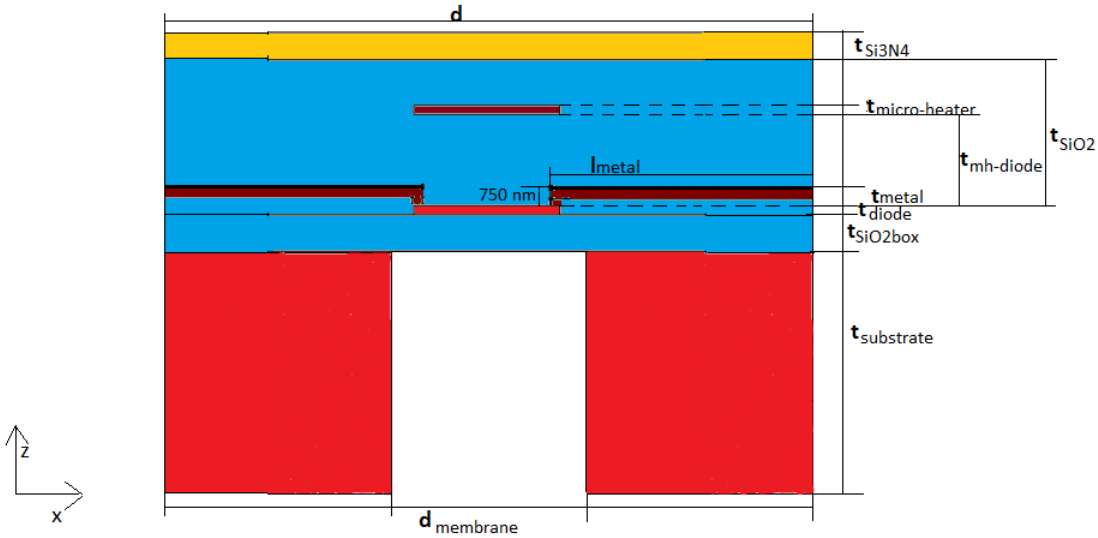

Figure 2.2: Die with substrate, the dimensions are the following: $t_{substrate} = 400\ \mu m, t_{SiO_2box} = 1\ \mu m$, $t_{diode} = 250\ nm$, $t_{metal} = 500\ nm$, $l_{metal} = 925\ \mu m$, $t_{mh-diode} = 2\ \mu m$, $t_{micro-heater} = 500\ nm$, $t_{SiO_2} = 4\ \mu m$ coated, $t_{Si_3N_4} = 500\ nm$, $d = 2\ mm$ and the diameter of the membrane $d_{membrane} = 600\ \mu m$. This schematic is not to the scale for readability purpose.

On figure 2.2, we can see a cross-section view of the die. For this die, the heat can come either from the micro-heater or from the power circuit on which it is glued. The Si_3N_4 layer is a passivation layer which acts as a coating on the die. The substrate layer is made of a cylinder of air with a diameter of $d_{membrane} = 600\ \mu m$ around which there is a torus in silicon with a width of 700 μm, leading to a total diameter of the device of 2 mm.
We are interested in studying the heat transmission along the z axis. The heat transfer through the sidewalls of the device in x=0 and x=2 mm is neglected and there is no heat exchange with the environment. The thermal resistance of the air, in x=0 and x=2 mm, are in parallel with the device and are much larger than the device resistance. Moreover, the z-dimension is about five times smaller than the x-dimension.
We consider convection is the main mechanism at the top of the passivation layer and the air and at the interface between the substrate and the air. In case the substrate is glued on a power device, convection on that side is replaced by heat conduction. We assume that the initial temperature of the die is 20 °C or 293.15 K and the temperature of the air surrounding the die is also 293.15 K.

2.2.2 Thinned die heated by the power device

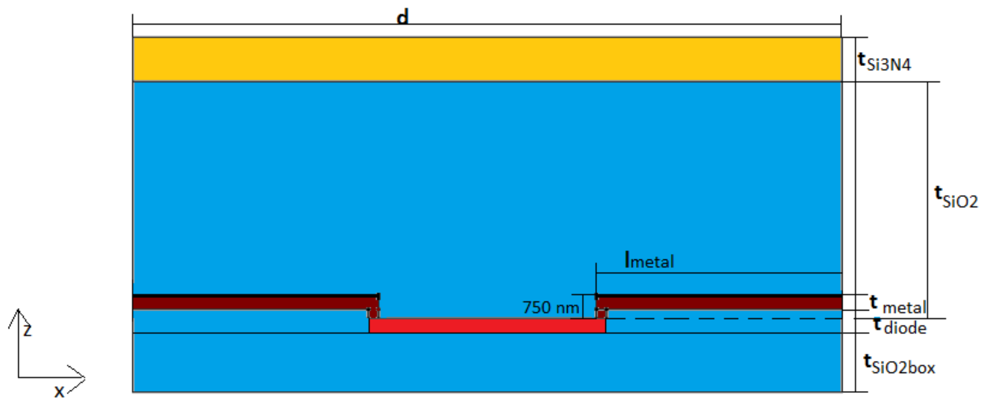

Figure 2.3: Thinned die with following dimensions: $t_{SiO_2box} = 1\ \mu m$, $t_{diode} = 250\ nm$, $t_{metal} = 500\ nm$, $l_{metal} = 925\ \mu m$ $t_{SiO_2} = 4\ \mu m$ coated and $t_{Si_3N_4} = 500\ nm$. The length of the sensor, d, is 2 mm and the length of the diode is 200 μm. this schematic is not to the scale.

On figure 2.3, we can see the thinned die heated by the power device glued below the SiO_2box layer. We are interested in studying the heat transfer along the z axis. For the same reason than the device shown on figure 2.2, we consider thermal insulation for $x = 0$ and $x = 2\ mm$. The die being glued on the power device, we only have convection at the interface between the passivation layer and the air. We also consider that the initial temperature of the die is 293.15 K and the temperature of the air surrounding the die is also 293.15 K.

2.3 Equivalent thermal circuit of the device

The conduction heat transfer is analogous to an electrical circuit where the temperature difference between two points is represented by the voltage difference and the heat flow is the equivalent current [22]. This representation will help us to know the time needed for the diode to respond to a temperature change at the sensor surface.

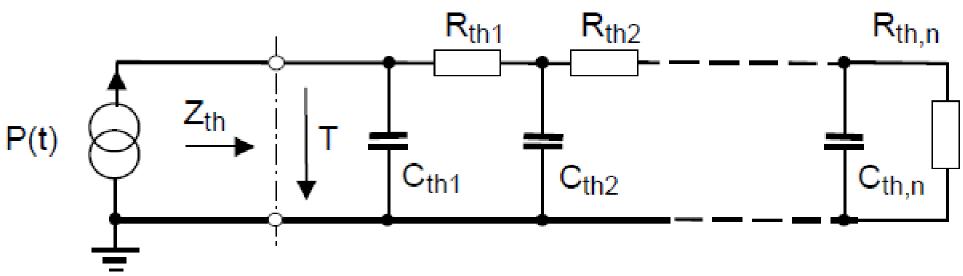

(a) Physical RC circuit

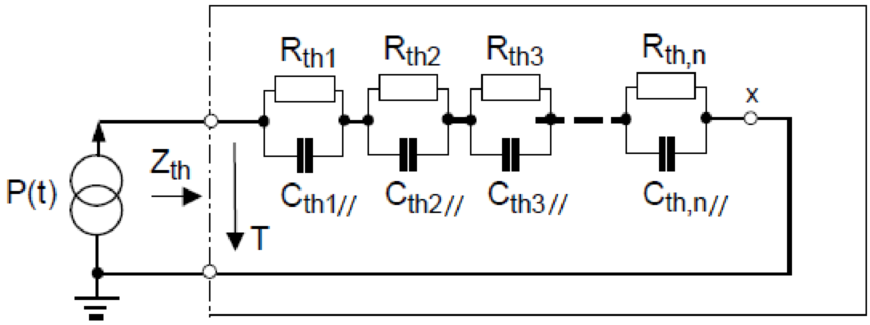

(b) Equivalent circuit

Figure 2.4: RC thermal circuits [23]

Two equivalent circuits can be used to model heat transfer and they can be seen on figure 2.4. Each layer is represented by a capacitance and a resistance. We can see that figure 2.4.(a) is equivalent to a transmission line and it models heat conduction properties with the physical parameters of the materials. Indeed, we could prefer the second representation, 2.4.(b), because we can say that the heat flows through all the different layers and first charges the first layer of material before charging the second layer, etc. As a consequence, the current flowing through the layers of the material is the same and this circuit is correct. However, this is not physically correct because in this representation, the energy stored in thermal capacitances depends on the temperature difference between two adjacent points, while in reality, the energy stored in materials, here modelled as the capacitance energy, is proportional to the absolute temperature in the material [24]. This is the reason why we prefer to use the RC thermal model shown on figure 2.4.(a) where the capacitances are all connected to the same reference voltage, corresponding to a reference temperature. The second model describes correctly the thermal behaviour at the entrance but as there is no link with the physical model, the temperature distribution inside the equivalent circuit does not have any meaning [24]. The advantage of the equivalent thermal circuit on figure 2.4.(b), is the fact that we can see the time constant, τ, for each material, independently from each other. Whereas the time constant of circuit 2.4.(a) is the same for all layers of material.

Nevertheless, we can switch from one representation to the other one by selecting the correct value for the capacitance and the resistance so that the time constant of each material is equal for both circuits. The corresponding resistances keep the same value for the two circuits. Once all the capacitances are fully charged, they behave like an open circuit, which means that circuits on figure 2.4 are equivalent. This implies that the resistance of each material must be the same. As a consequence, by also requiring the same value of the time constant, we obtain [24]:

$$C_{//} = \frac{\tau}{R} \tag{2.10}$$

2.3.1 Computation of thermal resistances and thermal capacitances

The equivalent thermal resistances and capacitances are computed based on material properties. But before computing their values, we need to define the heat transfer between the layer of materials.
As explained in section 2.2, the main heat transfer takes place by conduction, except at the interfaces with the air where there is convection. The equivalent thermal resistance for conduction can be computed by the following formula:

$$R_{cond} = \frac{t}{kA} \tag{2.11}$$

Where t is the thickness of the layer, k is the thermal conductivity and A is the cross-section area [25].
The equivalent resistance for convection is given by:

$$R_{conv} = \frac{1}{hA} \tag{2.12}$$

Where h is the convection coefficient and A is again the cross-section area [25].
The thermal capacitance, on figure 2.4.(a) can be given by the following formula:

$$C_{th} = c_p \rho t A \tag{2.13}$$

Where c_p is the heat capacity, ρ is the density, t is the thickness of the layer and A is the cross-section area [23].

Type of material	k [W/(m.K)]	c_p [J/(kg.K)]	ρ $[kg/m^3]$	h $[W/(m^2.K)]$
Si	130	700	2329	/
SiO_2	1.4	730	2200	/
Si_3N_4	20	700	3100	/
W	174	132	19350	/
Air	0.0257	1005	1.205	/
Convection	/	/	/	23.54

Table 2.1: Parameters of the different layers of materials for both devices

Materials parameters given in table 2.1 are taken from Comsol ® in order to be able to do a comparison with Comsol ® simulations and analytical results. Except for convection, air parameters do not come from Comsol ® and are found in [26].

Choice of convection coefficient, h, value

The value of convection coefficient, h, is comprised between 5 and 25 $W/(m^2.K)$ for the air, when there is no constraints. In order to determine the value of h corresponding to the device, Comsol ® allows to simulate external natural convection [27]. The temperature step was simulated by using a constant heat flux coming out of the SiO_2box layer. The value of h coefficient is obtained from:

$$h = \frac{q}{\Delta T} = \frac{1000}{42.48} = 23.54\ [W/(m^2.K)]$$

With q=1000 W/m^2 and $\Delta T = 42.48\ K$.

2.4 Die with substrate

2.4.1 Die heated by the power circuit

In a first time, we will study the heat transfer and the influence of the parameters on die shown on figure 2.2, when it is heated by a power circuit.

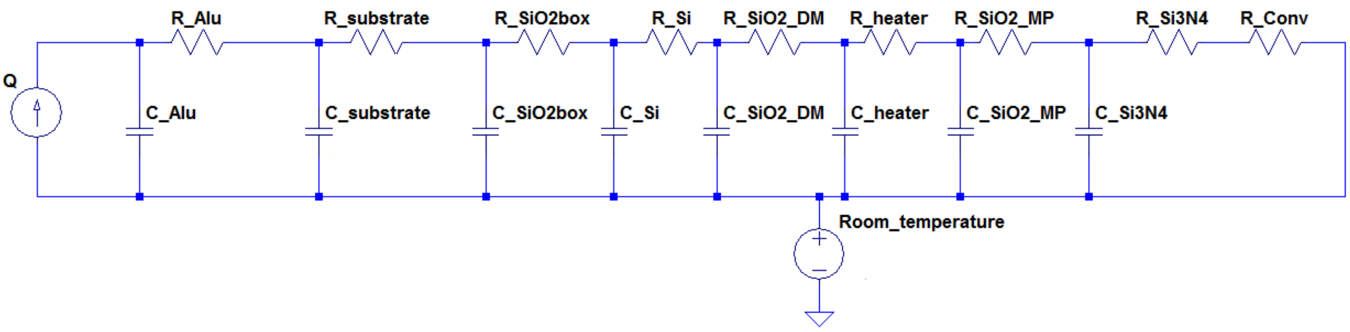

Figure 2.5: RC equivalent circuit of die shown on figure 2.2 when it is heated by a power MOSFET through the substrate

On figure 2.5, we can see the equivalent RC thermal circuit of the die shown on figure 2.2 when it is glued on a power MOSFET. The heat coming from the power transistor is represented by heat source Q. As the heat flux flowing through the die is observed in the centre of the device, in x=1 mm, the metallization is not taken into account.
As the tungsten micro-heater is embedded in the SiO_2 layer, we have to divide the SiO_2 layer into two parts. the first one, called SiO_2DM, represents the part of the SiO_2 between the diode and the micro-heater and the second part, called SiO_2MP, represents the part of the SiO_2 between the micro-heater and the passivation layer.
The aluminium layer between the heat source and the substrate represents the power circuit on which the die is glued. This layer allows to avoid a heat flux directly applied on the substrate surface. If this layer is not present, the limit condition forces the heat flux to be the same in the silicon and in the air, which is not the reality. Indeed, the thermal conductivity of the silicon is 5000 times higher than the thermal conductivity of the air. As the conductivity of the aluminium is important, this layer has almost no influence on the time constant of the device.

Computation of resistances and capacitances

We can now compute the values of the resistances and capacitances by using parameters values of table 2.1, dimensions on figure 2.2 and equations (2.11), (2.12) and (2.13). As the diameter of the die is 2 mm, for all the layer of material, the cross-section area is $\pi \times 10^{-6}$ except for the diode and the micro-heater which have a diameter of 200 μm, therefore their cross-section area is $\pi \times 10^{-8}$. As the substrate can be seen as a composite material composed of air and silicon, its resistance and capacitance will be computed in the following section. By using all these informations, we find the following values:

- $R_{Alu} = 13.4 \times 10^{-3} K/W$
- $R_{SiO_2box} = 0.227\ K/W$
- $R_{Si} = 0.06\ K/W$
- $R_{SiO_2DM} = 0.455\ K/W$

- $R_{heater} = 0.091\ K/W$
- $R_{SiO_2MP} = 0.341\ K/W$
- $R_{Si_3N_4} = 7.96 \times 10^{-3}\ K/W$
- $R_{Conv} = 13522\ K/W$
- $R_{Alu} = 7.67 \times 10^{-5} J/K$
- $C_{SiO_2box} = 5.045 \times 10^{-6}\ J/K$
- $C_{Si} = 1.28 \times 10^{-8}\ J/K$
- $C_{SiO_2DM} = 1.01 \times 10^{-5}\ J/K$
- $C_{heater} = 4.01 \times 10^{-8}\ J/K$
- $C_{SiO_2MP} = 7.57 \times 10^{-6}\ J/K$
- $C_{Si_3N_4} = 3.4 \times 10^{-6}\ J/K$

Computation of substrate resistance and capacitance [28]

The substrate shown on figure 2.2 is composed of a cylinder of air around which there is a torus in silicon and is treated as a composite material for which equivalent thermal resistance and capacitance must be computed. The heat flow is given by the following equation:

$$Q = A\frac{k}{t}\Delta T$$

where A is the cross section area, t is the thickness of the material, k is the thermal conductivity and ΔT is difference of temperature between the two surfaces of the layer. As the heat and temperature variation in the thermal circuit are respectively analogous to current and voltage in electrical circuit, the thermal resistance can be computed by the following way:

$$R_{th-subs} = \frac{\Delta T}{Q} = \frac{t}{kA}$$

We find the same expression than for equation (2.11). But as we have a composite material, we have to take into account the geometry. The total heat flowing through the substrate in z-direction is the sum of the one flowing in the silicon and in the air. Assuming the variation of temperature, ΔT, is the same for both materials, finally leads to [28]:

$$R_{th-subs} = \frac{t}{A_{air}k_{air} + A_{Si}k_{Si}}$$

And by using values given in table 2.1 and on schematic 2.2, we find:

$$R_{th-subs} = 1.076\ K/W$$

Now we would like to compute the thermal capacitance of the substrate layer. As a recall, the current through a capacitance is given by the following equation:

$$I = C\frac{dV}{dT} \tag{2.14}$$

The enthalpy, which is the variation of energy in a material as a function of the temperature, at a constant pressure, is given by:

$$dH = \rho c_P V dT$$

Where ρ is the density, c_p is the specific heat, V the volume and T the temperature. If we differentiate this equation in function of the time, we obtain:

$$\frac{dH}{dt} = \rho c_P V \frac{dT}{dt}$$

By looking at the units, we see that the left member correspond to J/s which is equivalent to W, so it is equivalent to the heat. Using again the fact that heat is analogous to the current and the temperature is analogous to the voltage, we can make a parallel with equation (2.14) and we find that $C_{th} = \rho c_P V$. Using the same method as to find the equivalent resistance, we obtain:

$$C_{th-subs} = \rho_{air} c_{Pair} V_{air} + \rho_{Si} c_{PSi} V_{Si}$$

By using values of parameters in table 2.1 and on schematic 2.2, we find that:

$$C_{th-subs} = 1.85 \times 10^{-3}\ J/K$$

Computation of equivalent capacitances

We have computed the values of physical resistances and capacitances of figure 2.5 but we would also like to compute the value of equivalent capacitances that can be seen on the circuit from figure 2.4.(b). Computing these capacitances allow us to know the time constant specific for each layer of material. To compute the time constant of each layer of material, we have to consider, in figure 2.4.(a), the input power source as an open circuit and all the capacitances which do not participate to the calculation of the time constant, as open circuit too. Then, the time constant is computed by the product of the capacitance of interest with the total equivalent resistance.
For example, if we consider the aluminium layer, the current source and all the capacitances, except the one of the aluminium, are in open-circuit. As the value of all resistances are negligible in comparison with the convection resistance, we have that $\tau_{Alu} \simeq 7.67 \times 10^{-5} \times 13522 = 1.04\ s$. Applying equation (2.10) gives $C_{Alu//} = 76.6\ J/K$. By using the same method for all the layers, we find the following values:

- $\tau_{Substrate} = 25.02\ s$ and $C_{Substrate//} = 23.25\ J/K$
- $\tau_{SiO_2box} = 68\ ms$ and $C_{SiO_2box//} = 299.6 \times 10^{-3}\ J/K$
- $\tau_{Si} = 173\ \mu s$ and $C_{Si//} = 2.88 \times 10^{-3}\ J/K$
- $\tau_{SiO_2DM} = 137\ ms$ and $C_{SiO_2DM//} = 0.3\ J/K$
- $\tau_{heater} = 542\ \mu s$ and $C_{heater//} = 5.96 \times 10^{-3}\ J/K$
- $\tau_{SiO_2MP} = 102\ ms$ and $C_{SiO_2MP//} = 0.3\ J/K$
- $\tau_{Si_3N_4} = 46\ ms$ and $C_{Si_3N_4//} = 5.78\ J/K$

In this case, we considered the time constant of the material, as being a part of the all system.

Transient case

We would like to know the time constant of each material when they are considered independently from each other. We only need to multiply the resistance of the material by the capacitance of the material. By using values computed in sections 2.4.1 and 2.4.1, we obtain:

- $\tau_{Alu} = 1.03\ \mu s$
- $\tau_{Substrat} = 1.99\ ms$

- $\tau_{SiO_2box} = 1.15\ \mu s$
- $\tau_{Si} = 0.77\ ns$
- $\tau_{SiO_2DM} = 4.6\ \mu s$
- $\tau_{heater} = 3.65\ \mu s$
- $\tau_{SiO_2MP} = 2.58\ \mu s$
- $\tau_{Si_3N_4} = 27.1\ ns$

By looking on these values, once the SiO_2box is heated, it takes 0.77 ns for the diode to heat up when all materials are considered independent from the others. In the global circuit, however the effective time constant is common to all materials and is mostly influenced by the highest capacitance and highest resistance.

Circuit at equilibrium

We have to determine the power flowing through the RC thermal circuit. We know that the convection flux is given by: $Q = h\Delta T$ and we know h=23.54 $W/(m^2.K)$ from section 2.3.1. If we assume the at equilibrium, the temperature is uniform across all layers, ΔT is equal to the temperature step observed on the power MOSFET. For $\Delta T = 150\ K$, we have $Q = 23.54 \times 150 = 3531\ W/m^2$.
In stationary case, the flux is identical in all layers and $Q_{in} = Q$. Q_{in} corresponds to the input flux to be set to reach the desired ΔT. Accounting for the die surface, $\pi \times 1O^{-6}$, we obtain P=11.1 mW.
The heat flux can also be used to determine the temperature at the interface between different materials. According to [25], the heat flux between two materials is given by:

$$q = \frac{T_{max} - T_{min}}{R_{tot}} \tag{2.15}$$

With T_{max} is the temperature of the hot surface and T_{min} is the temperature of the cold surface. R_{tot} is the thermal resistance between two surfaces. Using $T_{max} = 150\ K$, we find that the temperature at the interface between the aluminium and the substrate is given by:

$$T_{Alu-Subs} = T_{max} - qR_{Alu} = 442.9998513\ K$$

By applying this method successively, we can find:

- $T_{Subs-SiO_2box} = 442.9879077\ K$
- $T_{SiO_2box-Si} = 442.985388\ K$
- $T_{Si-SiO_2DM} = 442.984722\ K$
- $T_{SiO_2DM-heater} = 442.9796715\ K$
- $T_{heater-SiO_2MP} = 442.9786614\ K$
- $T_{SiO_2MP-Si_3N_4} = 442.9748763\ K$

Therefore, we can conclude that in equilibrium state, the temperature is approximately the same through all the device, which confirms the initial hypothesis used to determine Q.

LTSpice simulation

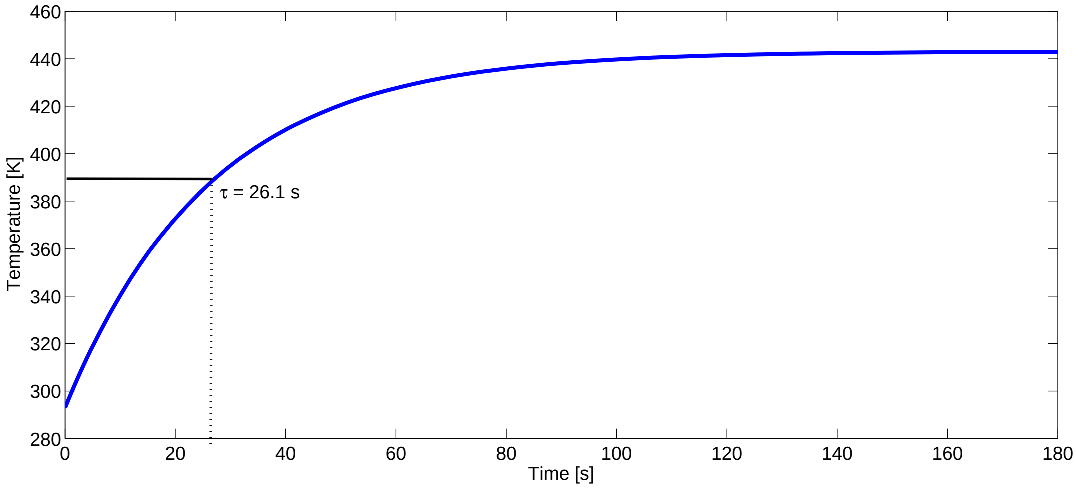

Figure 2.6: LTSpice simulation of RC thermal circuit shown on figure 2.5. The variation of the temperature as a function of the time is taken at the interface $Si - SiO_2DM$ layers.

On figure 2.6, we can see the LTSpice simulation of the thermal RC circuit shown on figure 2.5 and we can see that the time constant obtained is 26.1 s. We can notice that when we add all the time constants obtained in section 2.4.1, the sum is 25.37 s which is approximately the same value than the one obtained with LTSpice. It can be seen that the time constant of the system is dominated by the one of the substrate. As the thickness of the substrate is much important than the one of the membrane, 400 μm for 5 μm, the substrate layer absorbs more energy.

Comsol ® simulations

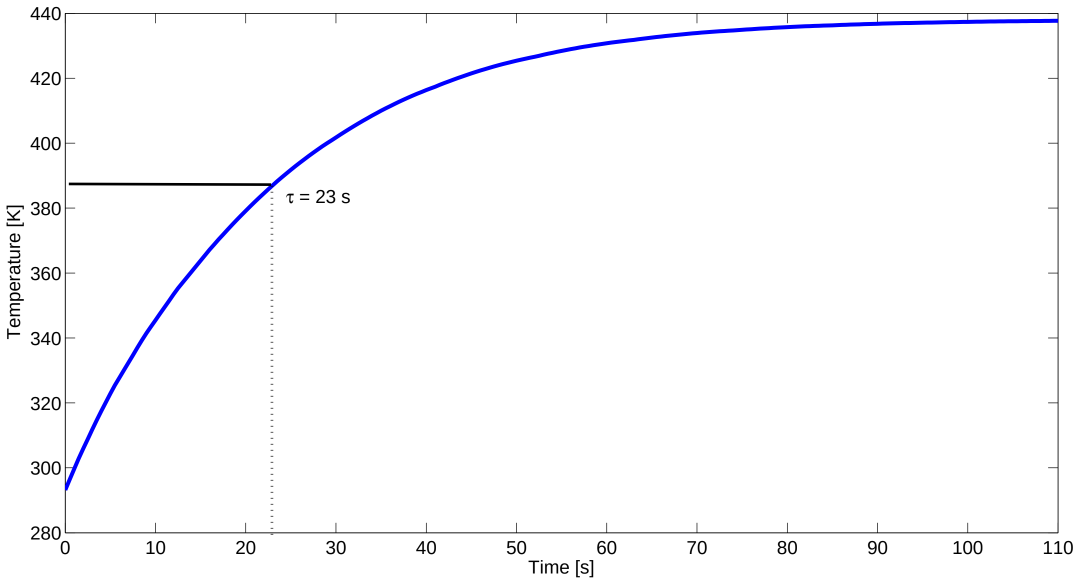

Figure 2.7: Comsol ® simulation of circuit shown on figure 2.2 for $h = 23.54$ and a heat flux of 3531 $W/(m^2.K)$. The variation of the temperature as a function of the time is taken at the interface $Si - SiO_2DM$ layers.

On figure 2.7, we can see the simulation obtained with Comsol ® for a convection coefficient of 23.54. A heat flux of 3531 $W/(m^2.K)$ is imposed on the substrate surface and corresponds to the flux required to reach a step of temperature of 150 K as previously computed. The obtained time constant is 23 s.

Comparison with LTSpice simulation
By comparing time constants obtained with Comsol ® and LTSpice simulations on figure 2.7 and 2.6, we can see that both values of time constants are close to each other, there is an error of approximately 13 %. This error comes from the fact that we made some approximations to compute the values analytically that we used for the LTSpice simulation.

Influence of the meshing
In finite elements, meshing plays an important role in the solution and its influence is studied. Indeed more the meshing is thin, more the solution will be accurate but the computation time will be increased. For this simulation we decided to test three different kinds of meshing, named: *extremely coarse*, *normal* and *extremely fine*. Their parameters can be found in the following table:

Type of meshing	Extremely coarse	Normal	Extremely fine
Degree of freedom	80178	121401	225982
Domain elements	38751	59170	111437
Boundary elements	9985	10637	10999
Maximum element size [m]	6.6×10^{-4}	1.3×10^{-4}	2×10^{-5}
Minimum element size [m]	10^{-4}	6×10^{-7}	4×10^{-8}
Maximum element growth rate	2	1.3	1.1
Curvature factor	1	0.3	0.2
Resolution of narrow regions	0.9	1	1
Computation time [s]	45	55	90

Table 2.2: Parameters of the meshings used in Comsol ® simulations

- The *maximum element size* allows to limit the maximum length of the elements
- The *minimum element size* specifies the minimum length allowed for the elements
- The *maximum element growth rate* fixes the maximum rate at which an element size can growth from a region with small elements to a region with larger elements
- The *curvature factor* "determines the size of boundary elements compared to the curvature of the geometric boundary and a lower value gives finer mesh along curved boundary"
- The *Resolution of narrow regions* controls the number of layers of elements in a narrow region, higher number leads to a finer mesh in narrow regions. If this number is lower than one, in narrow region, elements can be created with an anisotropic size.

These definitions are found in [29].

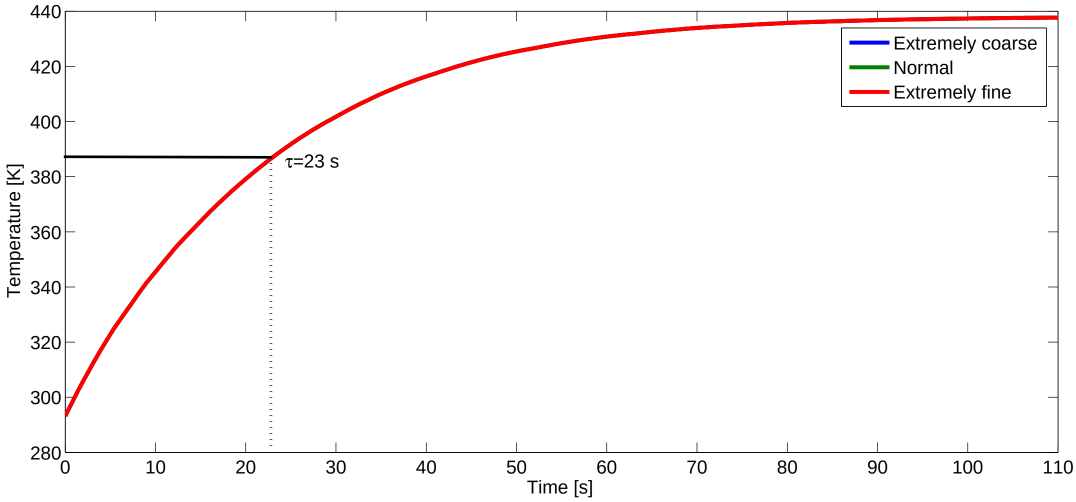

Figure 2.8: Influence of the meshing, the variation of the temperature as a function of the time is taken at the interface $Si - SiO_2DM$ layers. Simulation obtained with Comsol ®

On figure 2.8, we can see the influence of the meshing and we can see that all the curves overlay each other, which means that the meshing does not influence the time response of the die. The curves represent the variation of the temperature in the diode as a function of the time. We will use the *extremely coarse* meshing because the result is the same when using the *extremely fine* meshing and the computation time is reduced.

Influence of the symmetry

As it can be seen on figure 2.2, the die is entirely symmetrical along the x axis. Therefore, we can only simulate the half of the device and impose a condition of symmetry on the central axis. We decide to simulate the die from $x = 0$ to $x = d/2 = 1\ mm$ and to require a condition of symmetry in $x = 1\ mm$.

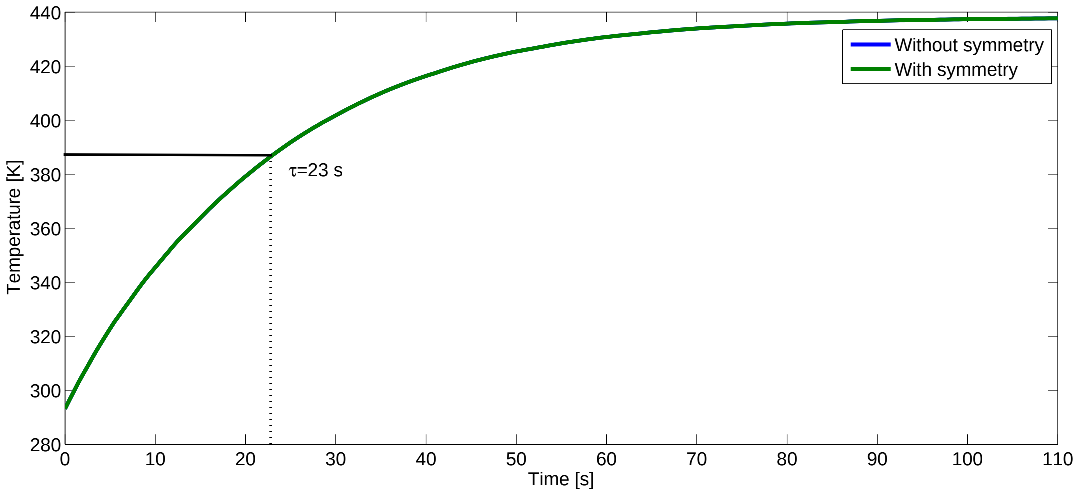

Figure 2.9: Influence of the symmetry on the response time, the variation of the temperature as a function of the time is taken at the interface $Si - SiO_2DM$ layers. Simulation obtained with Comsol ®

As we can see on figure 2.9 the curves overlay each other, which implies that the condition of symmetry can be used to reduce the computation time. For the extremely coarse meshing, the computation time is reduced by 8 s.

Influence of the material of substrate layer

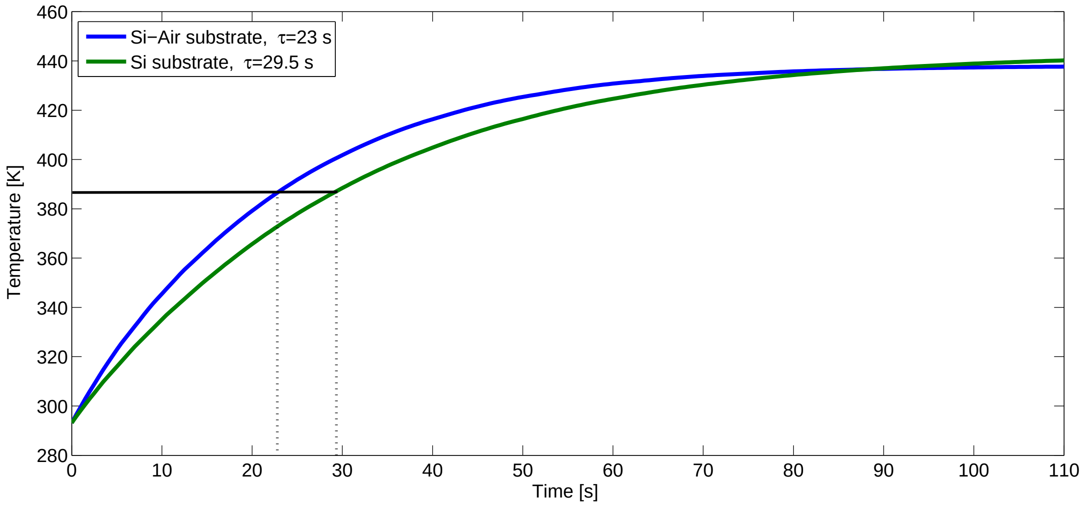

Figure 2.10: Influence of the material for the substrate layer. The variation of the temperature as a function of the time is taken at the interface Si-SiO_2DM layers. Simulation obtained with Comsol ®

On figure 2.10, we can see the influence of the materials which compose the substrate layer. As described on figure 2.2, the substrate layer is a composite material made of air and silicon. As the thermal conductivity of the silicon is about 5000 times greater than the one of the air, almost all the heat flows through the silicon material. Therefore, we could think that the time constant will be reduced if the substrate is only made in silicon, but as we can see on figure 2.10 this is not the case. The time constant of all the die is influenced by the dominant response time which is for the substrate layer. As it was explained in section 2.4.1, the time constant of a layer depends on the value of its capacitance and the value of the convection resistance. All the other resistances being negligible in comparison with the convection resistance. If we use the dimensions described on figure 2.2, the capacitance of the composite layer is almost equal to the capacitance of the silicon. As a recall, the equation used to find the thermal capacitance of a material is given by:

$$C_{th} = \rho c_p t A$$

In the case of the composite material, the capacitance is almost equal to the one of the silicon, which has a volume of $1.14 \times 10^{-9}\ m^3$, a capacitance of $1.85 \times 10^{-3}\ J/K$ and a time constant is 25.02 s. If we consider that all the substrate is in silicon, the volume of the substrate is $1.25 \times 10^{-9}\ m^3$, the capacitance is $2.04 \times 10^{-3}\ J/K$ and as a consequence, the time constant of the substrate layer is 27.56 s.

Influence of the metallization

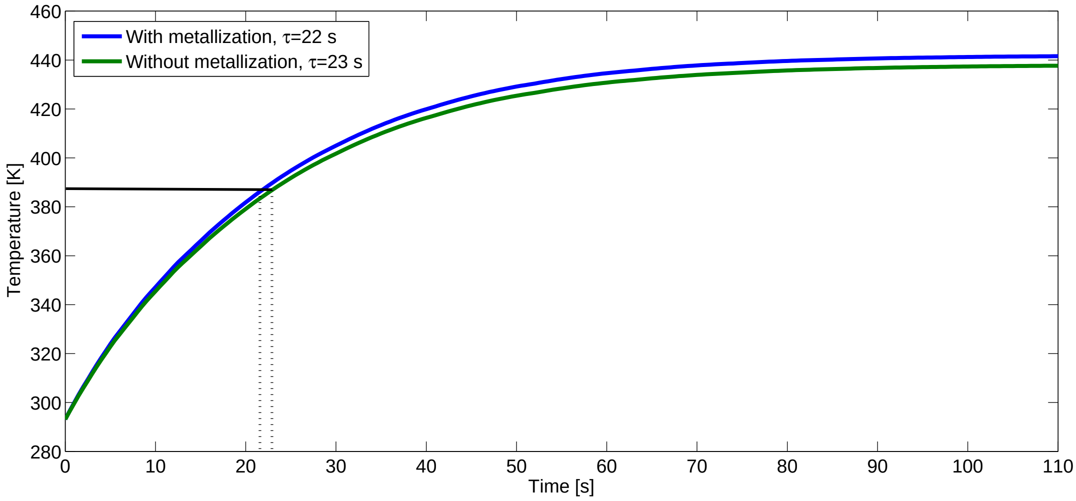

Figure 2.11: Influence of the metallization, simulation obtained with Comsol ® , the variation of the temperature as a function of time is taken at the interface between the Si layer and the SiO_2DM layer

Another parameter which is interesting to study is the influence of the presence of the metallization allowing to measure the current or the voltage through the diode. As we can see on figure 2.11, when there is no metallization, the time constant obtained is greater than when there is metallization and the error is about 4.5 %. This can be explain by the fact that the diode is on-membrane and the heat does almost not flow through the air and so it has to flow from the silicon to the SiO_2box layer. As the thermal conductivity of the tungsten, which is the material of the metallization, is about 100 times higher than the thermal conductivity of SiO_2, the heat will reach faster the diode by flowing through the metallization. Nevertheless, as the error when there is no metallization is negligible, the metallization will be neglected because it allows to reduce the time of simulation.

Influence of the convection coefficient

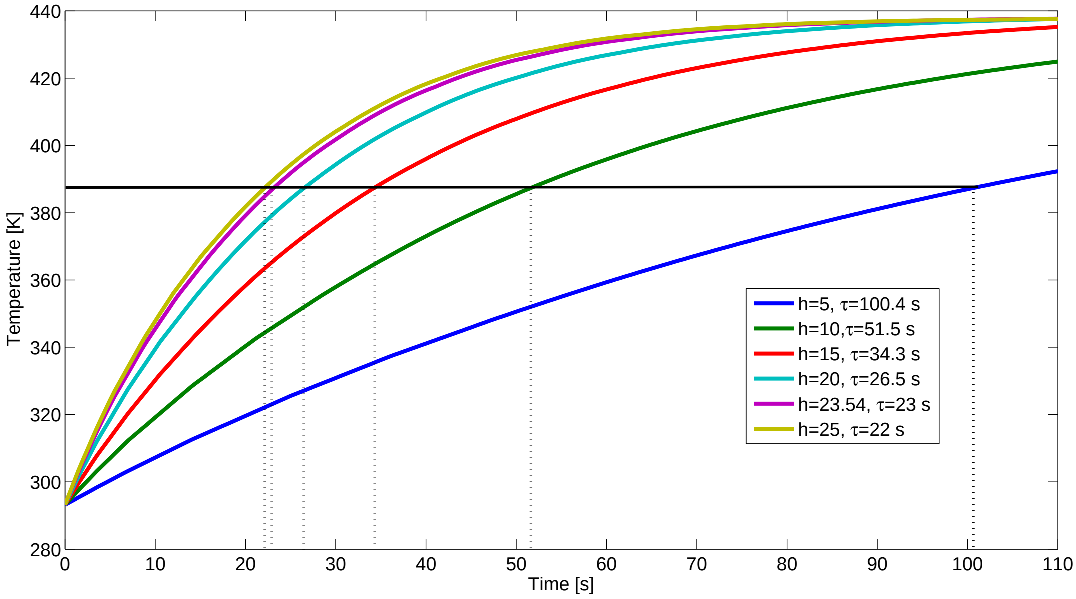

Figure 2.12: Influence of the convection coefficient on the time response of the die. Simulation obtained with Comsol ®. The value of temperature as a function of the time is taken at the interface between the Si layer and the SiO_2DM layer

On figure 2.12, we can see the influence of the convection coefficient on the time response of the system. The heat flux on the substrate is selected to reach the same final temperature independently of the value of h. As it was explain in section 2.4.1, the initial flux coming from the power circuit is constant and as once the die is in stationary case, the flux is the same through all the device and equal to convection flux, the initial flux is equivalent to the final convection flux. As a recall, the convective flux is given by: $Q = h\Delta T$. As we keep the value of ΔT constant and equal to 150 K, the value of the applied heat flux will increase with an increasing value of the convection coefficient.

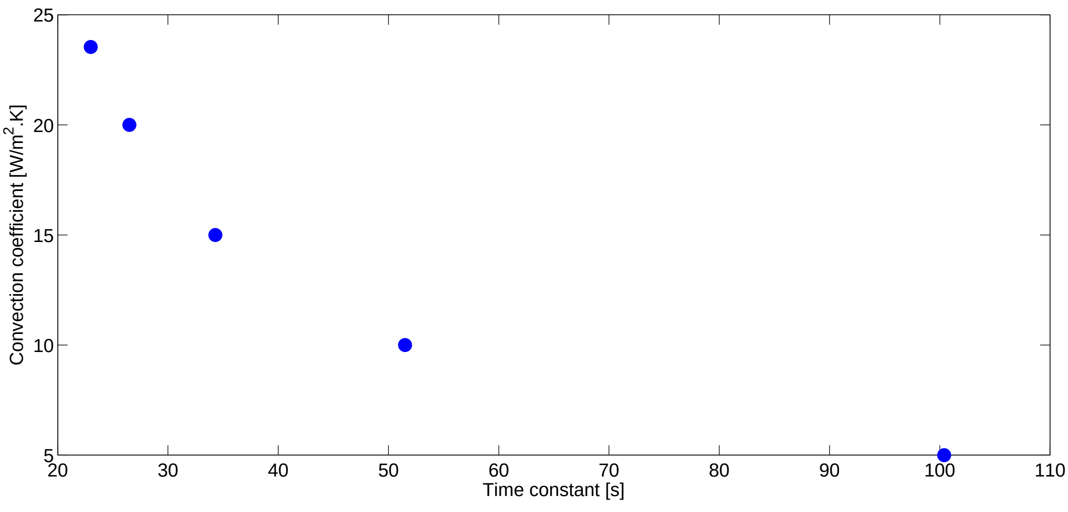

Figure 2.13: Value of the time constant in fuction of the convection coeffcient value

By looking on figure 2.13, we can see that the value of the time constant decreases with the rise of the convection coefficient. This is explain by the fact that the heat flowing through the die increases with h and therefore, the diode will be heated more rapidly. We can also noticed that when the value of the convection coefficient double, the value of the time response is approximately divided by a factor two.

Influence of the step of temperature

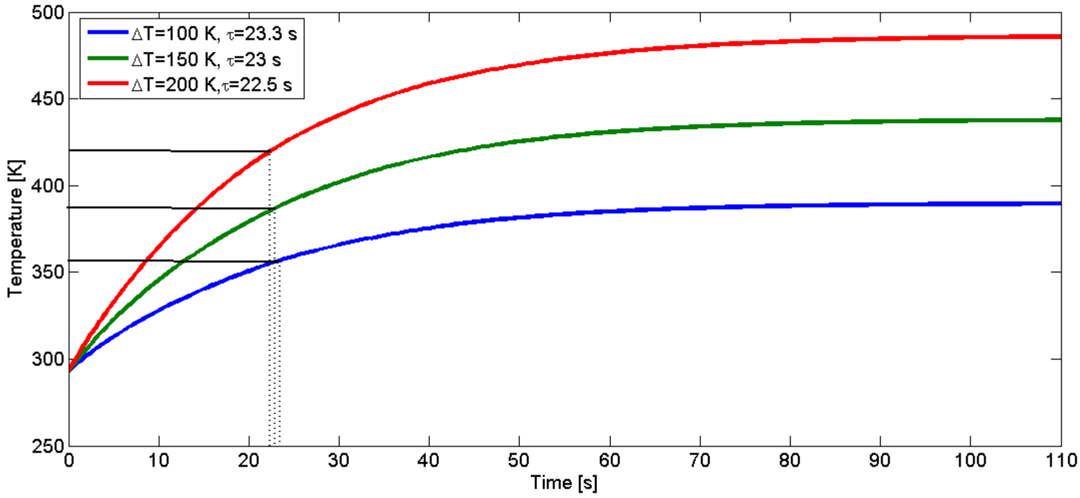

Figure 2.14: Influence of the step of temperature, simualtion obtained with Comsol ®. The variation of the temperature as a function of the time is taken at the interface between the Si layer and the SiO_2DM layer.

A last parameter for which it is interesting to study the influence is the value of the step of temperature. On figure 2.14, we can see the Comsol ® simulations obtained for a step of 100 K, 150 K and 200 K. As the initial temperature is always 293.15 K, the final temperature reached will be 393.15 K, 443.15 K and 493.15 K for a step of 100 K, 150 K and 200 K respectively. As a consequence, we have to change the value of the heat flux coming from the substrate layer. Therefore, as the final temperature varies, the temperature corresponding to the time $t = \tau$ is not the same for the three steps. But as we can see on figure 2.14, the time constants obtained for these steps are really close to each other and the error is about 2%.

2.4.2 Die heated by the embedded micro-heater

The case where the die is heated by the embedded micro-heater is studied. This case is different than the previous one because the heat source in embedded in the die. Therefore, the heat does not only flow in one direction but flows in the direction of the top of the die, which is the passivation layer and in the direction of the substrate.
In a first time, it is assumed that there are two convection resistances, one between the passivation layer and the air and another one between the substrate layer and the air, both having a convection coefficient of 23.54 $[W/(m^2.K)]$ as it is explained in section 2.3.1. The sidewalls remain insulated. One way to know the power generated by the micro-heater in the die, is by using the following equation [25]:

$$q = \frac{\Delta T}{R_{tot}} \tag{2.16}$$

Where q is the power expressed in W. As shown previously, the convection resistances are big in comparison with the other ones and in steady state, they are in parallel. Therefore, the heat flow required to reach a step of 150 K is:

$$q = \frac{150}{6761} = 22\ mW$$

In Comsol ® , the heat flowing through the die is expressed in $[W/m^2]$, therefore, we have to divide the obtained value by the surface of the micro-heater. This last one is a cylinder with a thickness of 500 nm and a diameter of 100 μm. Finally, we obtain a heat flow of 348399 W/m^2.

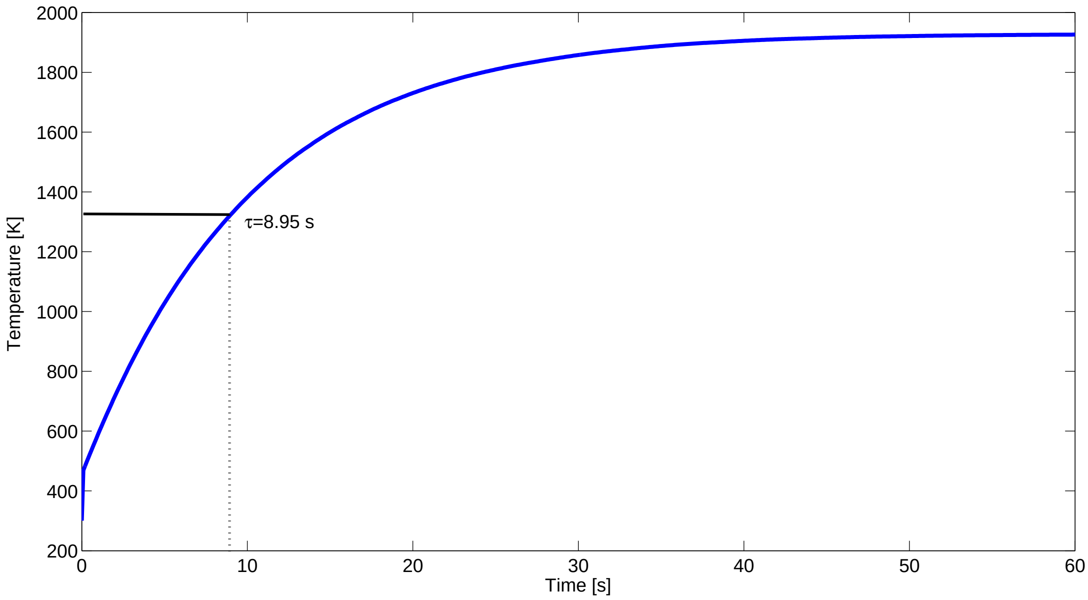

Figure 2.15: Temperature in the diode as a function of time, simulation obtained with Comsol ® for the die shown on figure 2.2 when it is heated by the embedded micro-heater and it is assumed that there are two interfaces with the air

On figure 2.15, we can see the variation of the temperature in the diode as a function of the time when there is convection at two interfaces: between the passivation layer and the air and between the substrate layer and the air. But as it can be seen on figure 2.15, the final temperature reached by the diode is approximately 1900 K which is much higher than the targeted temperature, 443 K.

One solution to explain this difference is that we considered convection between the substrate and the air but in reality, the die is fixed on a package, which can be considered as a heat sink, therefore the main transfer mechanism in the substrate is conduction rather than convection. As a consequence we can assume that most of the heat will flow through the substrate layer in the heat sink and we can consider that the temperature at the bottom layer of the substrate is 293 K. As only the convection resistance from the passivation layer remains, the power required to heat the device will decrease. By still requiring a convection coefficient of 23.54 and a final temperature of 443 K, by using equation (2.16), we obtain $q = 11.9\ mW$ and the heat flow is 188452 $[W/m^2]$.

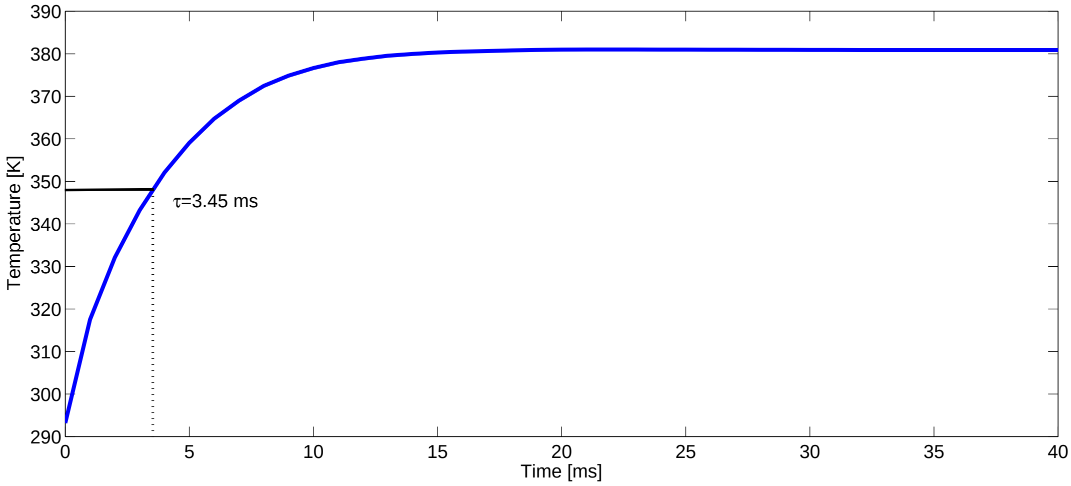

Figure 2.16: Temperature in the diode in function of the time when all the heat flows through the substrate layer. simulation obtained with Comsol ®

On figure 2.16, we can see the temperature in the diode as a function of the time when it is considered that all the heat flows through the substrate layer and as a consequence, the temperature of the substrate layer is 293 K, like the temperature of the air. This time, we can see that the reached temperature is below 443 K and the time constant is 3.45 ms.

This case is closer to the reality but it is not right because the heat will flow in the package and therefore, the temperature at the interface between the substrate and the package will not be exactly 293 K. The package can be represented by a metallic layer of arbitrary thickness and thermal conductivity. The thickness is fixed to 100 μm and the thermal conductivity is selected to reach the desired temperature, 443 K, in stationary case.

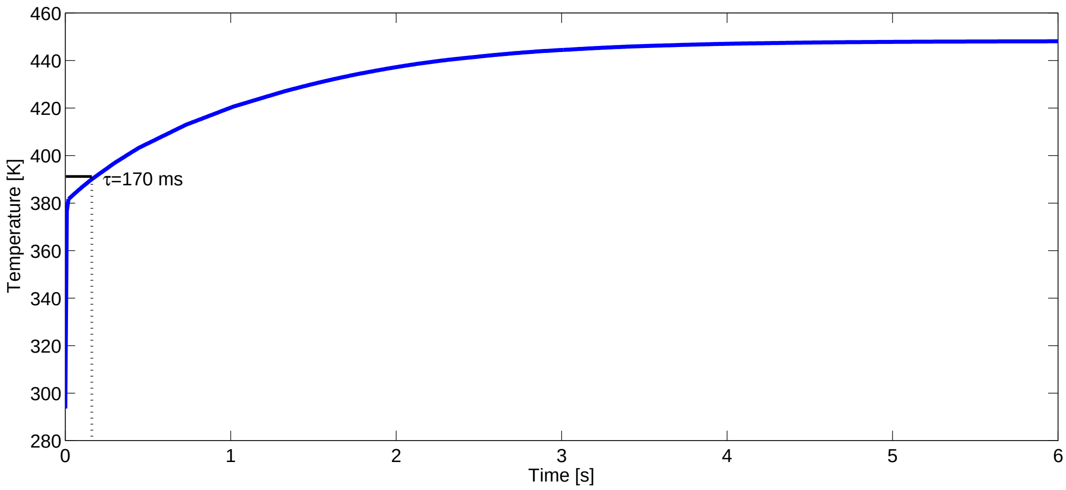

Figure 2.17: Temperature in the diode when the resistance of the package is taken into account and the bottom of the package is considered to be at 293 K. Simulation obtained with Comsol ®

On figure 2.17, we can see the temperature in the diode as a function of the time when a resistance is taken into account to represent the package layer. This resistance was artificially fixed to 500 Ω in order to obtain a temperature of 448 K, in the diode, which is really close to the desired temperature, 443 K. It can be seen that for a temperature of 380 K, the curve is bent and the value of the slope decreases rapidly.

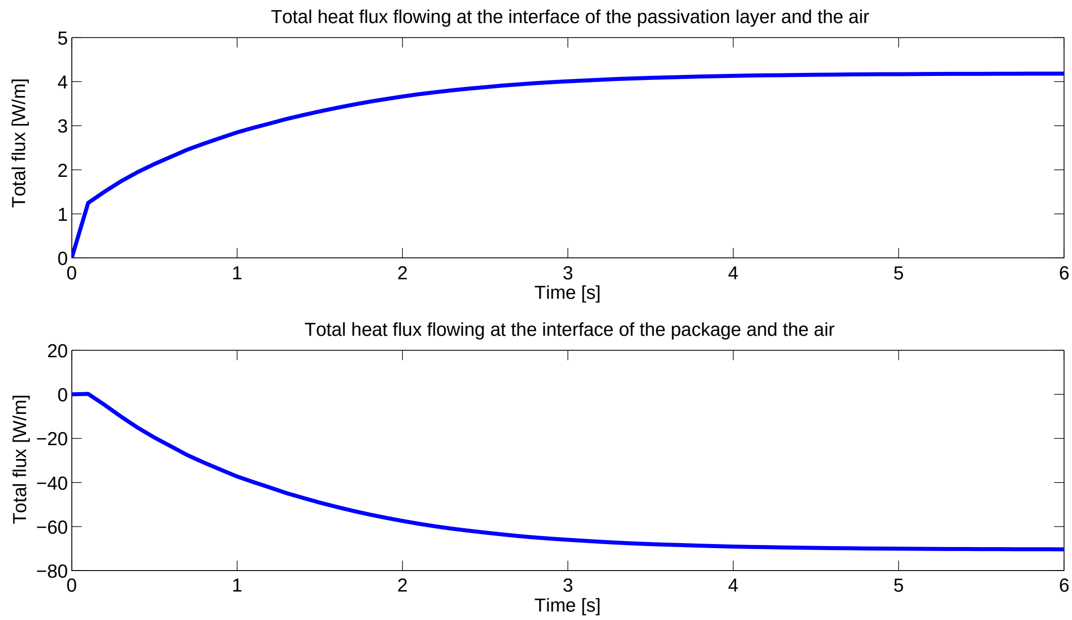

Figure 2.18: Flux at the both interfaces with the air as a function of time

We decided to the look at the total heat flux at both interfaces with the air. We can see that at the same time, both curves are bent. This can be explained by the fact that it is ultra fast, a few ms, to heat all the die and the diode but as the resistance of the package layer is high in comparison with the resistance of the other layer, the time needed to heat all the package is increased and therefore influence the time constant of the die.

This approximation is the closest to reality but is not true because it does not account for leak flux, in x=0 and x=2 mm, and if we want to simulate exactly the thermal model of the die, we also have to simulate the entire thermal model of the package which is not known.

One solution which could improve the curve is to study the influence of the meshing.

Influence of the meshing

As for the case when the die is heated by a power circuit, we will study the influence of three different meshing: *extremely coarse*, *normal* and *extremely fine*.

Type of meshing	Extremely coarse	Normal	Extremely fine
Degree of freedom	113359	166204	301345
Domain elements	55263	81516	148909
Boundary elements	15661	16711	17577
Maximum element size [m]	6.6×10^{-4}	1.3×10^{-4}	2×10^{-5}
Minimum element size [m]	10^{-4}	6×10^{-7}	4×10^{-8}
Maximum element growth rate	2	1.3	1.1
Curvature factor	1	0.3	0.2
Resolution of narrow regions	0.9	1	1
Computation time [s]	116	151	251

Table 2.3: Parameters of the meshings used in Comsol ® simulations

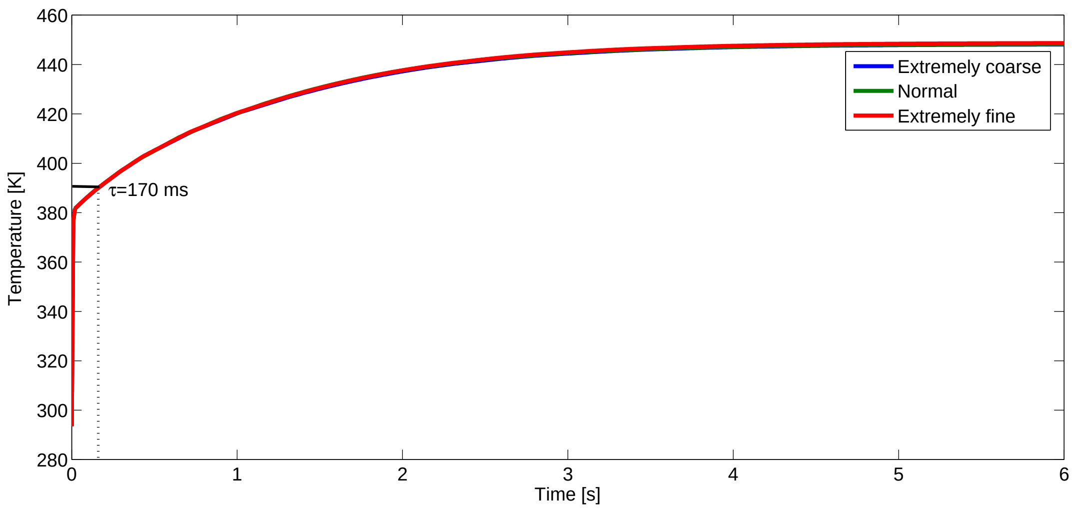

Figure 2.19: Influence of the meshing on the time response. The variation of the temperature as a function of the time is taken at the interface $Si - SiO_2DM$. Simulation obtained with Comsol ®

By looking on figure 2.19, we can see that using a more precise mesh does not improve the bent of the curve. Moreover, when we look at values given in table 2.19, we can see that the time of simulation is divided by two when using the *extremely coarse* mesh instead of using the *extremely fine* mesh. For that and reason and because the bent of the curve is not influenced by the meshing, we will use the *extremely coarse* mesh.

2.5 Thinned die

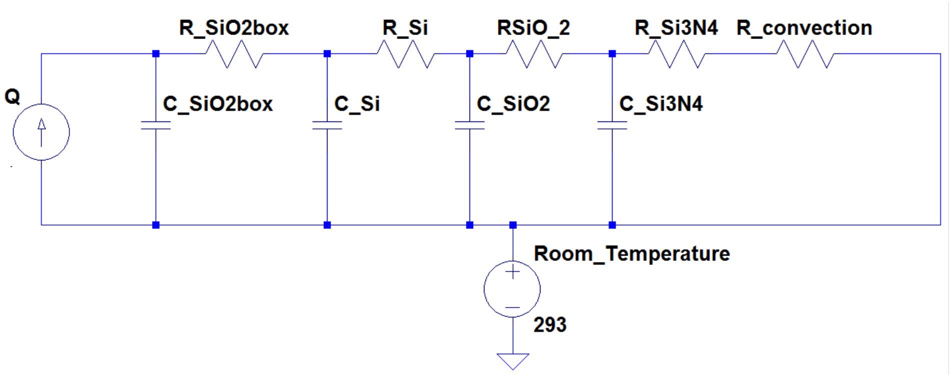

(a) Physical RC circuit

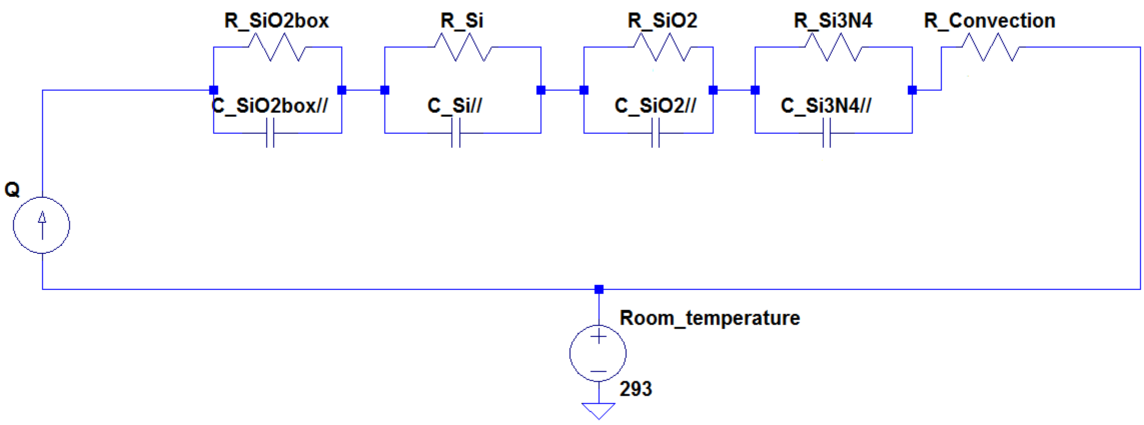

(b) Equivalent circuit

Figure 2.20: RC thermal circuits applied to the special case of die shown in section 2.2.2

On figure 2.20, we can see both equivalent circuits corresponding to the design shown on figure 2.3, where the heat comes from the power MOSFET and flows through the die by first heating the SiO_2box layer, then the Si diode, then the SiO_2 layer and finally the passivation layer.
The metallization is not taken into account in a first time because we consider the heat transfer along the z axis in the centre of the device, in x=1 mm.
In this case, we do not have to add an aluminium layer to simulate the power device. Indeed, the layer which is glued on the power MOSFET is uniform and is the SiO_2box. As a consequence, the heat will be the same through all the layer. For this part, we only focus on the heat transfer through the die. The simulation with the thermal model of the power transistor and the die will be done in chapter 3.

2.5.1 Computation of resistance, capacitances and equivalent capacitances

We can now compute the value of the resistances and capacitances on circuit 2.20.(a) by using the values given in table 2.1 and the thickness of the different layers given on figure 2.3. As the diameter of the diode is 200 μm, its cross-section area is $\pi \times 10^{-8}$ and for the other layers, as the diameter of the die is 2 mm, their cross-section area is $\pi \times 10^{-6}$. Using all of these informations, and equations (2.11), (2.12) and (2.13), we find the following values:

- $R_{Si0_2box} = 0.227\ K/W$

- $R_{Si} = 0.06\ K/W$
- $R_{SiO_2} = 0.909\ K/W$
- $R_{Si_3N_4} = 7.96 \times 10^{-3}\ K/W$
- $R_{Conv} = 13522\ K/W$
- $C_{Si0_2box} = 5.045 \times 10^{-6}\ J/K$
- $C_{Si} = 1.28 \times 10^{-8}\ J/K$
- $C_{SiO_2} = 2.02 \times 10^{-5}\ J/K$
- $C_{Si_3N_4} = 3.4 \times 10^{-6}\ J/K$

The value of resistances and capacitances are known for circuit 2.20.(a) so we would like to apply equation (2.10) to compute the equivalent capacitances. By using the method described in section 2.4.1 and values of resistances and capacitances previously computed, we find:

- $\tau_{SiO_2box} = C_{SiO_2box} \times R_{eq} = 68\ ms$ and $C_{SiO_2box//} = 299.6 \times 10^{-3}\ J/K$
- $\tau_{Si} = 0.173\ ms$ and $C_{Si//} = 2.88 \times 10^{-3}\ J/K$
- $\tau_{SiO_2} = 273\ ms$ and $C_{SiO_2//} = 0.3\ J/K$
- $\tau_{Si3N4} = 45.9\ ms$ and $C_{Si3N4//} = 5.78\ J/K$

2.5.2 Transient case

In the previous section, we computed the time constant for all the system. We can also compute the time constant of each material by considering one material independent of the other layers. The time constant for each material was computed in section 2.4.1, except for the SiO_2 layer, which is:
$\tau_{SiO_2} = 18.4\ \mu s$
Once the SiO_2box layer is heated, the silicon diode takes 0.77 ns to heat up. As it was explained previously 2.4.1, the effective time constant of the global circuit is mostly influenced by the highest capacitance and highest resistance.

2.5.3 Circuit at equilibrium

As we have the same value of h than for circuit shown on figure 2.5, we can apply the method described in section 2.4.1. Therefore, we find the following values:

- $T_{SiO_2box-Si} = 442.9974803\ K$
- $T_{Si-SiO_2} = 442.9968143\ K$
- $T_{SiO_2-Si_3N_3} = 442.9867244\ K$
- $T_{Si_3N_4-air} = 442.986636\ K$

We can conclude that once the thermal circuit will be in the stationary case, the temperature through all the material is approximately the same.

2.5.4 LTSpice simulation

In a first time, the equivalent RC thermal circuit shown on figure 2.20.(a) is simualted with LTSpiceIV ®.

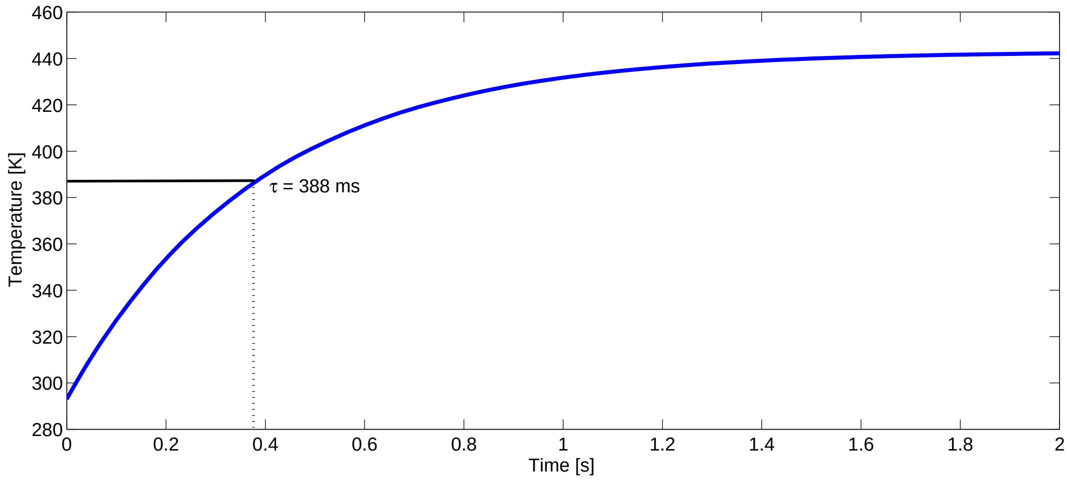

Figure 2.21: Time response of RC thermal circuit obtained with LTSpiceIV. The variation of the temperature in function of the time is taken at the interface between the diode and the SiO_2 layer

On figure 2.21, it can be seen that the time constant for all the system is 388 ms. If we look at the time constant computed for each material in section 2.5.1, we notice that if we add all the time constants, we obtain a similar value to the one obtained with the LTSpice simulation.

2.5.5 Comsol ® simulations

The time constant of the system is computed by simulating the device shown on figure 2.3 in Comsol ® .

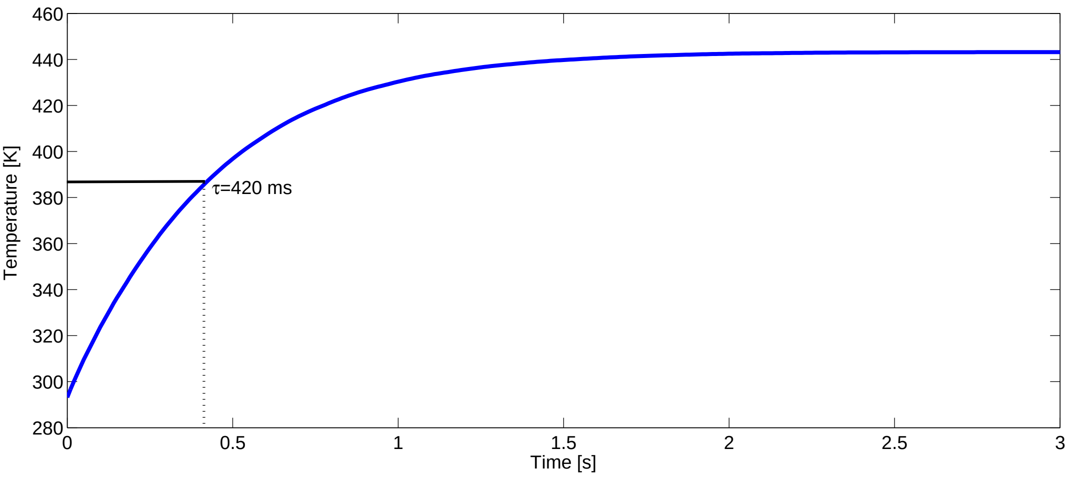

Figure 2.22: Time response of sensor showed on figure 2.3. Simulation obtained with Comsol ®. The variation of the temperature in function of the time is taken at the interface between the diode and the SiO_2 layer

On figure 2.22, the response time of the diode obtained with Comsol ® can be seen and this value is 420 ms. The parameters used are a convection coefficient of 23.54 $W/(m^2.K)$ and a heat flux of 3531 W/m^2 in order to reach a temperature of 443 K in stationary case.

Comparison with LTSpice simulation

By looking on figures 2.21 and 2.22, we can see that there is a difference in the obtained time constants. Indeed, the one obtained with Comsol ® is approximately 7 % higher than the one obtained with LTSpice. This difference is negligible and can be explained by the fact that for the LTSpice simulation, the values of resistances and capacitances of materials were computed analytically and therefore some approximations were made.

Now that we have the simulation of die shown on figure 2.3, we can vary some parameters of the simulation to evaluate their influence.

Influence of the meshing

The first parameter that will be studied is the meshing. Indeed, if the number of elements in the meshing increases, the solution should be more accurate. The different meshing are: *extremely coarse*, *normal* and *extremely fine*. Their characteristics can be seen in table 2.4.

Type of meshing	Extremely coarse	Normal	Extremely fine
Degree of freedom	50672	67111	80319
Domain elements	24373	32456	39036
Boundary elements	7525	8184	8269
Maximum element size [m]	3.3×10^{-4}	6.7×10^{-5}	10^{-5}
Minimum element size [m]	5×10^{-5}	3×10^{-7}	2×10^{-8}
Maximum element growth rate	2	1.3	1.1
Curvature factor	1	0.3	0.2
Resolution of narrow regions	0.9	1	1
Computation time [s]	39	42	45

Table 2.4: Parameters of the kind of meshing used in Comsol ® simulations

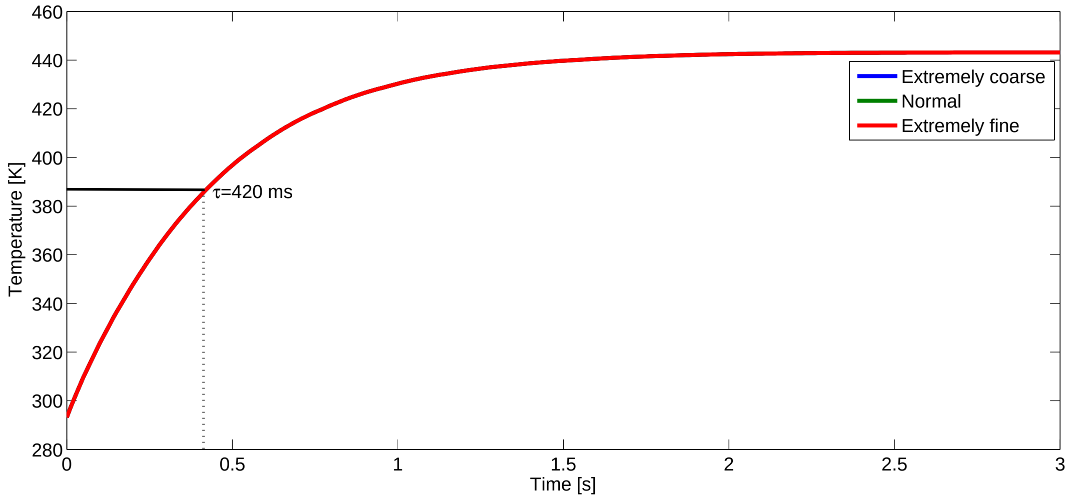

Figure 2.23: Influence of the meshing on the time response of the sensor. The variation of the temperature in function of the time is taken at the interface between the diode and the SiO_2 layer. Simulation obtained with Comsol ®

By looking the value of table 2.4, we can see that the *extremely fine* mesh should give a more accurate mesh but when we look at figure 2.23, we can see that the obtained curves overlay each others. We can conclude that the size of the meshing does not have influence on the obtained curve and this is the reason why we will use the *extremely coarse* meshing. Indeed, its number of degree of freedom is the lowest and its computation time is also the lowest.

Influence of the symmetry

The die shown on figure 2.3 is symmetric in the x-direction. As a consequence, we can simulate only the half of the die, from x=0 to x=1 mm and impose a symmetry condition in x=1 mm.

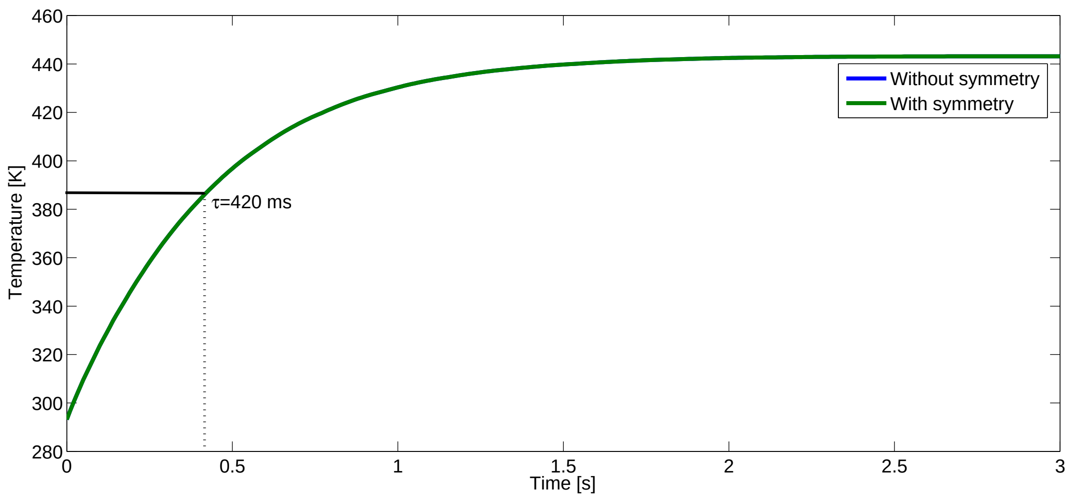

Figure 2.24: Influence of the symmetry on the time constant. The variation of the temperature in function of the time is taken at the $Si - SiO_2$ interface. Simulation obtained with Comsol ®

On figure 2.24, the influence of the symmetry on the time response can be seen. It can be concluded that this condition does not have any influence as the two curves overlay. Using the symmetry condition allows to reduce the computation time of 4 s when the *extremely coarse* meshing is used.

Influence of the metallization

A third parameter which can influence the solution is the presence of tungsten metallization, which can be seen on figure 2.3.

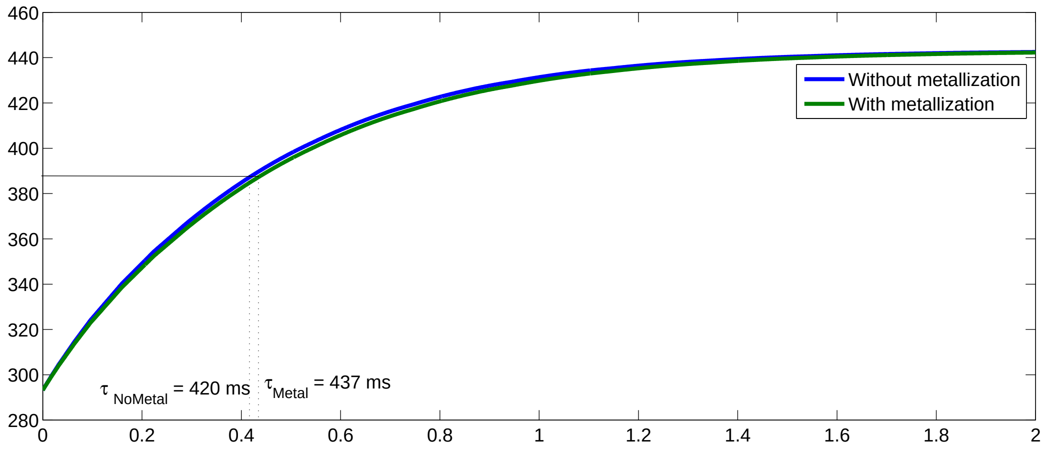

Figure 2.25: Influence of the metallization on the time response. The variation of the temperature in function of the time is taken at the $Si - SiO_2$ interface. Simulation obtained with Comsol ®

On figure 2.25, we can see the influence of the metallization on the time response of the diode. We can see that without the metallization, the time response is 420 ms and with the metallization, the time response is 437 ms.The difference in time constants when using metallization or not is about 4 %, which is negligible. Therefore, the initial hypothesis to not take into account the metallization in the equivalent thermal circuit is verified.

Influence of the micro-heater

A parameter that we would also like to study is the consequence if a micro-heater is added on the schematic of figure 2.3. In order to analyse this effect, we add a tungsten micro-heater, having the same dimensions and the same distance from the diode that what can be seen on figure 2.2.

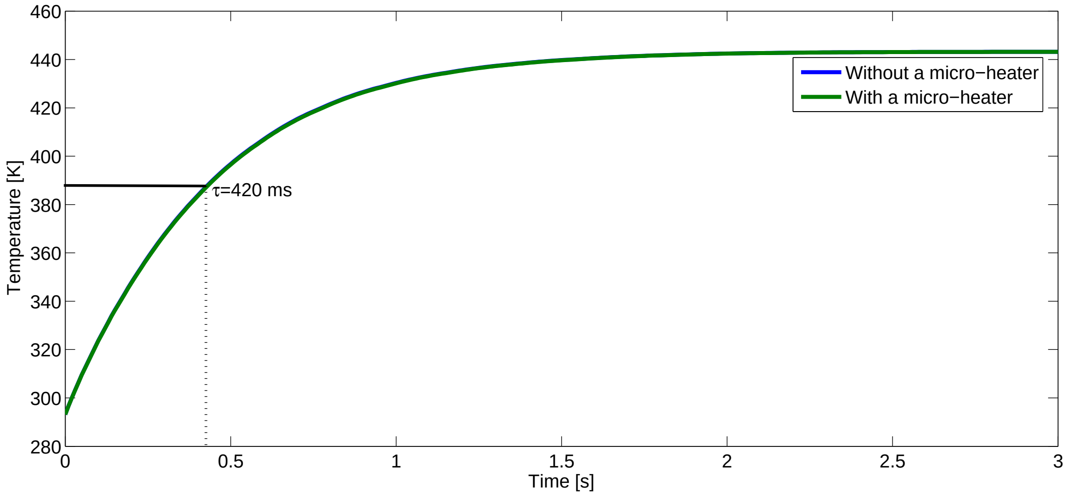

Figure 2.26: Influence of a tungsten micro-heater on the time response. The variation of the temperature in function of the time is taken at the $Si - SiO_2$ interface. Simulation obtained with Comsol ®

On figure 2.26, we can see the temperature in the diode when a tungsten micro-heater is added on the die shown on figure 2.3. We can see that both curves overlay each other so there is no influence of the micro-heater and this one can be neglected when the simulations are made. The initial hypothesis to not take into account the presence of the micro-heater for equivalent thermal circuit is verified.

Influence of the convection coefficient

When there is air around a structure, the convection coefficient vary from 2 to 25 $[W/(m^2.K)]$ [27], therefore, it is interesting to study the influence of this coefficient on the time response of the diode.

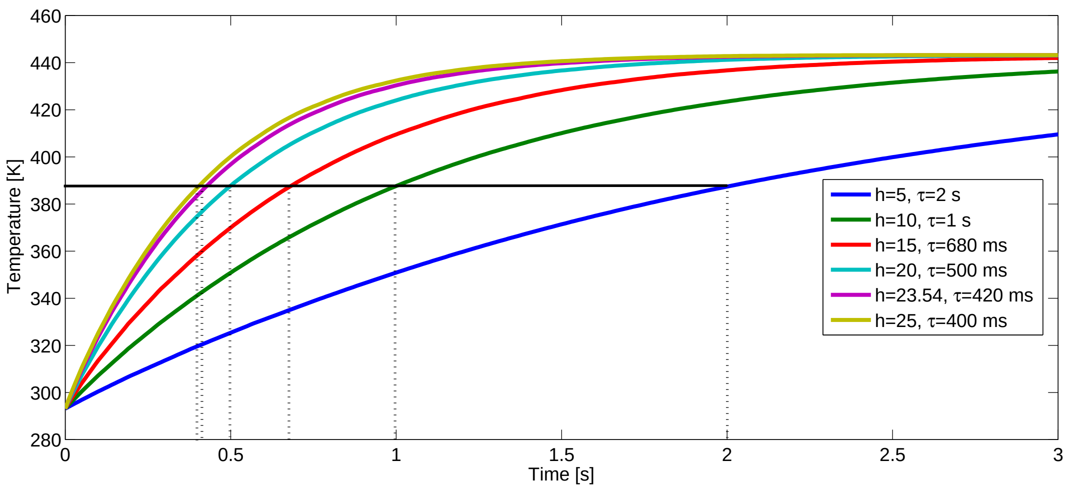

Figure 2.27: Influence of the value of convection coefficient on the time response of the diode. The variation of the temperature in function of the time is taken at the $Si - SiO_2$ interface. Simulation obtained with Comsol ®

On figure 2.27, we can see that if the value of h increases, the value of the time response decreases. We can see that for $h = 10$, the time constant is equal to 1 s and for $h = 23.54$, the time constant is 420

ms. Therefore, we can see that if the value of h is decreased by 13.54, the time response is increased by 150 %.
The value of Q is selected so that the final temperature reached is always the same, 443 K. Because $Q = h\Delta T$, the heat flux decreases when h decreases. As the heat fed to the die is lower, it will take more time for the die to reach the final temperature. This explains the result shown on figure 2.27.

Influence of the step of temperature

A last parameter which is interesting to study is the influence of the step of temperature on the time response of the diode.

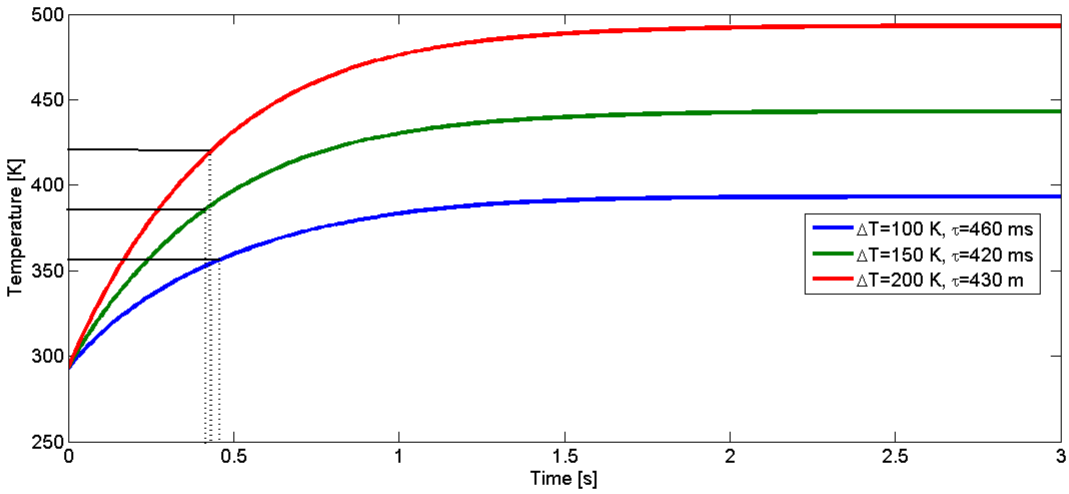

Figure 2.28: Influence of the step on temperature on time constant. The variation of the temperature in function of the time is taken at the $Si - SiO_2$ interface. Simulation obtained with Comsol ®

On figure 2.28, the influence of the step of temperature on the time constant of the system is studied. As the step of temperature of 150 K is a requirement, it is taken as the reference. By looking on the values of response time obtained on figure 2.28, it can be seen that the maximum error to reference time constant is less than 10 %. As a consequence, it can be concluded that the step of temperature does not influence the time constant of the system.

2.6 Comparison between the results obtained for the die with substrate and the thinned die

Type of die	Die with substrate heated by a power circuit	Die with substrate heated by an embedded micro-heater	Thinned die heated by a power circuit
Meshing used	Extremely coarse	Extremely coarse	Extremely coarse
Computation time [s]	45	116	39
Time constant [s]	23	0.17	0.42

Table 2.5: Comparison between the simulation of the different implementations of the temperature sensor

On table 2.5, we can see the most important parameters for the different kinds of dies studied. We can see that the die having the smallest time constant is the die with substrate heated by an embedded tungsten micro-heater. But as the goal of the work is to detect the variation of temperature of a power circuit, we have to compare the two dies heated by a power circuit.
We can see that the time constant of the thinned die is approximately 50 times smaller than the one for the die with substrate. This can be explained by the fact that the substrate layer is very thick in comparison with the thickness of the membrane and therefore, it takes more time to heat the diode.
If we look to the parametric study made in section 2.4.1 and 2.5.5, we can see that both dies behave in the same way, which means that when the value of the convection coefficient increases, the time response of the die decreases. We can also see that the step of temperature does not influence the time response as well as the presence of metallization or not.

Chapter 3

Power Circuit

This chapter focusses on the power circuit, indeed the power circuit is an important part of this work as the temperature sensor will be glued on it in the order to detect a variation of temperature. In a first time, the power circuit will be chosen and then its working principle will be explained. Finally, the thermal model of the chosen power circuit will be studied and simulated in combination with the thermal models of the temperature sensors.

3.1 Choice of the power transistor

As the temperature will be glued on a power transistor, it is important to understand the working principle of this transistor as well as its thermal model. Before, we need to choose either the power bipolar junction transistor (BJT) or the power MOSFET transistor.
The power MOSFET is chosen due to the limitations of the BJT, which are the followings [30]:

1. The bipolar transistor is driven in current and to keep the device in its ON state, it is necessary that the base current is equal to one-fifth of the collector current.
2. As a consequence, the required base reversed current is higher to switch off the device.
3. In a BJT, both electrons and holes participate in conduction, moreover, as holes have longer carriers lifetime, it implies that the switching speed is lower than for a power MOSFET with similar size.
4. The last limitation of the BJT is that the forward voltage drop decreases with increasing temperature. As a consequence, it is difficult to have several BJT in parallel.

In comparison, the advantages of the power MOSFET are the followings [30]:

- They have a faster switching frequency than the BJT, therefore, they have less switching losses.
- They can support applications with high current and high voltage.
- They can be put in parallel because the forward voltage drop increases with an increasing temperature, this ensures a uniform distribution of the current through the different components.

The advantage of BJT compared to the MOSFET is that at high breakdown voltage, >200 V, the voltage drop for the on-state of the power MOSFET is higher than the one for a power bipolar transistor with similar size and similar range of voltage [30].

3.2 Working principle of power MOSFET

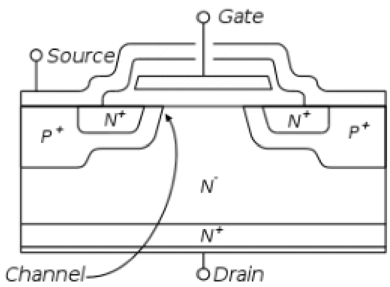

Figure 3.1: Cross-section of a power MOSFET [31]

On figure 3.1, we can see the cross-section view of a power transistor. The power MOSFET is also called *Vertical Diffused MOS* because when the transistor is ON, the current flows from the source to the drain, vertically through the device unlike planar MOSFET where the current flows from the left to the right or inversely.

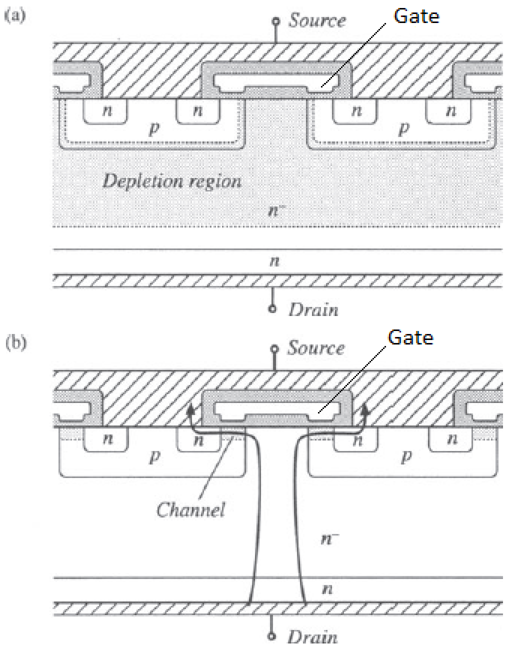

Figure 3.2: Off-state (a) and on-state (b) of a power MOSFET [32]

On figure 3.2.(a), the off-state of a power MOSFET can be seen and the voltage between the drain and the source appears across the $p - n^-$ junction. In this case, both p-n junctions are reversed-biased. On figure 3.2.(b), the on-state of the power MOSFET can be seen. It appears when the voltage between the gate and the source is higher than the threshold voltage as a consequence, a channel forms below the gate. The drain current flows through the n^- region, the channel, the n region and goes out through the source contact. For this operating mode, for which $v_{ds} \geq 0$ both p-n and $p - n^-$ junctions are reversed-biased [32].
When the transistor is in on-state, it shows a resistive behaviour between the drain and source terminal. The equivalent resistance is called $R_{DS_{ON}}$, which is the resistance seen between the drain and source terminals during the on-state of operation. The value of this resistance is given by the following equation:

$$R_{DS_{ON}} = R_{source} + R_{channel} + R_{n^{-}region} + R_{nregion} + R_{drain}$$

When the breakdown voltage is significantly increased, the value of the on-resistance is dominated by the resistance of the n^- region. This on-resistance increases rapidly because there are no minority carriers to modulate the conductivity [32].
The $p - n^-$ junction is the body the diode and it is an effective diode in parallel with the channel. This diode is forward biased when the applied voltage v_{ds} is negative, which is not allowed for a nMOS.

3.3 Thermal model of a power transistor

3.3.1 Thermal resistances

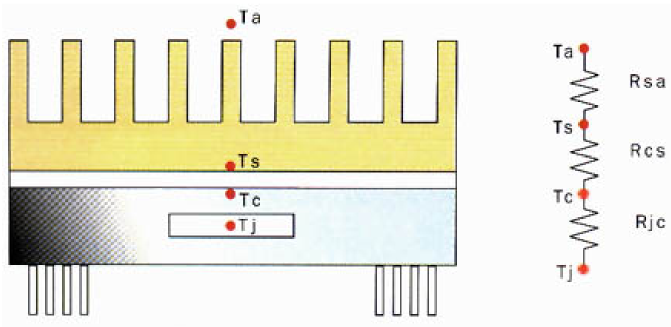

Figure 3.3: Junction, case and sink temperature of a power MOSFET [33]

On figure 3.3, the different resistances given in [34] can be seen as well as their location of the power MOSFET. The meaning of these resistances can be found [35]:

- $R_{\theta JC}$, junction-to-case resistance, is the resistance between the junction and the case, it is a small layer of copper used for cooling by conduction with a radiator
- $R_{\theta CS}$, case-to-sink resistance, is the resistance between the case and the sink, used for example if a heat sink is glued on the power MOSFET. The sink temperature being the point closest to the power MOSFET, the value of this resistance also represents the glue used to stick the sink
- $R_{\theta JA}$, junction-to-ambient resistance, is the resistance between the junction and the air when there is only natural convection

3.3.2 Power derating curve

A main parameter for the thermal model of a power transistor is the *power derating curve*. The power dissipation as a function of the temperature, defined the junction temperature under which the power MOSFET should always operate [36].

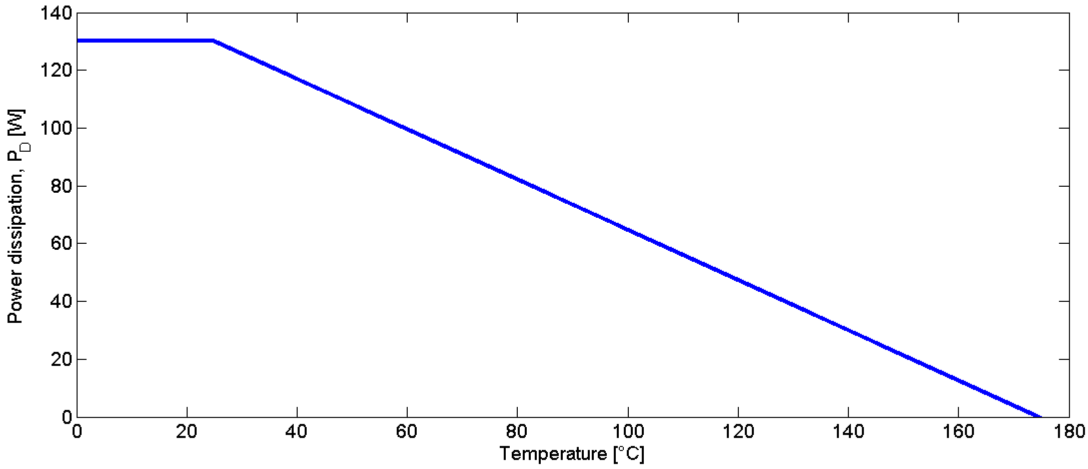

Figure 3.4: Power derating curve of power transistor with channel N (IRF540NPBF), obtained with value given in [34]

The power derating curve shown on figure 3.4 has been obtained with the value given in the datasheet [34] of the power transistor IRF540NPBF which has a N channel. Until 25 °C, the power dissipation is constant and the value is directly given in the datasheet. Then in order to be able to draw all the curve, we have to use the *derating factor* given in [W/°C] and it means that each time the temperature is increased by one Celsius degree, the power dissipation is reduced by the derating factor.

3.3.3 Safe operating area

When a voltage pulse is applied on the gate of the power MOSFET, the maximum alternating drain current is 110 A, which is much higher than the maximum continuous current, 33 A. We have to pay attention to not damage the device, therefore we have to define the *safe operating area*.

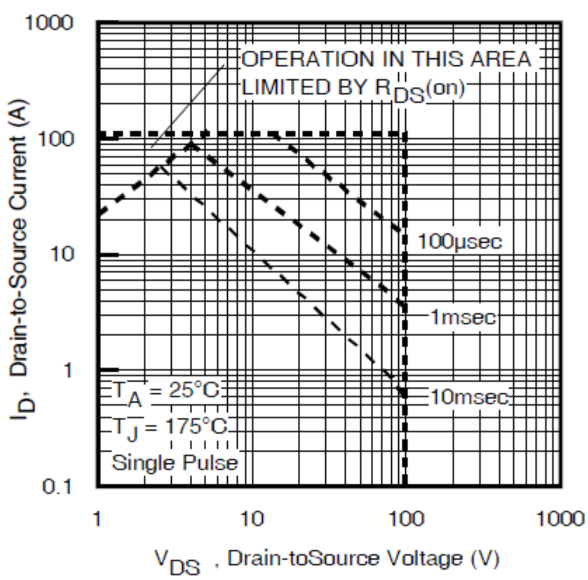

Figure 3.5: Safe operation area of power transistor used, IRF540NPBF [34]

On figure 3.5, we can see the safe operating area of the power transistor IRF540NPBF. The maximum drain-to-source voltage is limited by the breakdown voltage and the maximum current is limited by the the *pulsed drain current*. On the left side, the safe operating are is limited by the $R_{DS(ON)}$ resistance which in this case is equal to 44 $m\Omega$ [34]. On the right side, the safe operating area is limited by the increase of temperature which is induced by the power dissipation as it can be seen on figure 3.4, as a consequence, it is impossible to operate at the maximum voltage and the maximum current at the same time. But for a pulse of short duration, order of μs, a higher current and voltage can be simultaneously applied, depending on the pulse width. The current is determined with the transient thermal impedance [35].

3.3.4 Switching characteristic

If a voltage pulse is applied on a power transistor, it is important to know the time it takes to the the MOSFET to react to the pulse signal. This behaviour is given by the switching characteristics.

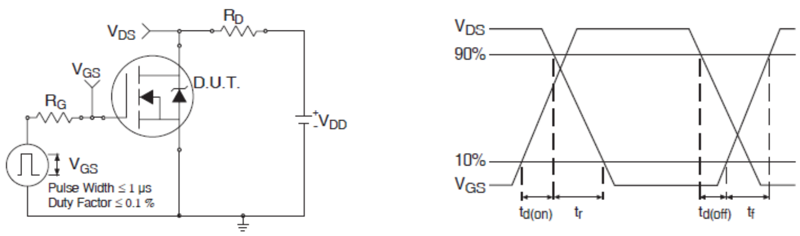

(a) Switching test circuit (b) Switching waveforms

Figure 3.6: Switching characteristic of the power transistor IRF540NPBF [34]

On figure 3.6, we can see the test circuit and the waveforms obtained for the power transistor with channel N which is used for this work. The switching characteristic depends on the gate resistance, R_G and on the capacitances: input capacitance, C_{iss} and reverse transfer capacitance, C_{rss} [35] and R_D is the load resistance. The different parameters, $t_{d(on)}$, t_r, $t_{d(off)}$ and t_f are explained just below [35]:

- $t_{d(on)}$ is the turn-on delay time, it is the time when the gate-to-source voltage (V_{gs}) increases over 10 % of the gate drive voltage and the drain current rises over 10 % of the specified current. In $t = t_{d(on)}$, the gate-to-source voltage is equal to the threshold voltage. This period is controlled by the time constant given by $R_G \times C_{iss}$.
- t_r is the rise time, it is the time that it takes for the drain current to rise from 10 % to 90 % of the load current. This value depends on the threshold voltage, the transconductance and the time constant given by $R_G \times C_{rss}$.
- $t_{d(off)}$ is the turn-off delay time, it is the time when the gate-to-source voltage decreases below 90 % of the gate drive voltage when the drain current drops below 90 % of the load current. It depends on time constant give by R_G and C_{iss}.
- t_f is the fall time, it is the time that it takes for the drain current to fall from 90 % to 10 % of the load current. The value of the fall time is influenced by the same parameters than for the rise time.

The values of these parameters found in the datasheet [34] are: $t_{d(on)} = 11\ ns$, $t_r = 35\ ns$, $t_{d(off)} = 39\ ns$ and $t_f = 35\ ns$.

3.3.5 Thermal transient impedance

The thermal transient impedance is used when a pulse is applied on the power MOSFET. The value of the impedance depends on the duty-cycle D and the time during which the heat source is ON.

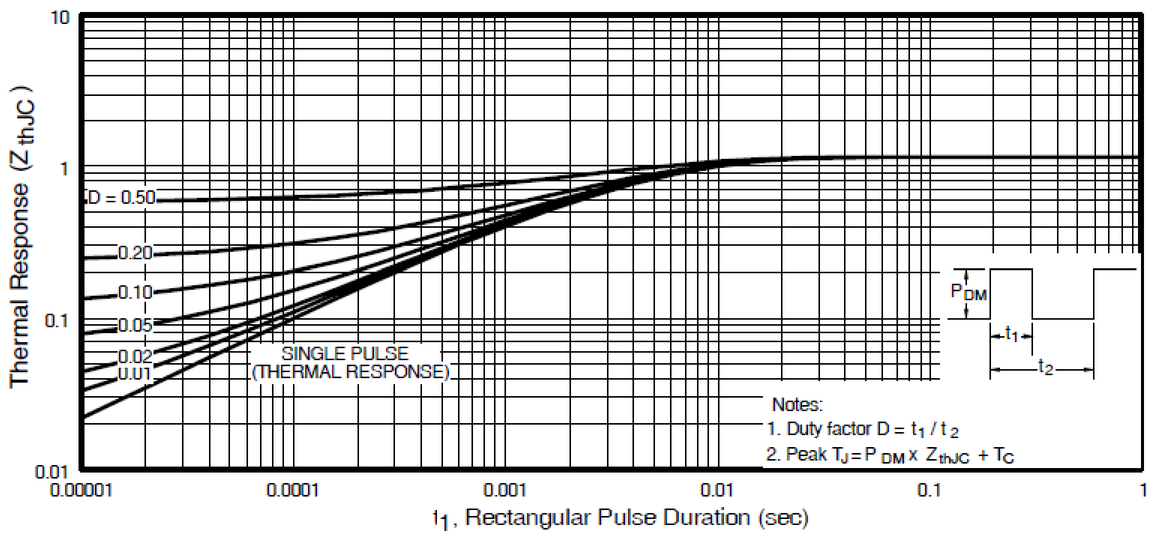

Figure 3.7: Thermal transient impedance of power transistor used, IRF540NPBF [34]

On figure 3.7, it can be seen that for a pulse width larger than 10 ms, the thermal impedance becomes equivalent to the value of junction-to-case thermal resistance which is 1.15 °C/W [34].

Determination of the transient thermal impedance [24]

As it can be seen on figure 3.7, the value of the thermal impedance depends on the duty-cycle, D, and the time during which the heat source, P_{DM}, is ON. During the time, t_1, the temperature next to heat source increases according to:

$$T(t) = P_{DM} \times R_{thJC} \left(1 - e^{-t/R_{thJC} \times C_{thJC}}\right) + T_{MIN} \times e^{-t/R_{thJC} \times C_{thJC}}$$

And the maximum temperature corresponding to the time $t_0 + t_1$, where t_0 is the time at which the heat source switches ON, is:

$$T_{MAX} = T(t_0 + t_1) = P_{DM} \times R_{thJC} \left(1 - e^{-t_1/R_{thJC} \times C_{thJC}}\right) + T_{MIN} \times e^{-t_1/R_{thJC} \times C_{thJC}}$$

When the heat source is off, temperature decreases according to the relationship:

$$T(t) = T_{MAX} \times e^{-t/R_{thJC} \times C_{thJC}}$$

Therefore, the minimum temperature corresponding to the time $t_0 + t_2$, where t_2 is the period of the signal, is given by:

$$T(t) = T_{MAX} \times e^{-(t_2 - t_1)/R_{thJC} \times C_{thJC}} = T_{MAX} \times e^{-t_1(1-D)/D \times R_{thJC} \times C_{thJC}}$$

Where $D = \frac{t_1}{t_2}$. Finally the maximum temperature is given by:

$$T_{MAX} = P_{DM} \times R_{thJC} \frac{1 - e^{-t_1/R_{thJC} \times C_{thJC}}}{1 - e^{-t_1/D \times R_{thJC} \times C_{thJC}}}$$

And the minimum temperature is given by:

$$T_{MIN} = P_{DM} \times R_{thJC} \frac{1 - e^{-t_1/R_{thJC} \times C_{thJC}}}{1 - e^{-t_1/D \times R_{thJC} \times C_{thJC}}} e^{-t_1(1-D)/D \times R_{thJC} \times C_{thJC}}$$

The mean value of the heat source is given by:

$$\bar{T} = P_{DM} \times R_{thJC} \times D$$

The thermal impedance is given by:

$$T_{MAX} = P_{DM} \times Z_{thJC}$$

Therefore, by using the expression for the maximum temperature, we find that the expression of the thermal impedance is:

$$Z_{thJC}(t_1) = R_{thJC} \frac{1 - e^{-t_1/R_{thJC} \times C_{thJC}}}{1 - e^{-t_1/D \times R_{thJC} \times C_{thJC}}}$$

Typical value of the transient thermal characteristics

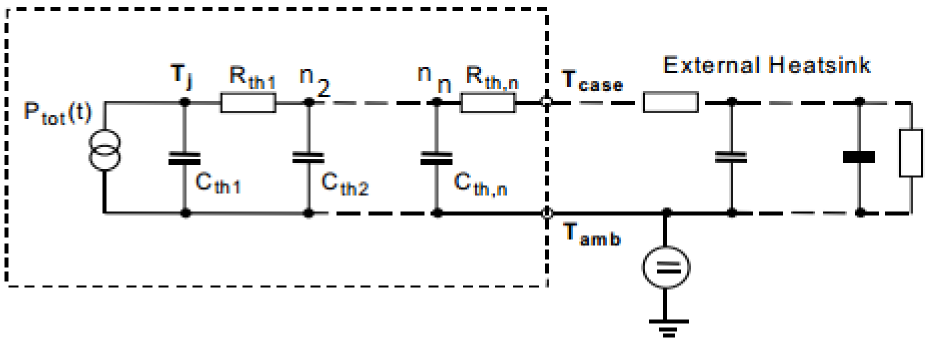

Figure 3.8: Thermal model of a power transistor [24]

On figure 3.8, we can see the thermal model of the power MOSFET which is framed by a dot line and then, we have to add the thermal model of the die for the application of this work. In spice simulation file for the power transistor IRF540NPBF [37], we find:

Thermal resistance [°C/W]	Thermal capacitance [J/°C]
$R_{thTJ-n2}$=0.158	$C_{thTJ-n2} = 0.00131$
$R_{thn2-n3}$=0.274	$C_{thn2-n3} = 0.001686$
$R_{thn3-TC}$=0.29	$C_{thTJ-n2} = 0.022562$

This means that for the power transistor IRF540NPBF, the n is equal to 3.

Combination of thermal model of the power transistor and the one of the dies

In chapter 2, the RC equivalent thermal circuit of the devices shown on figures 2.2 and 2.3 are studied and in the previous section the equivalent RC thermal model of the power transistor is analysed. As the device will be glued on the power MOSFET, we are now able to study the device formed by the die with substrate and the power MOSFET.

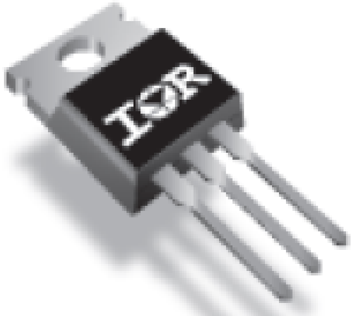

(a) Front side of the transistor [34]

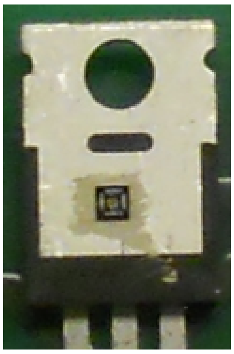

(b) Back side of the transistor with die glued on it

Figure 3.9: Front side and back side of the nMOS transistor used

On figure 3.9, both sides of the transistor used can be seen and on figure 3.9.(b), the temperature sensor glued on it. It is assumed that the heat flux generated by the power MOSFET is uniformly distributed through all its metallic surfaces. The ratio between the area of the die and the one of the MOSFET is approximately 1/65, which implies that the heat flowing through the die is 65 times smaller than the total heat generated by the power MOSFET.

Die with substrate

The RC thermal circuit of the device with substrate is combined with the one of the power MOSFET and is simulated with LTSpiceIV.

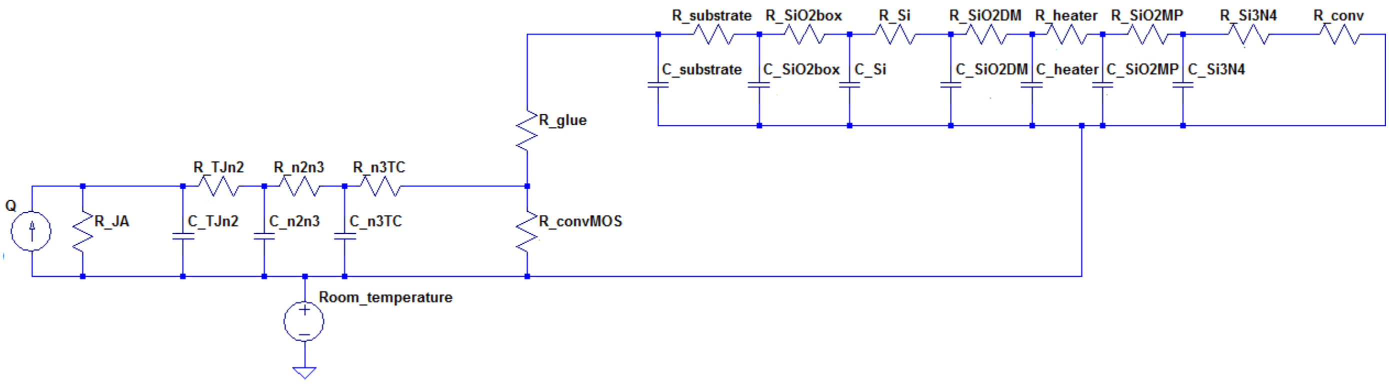

Figure 3.10: Combination of thermal circuit of the die with substrate and the MOS transistor

On figure 3.10, the complete thermal circuit of the power MOSFET and the die with substrate can be seen. R_{glue} is the resistance of the glue and is given in datasheet [34] as the case-to-sink resistance. The current flowing through the resistance $R_{convMOS}$ represents the heat generated by the power MOSFET which is not flowing in the die. In order to respect the ratio of 65, in stationary case, we have:

$$R_{convMOS} = \frac{R_{totdie}}{65} \simeq 208\ \Omega$$

With the R_{totdie} being the total resistance of the die, which is dominated by the convection resistance.

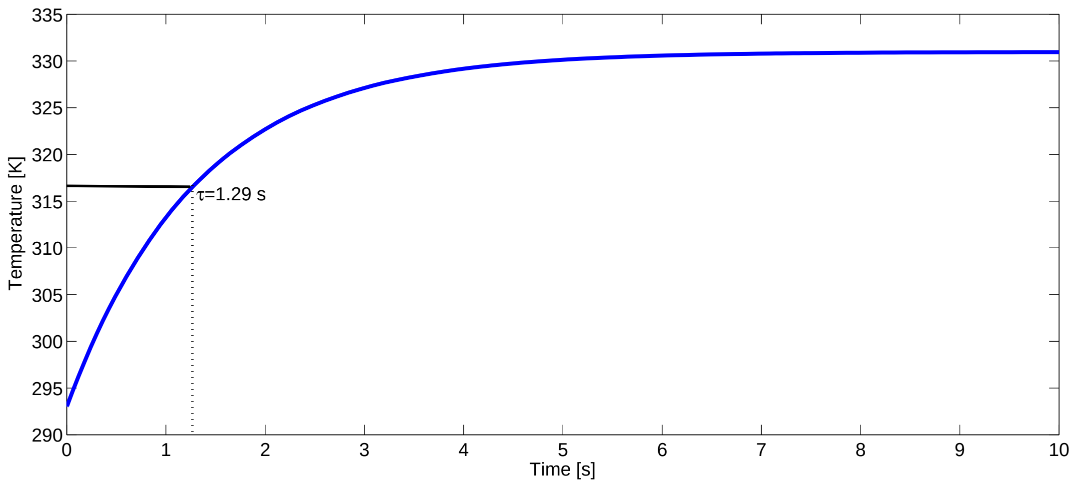

Figure 3.11: LTSpice simulation of the temperature of the diode in function of the time. The temperature is taken at the interface $Si - SiO_2DM$. The input heat source is equal to 0.8 W

On figure 3.11, the variation of temperature of the diode in function of the time can be seen. The maximum temperature reached is about 30 °C which correspond to measured temperature for the same conditions. The time constant is 1.29 s which is much lower than the one obtained in section 2.4.1. This value of response time can be explained by the fact that the thermal model of the power transistor is not exactly known.

Thin die

We can do the same analysis but this time when the die used is thinned down. The equivalent thermal circuit of all the device is:

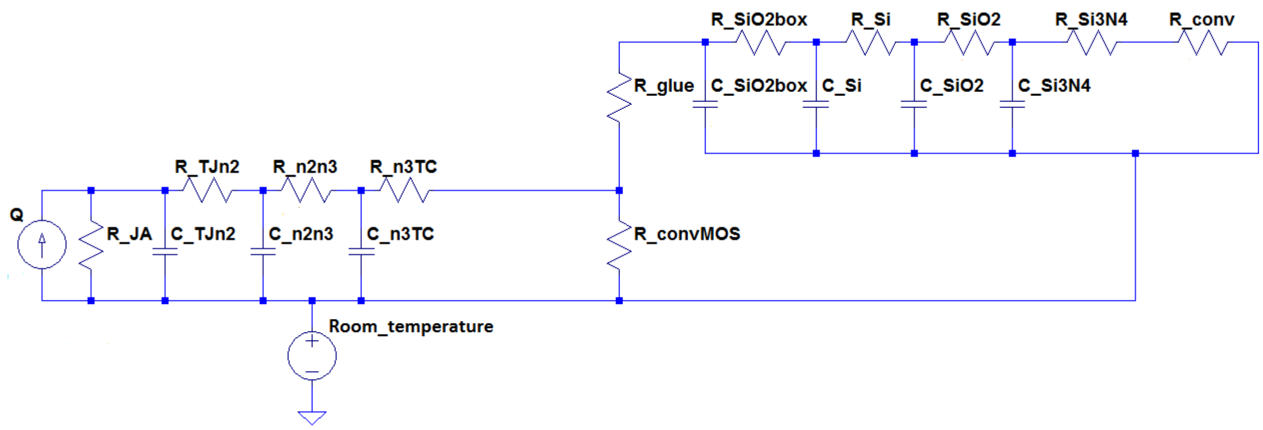

Figure 3.12: Combination of thermal circuit of the thin die with the one of the MOS transistor

The values of circuit shown on figure 3.12 are taken from section 2.5.1 and from the thermal model of the power transistor studied previously. The R_{glue} and $R_{convMOS}$ have the same meaning and value than for the case with the non thin die. This circuit is simulated with LTSpiceIV.

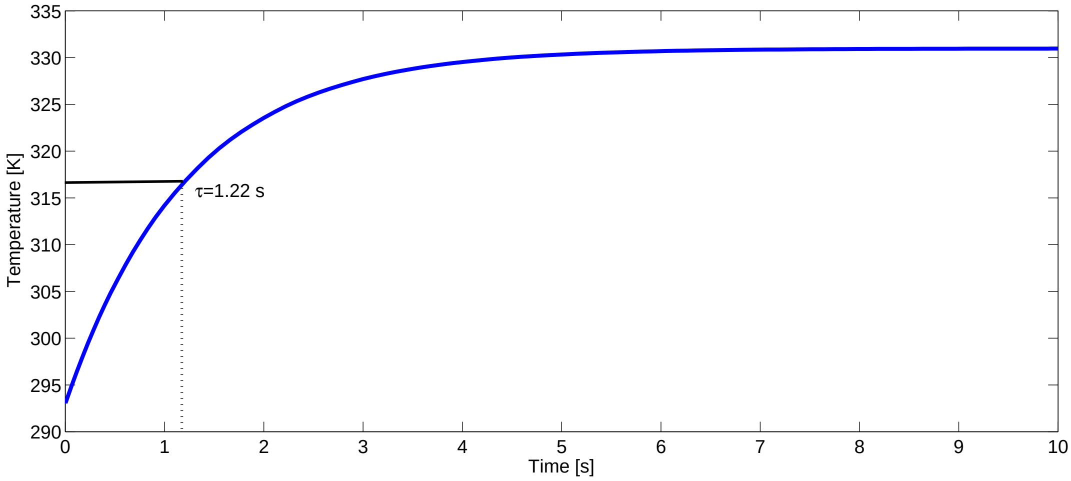

Figure 3.13: LTSpice simulation of the temperature of the diode in function or the time. The temperature is taken at the interface $Si - SiO_2$. The input heat source is equal to 0.8 W

On figure 3.13, it can be seen that the time constant is 1.22 s. When looking at the time constant obtained in section 2.5.5, using the thermal model of the transistor instead of heat source increases the response time of the system.

Comparison between die with substrate and thin die

By looking on the curves shown on figures 3.11 and 3.13, it can be seen that the two time constants are close to each other, 1.29 s and 1.22 s, respectively for the non thin die and the thin die. Therefore, we can conclude that the response time is not influenced by the thickness of the die anymore but is influenced by the thermal circuit of the power device.

Chapter 4

Thin film and transfer on a PCB

This chapter aims to study the thinning and transfer processes. Indeed, the heat transfer through the temperature sensor and that the thermal model of the power transistor are known. Before doing the measurements, the thinning and transfer processes have to be studied. The last part of this chapter will study the possibility of directly build a die on the final substrate.

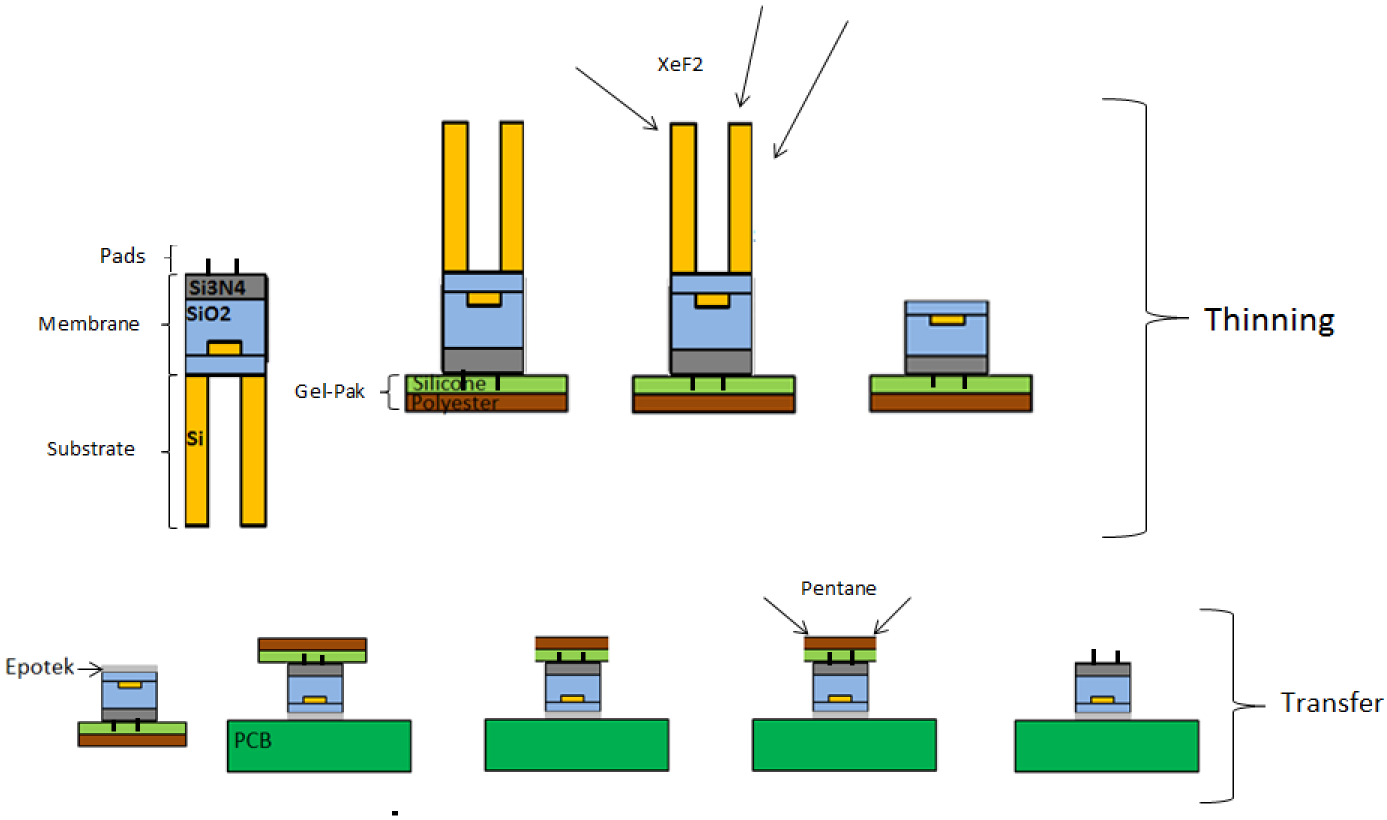

Figure 4.1: Thinning procees and transfer of the die

On figure 4.1, we can see all the steps to thin down a die and to transfer it on a PCB or another shelf. The steps will be described in the two following sections.

4.1 Thinning process

4.1.1 Gel-pak

The first step consists in the bonding on a sheet of *gel-pak*.

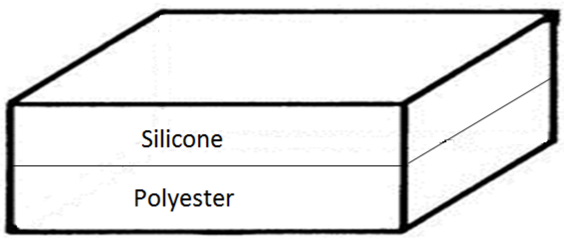

Figure 4.2: Sheet of Gel-Pak

As we can see on picture 4.2, the sheet of Gel-Pak is composed of a layer of polyester and another one with silicone. The surface below the polyester layer is adhesive and can be stick on a glass or something else. The chip is stick on the silicone layer by the *Flip-chip* technique, which means that the top side of the chip (the one which is the passivation layer) is glued on the silicone layer thanks to Van der Waals forces. The pads for the wire-bonding are on the passivation layer.

4.1.2 Chemical dry etching with xenon difluoride (XeF_2)

The xenon difluoride is chosen for the etching of the silicon because it is very selective [38]. Indeed, XeF_2 allows to remove the silicon without removing the oxide. Therefore, the die is flat after the etching.
The chemical reaction between XeF_2 and Si is given by the following equation [39]:

$$2\ XeF_2\ + Si\ \rightleftharpoons\ 2\ Xe\ + SiF_4 \tag{4.1}$$

With this chemical reaction, it can be seen that when the silicon is mixed with the xenon difluoride, it evaporates. In order to correctly etch the silicon, it is necessary to have between 80 and 100 cycles. It is better to do less cycles and then increase them because we do not want to have over-etching and removing SiO_2box layer. Each cycle goes on during 175 s with a pressure of 3,4 Torr for the XeF_2. Only the first cycle is longer because it is necessary to flush out the chamber.

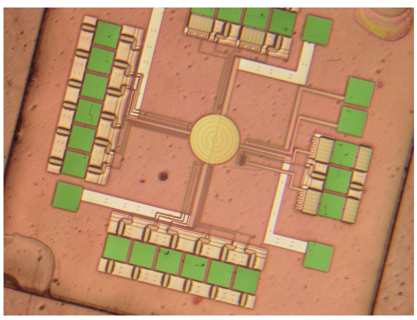

Figure 4.3: Backside of the chip after thinning process

On figure 4.3, we can see the result after the thinning process and we can observe that the substrate has been removed. This means that on figure 4.3, we see the pads of the die through the SiO_2box layer The thickness of the thin die is 5 μm instead of 400 μm.

4.2 Transfer of the thinned die

Once the die is thinned down, it is necessary to transfer it on the final substrate which can be a PCB, a power circuit for this application and so on. The first step is to put the glue *epotek* on the final substrate. This glue is a silver lacquer and becomes electrically conductive with an annealing. Before doing the annealing, it is necessary to do another flip-chip of the thin die to glue it on the power transistor. The minimum time for the annealing is one hour at 120 °C and three hours at 100 °C.
Mostly, when the epotek is dried, the noise is reduced. The last step of the transfer consists in removing the gel-pak from de substrate in order to be able to do the wirebonding or to use probes on the die. In a first time, we can cut the part of the gel-pak which is out of the die and then, pentane is used to remove Vander Waals forces.

The first critical step is to put the glue on the final substrate. If there is not enough epotek, it is possible that the die could not stick on the substrate. If there is too much glue, holes can be created below the die, which is unwanted because the die could be broken when removing the gel-pak.
The second step which is the annealing is quite easy to do but to be sure that the thin die glues on the final substrate, it is better to put a PCB over the device and apply a weight on it. We have to pay attention to have the same amount of forces applied everywhere on the die to be sure that it stays flat. We also need to pay attention to the weight of the load. If the load is too light, it is useless and the die should not be very well glued on the die but if the weight of the load is too heavy, the die could be flattened because it is only 5 μm thick.
Concerning the annealing, the time is also important. If the glue is not dried at the end of the annealing, it will not be possible to do the wirebonding or to use probes to do the measurements. Even if the *epotek* is electrically conductive.
The last part of the process is the most critical one because we have to remove all the gel-pak which cover the die but without break the die. When removing the gel-pak with a pliers, if the die is touched, we could break a diode, the micro-heater or another component of the die.

The transfer of a die which is not thinned down is less critical because we only need to put the epotek of the power circuit and then put the die on it. The wirebonding will always work because the die is sufficiently thick, 400 μm. Even if the glue is not totally dried, this will not have any influence.

4.2.1 Result of transfer

Transfer of the die with substrate

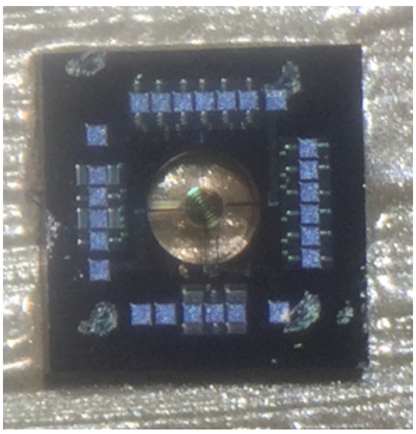

Figure 4.4: Transfer of the die with substrate on the power MOSFET

On figure 4.4, we can see the transfer of the die with substrate on the power transistor. We can see that all the die is well transferred and there is no broken part. The non flat part below the die is the glue *epotek*.

Transfer of the thin die

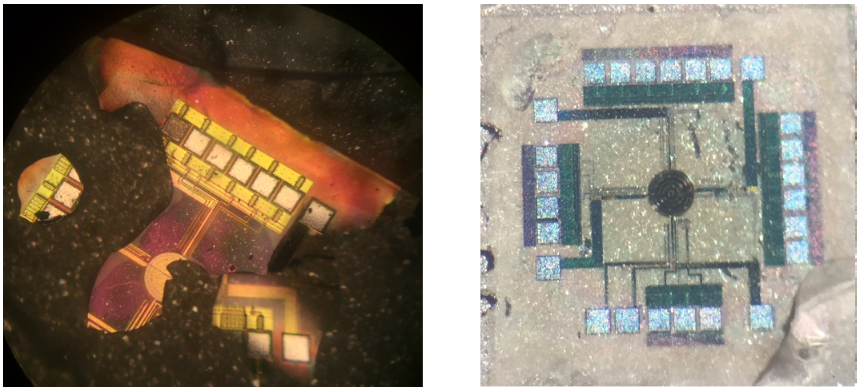

Figure 4.5: Transfer of the thinned die on the power MOSFET

On figure 4.5, we can see the result of the transfer for the thinned die. On the picture on the left, we can see that the die is totally broken and this happened because there was not enough glue on the power transistor. On the right picture of figure 4.5, it can be seen that the thin die is well transferred.

4.3 Monolithic integration

The monolithic integration allows creation of flexible skin technologies by two possible methods. The first one consists to directly fabricate the device on the flexible substrate. The second one is divided into two parts. The first part consists in creating the CMOS circuit or the MEMS device on a silicon wafer and then create the flexible substrate. According to [40], the second method is preferred because the process for flexible substrate is not limited in temperature. Indeed, the first method require only low temperature process. As a consequence, devices involving high temperature during the process can not be directly created on the flexible substrate [40].

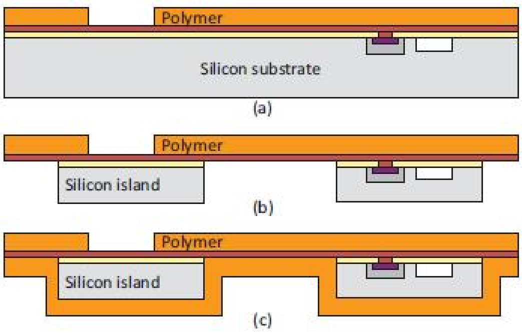

Figure 4.6: Simplified steps of the process to create flexible skin technologies [40]

On figure 4.6, we can see the steps for the fabrication of flexible substrate according to [40]. The first step consists in the deposition of a polymer layer on the top side of the wafer. Then the next one resides in the etching of the silicon substrate to create an array of silicon islands which are bound by

flexible cables, made with polymers. In the last step, another layer of polymer is coated on the silicon substrate to encapsulate the silicon islands.
Polymer cables could be replaced by silicon because hermetic sealing is possible for conductors fabricated on them [40]. However, silicon cable are not so strong than polymer in the special case of flexible substrate.

Chapter 5

Results and discussion

In this chapter, measurements of dies studied in chapter 2 will be done. In a first time, the reference curves will be obtained, then static and pulsed measurements will be realized.

5.1 Noise floor

A first important parameter to take into account is the noise floor. Indeed, the noise floor being the level of noise introduced by the system, if the result signal is below the noise floor, it is impossible to distinguish the useful signal from the noise. It was measured with B1500, in this case, the noise current is measured when there is no contact between the probes and the die. With the test fixture, the noise is measured by putting an empty package instead of the one containing the die. This means that all the cables are present. Both measurements gave a level of noise in the order of tens of fA.

5.2 Reference curves

In order to correctly interpret the obtained results, we need to have reference curves of the voltage drop in function of the temperature for a constant current. In order to know the temperature everywhere, we used a heating chuck and we put the dies on it.The temperature varies from 25 to 125 °C by steps of 25 °C. In order to obtain the best curves as possible, the dies are put on a sheet of Gel-Pak to avoid displacement of the die when it is measured by the prober and this sheet of gel-pak was glued on a thin PCB to have the same temperature on the dies than the one of the chuck.

5.2.1 Forward voltage drop in function of temperature at constant current

When measuring the temperature on a diode, the method of constant current is preferred because of the almost linear relationship between the forward voltage drop and the temperature. This equation describing this relationship is:

$$V = V_g + \frac{kT}{q}(lnI - lnC - \eta lnT)$$

Existing devices

We first obtain the reference curves for the existing temperature sensors. We choose two different design which can be seen on the following on figure 5.1.

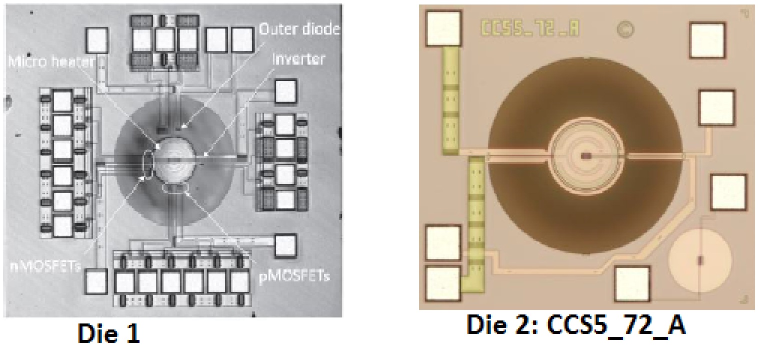

Figure 5.1: Existing dies for temperature sensor. Both dies are made in technology Xfab SOIHITS, the first one, on the left, is designed by UCL and the second one, on the right, is CCS5-72-A [41].

As it is explained in section 1.2.2 of chapter 1, the *Die 1* on the left side is composed of a central diode, which is a membrane diode, located just below a tungsten micro-heater, an external thermodiode, a CMOS inverter and two nMOS and two pMOS transistors. By looking the top-view and taking into account the pads, the size of this die is 2 mm × 2 mm [18]. The *Die 2* is only composed of a membrane diode located just below a micro-heater and a substrate diode. By looking the top-view of the die and taking into account the pads, the size of the die is 1 mm × 0.9 mm [41]. We can now compare the reference curves obtained for these dies.

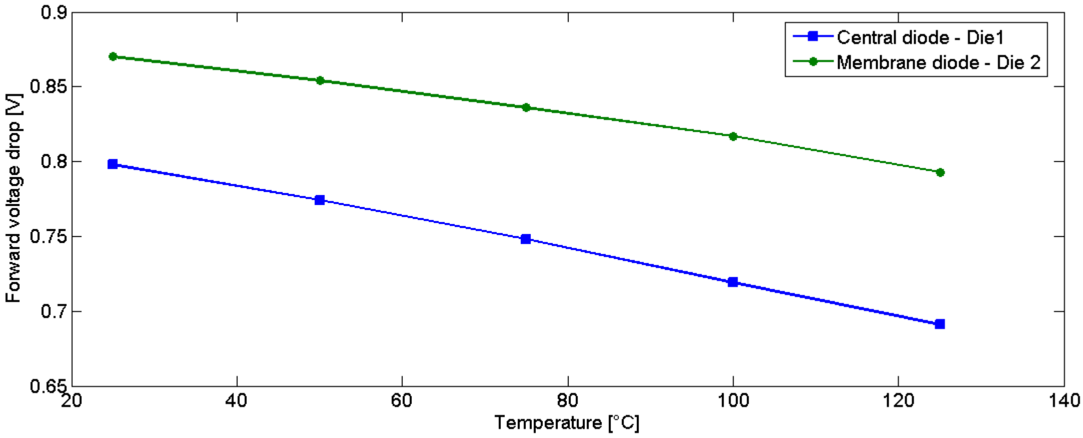

Figure 5.2: Forward voltage drop as a function of temperature, for a constant current of 65 μA.

On figure 5.2, we can see the reference curves as a function of the temperature. We can observe that the obtained reference curves are consistent with the equation because the straight line has a constant slope. Indeed at 150°C, we will be always in the linear relationship between voltage and temperature. With these curves, we are able to compute the diode temperature coefficient (d). This coefficient can be found with the following equation:

$$V_d = V_0 - d(T - T_0) \Rightarrow d = \frac{V_0 - V_d}{T - T_0} \tag{5.1}$$

Where V_0 is the voltage across the diode at 25°C, T_0 is the room temperature, 25°C, and we keep a constant current of 65 μA. We choose a temperature of 100°C to compute the coefficient.
For *Die 1*, at 25°C, the voltage is 798 mV and at 100°C, the voltage is 719 mV. For *Die 2*, at 25°C, the voltage is 870 mV and at 100°C the voltage is 817 mV. Therefore, by using equation (5.1), we find: $d_{Die1} = 1.1\ mV/K$ and $d_{Die2} = 0.71\ mV/K$.

By looking on figure 5.2, it can be seen that for a same temperature, the voltage reached by the membrane diode of *die 2* is 8 % higher than the one reached by the membrane diode of *die 1*. But as we would also like to study the time response of the membrane diode when a micro-heater is heated, for the rest of this chapter, all the measurements will be made with *die 1*.

5.2.2 Current through the diode in function of the temperature at constant voltage

For pulsed measurement, the equipment K4200 is used because it allows to do ultra-fast pulsed measurement. But the pulser is in constant voltage mode and not in constant current mode. Therefore, we are not able to bias the diodes with a current and this is why we have new reference curves for a constant voltage mode.
As a recall, for a constant voltage, the relationship between the current and the temperature is exponential and is given by the following formula:

$$lnI = \frac{q(V - V_g)}{kT} \tag{5.2}$$

When the nonlinear terms are neglected.

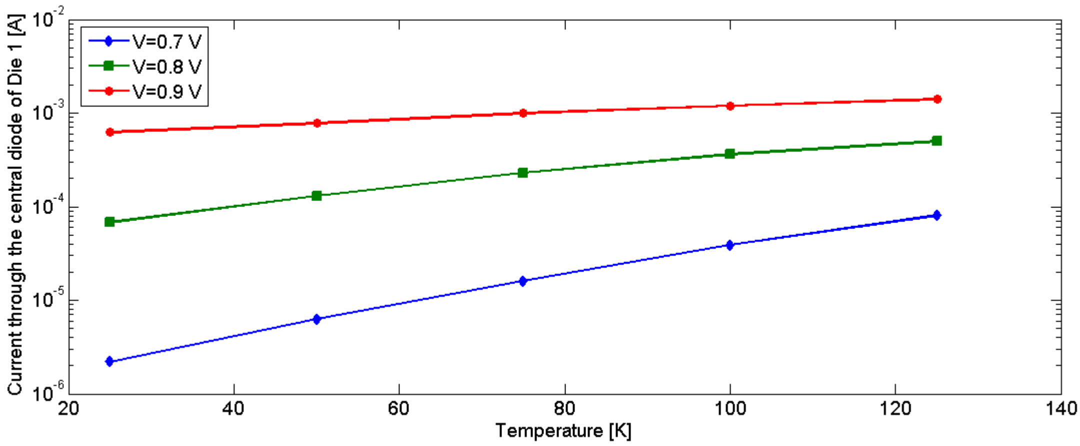

Figure 5.3: Currrent through the centrale diode of *Die 1* as function of temperature for three different voltages

On figure 5.3, we can observe the variation of the current through the central diode of *Die 1* as a function of the temperature for three different voltages, the temperature varies between 25 and 125 °C. We can see that more the value of the constant voltage increase, more the current is high. The sensitivity of these curves can be studied.

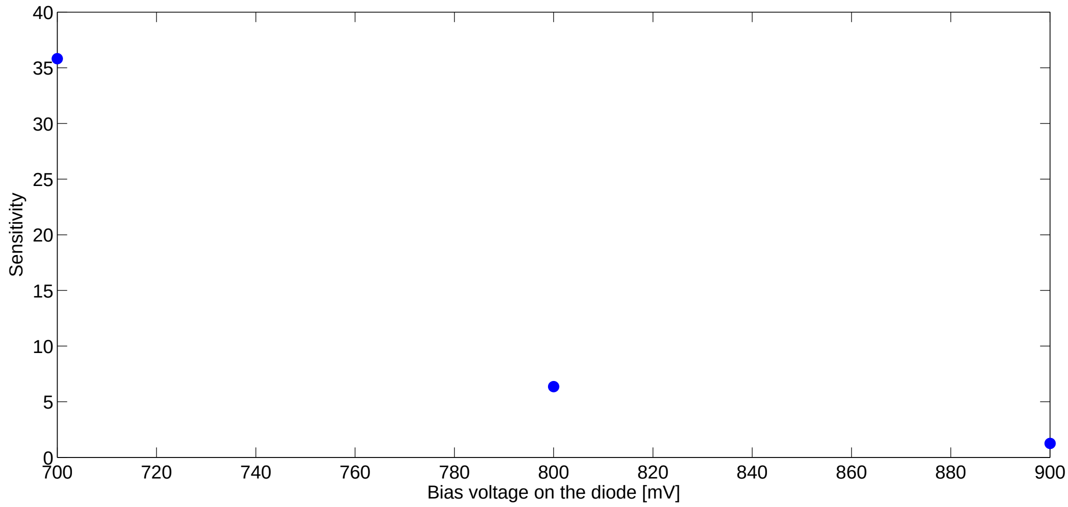

Figure 5.4: Sensitivity of the curves obtained on figure 5.3

On figure 5.4, we can see the sensitivity of the curves obtained on figure 5.3. The sensitivity, S, is computed in the following way:

$$S = \frac{\Delta I}{I}$$

It can be observed that for a constant voltage of 0.7 V, the sensitivity is more than 6 times better than for a constant voltage of 0.9 V. But by looking on figure 5.3, the maximum current obtained for a constant voltage of 0.7 V is approximately 17 times lower than the maximum current obtained for a constant voltage of 0.9 V. As a consequence, it is necessary to do a trade off between the best sensitivity and the maximum current, this why a constant voltage of 0.8 V will be chosen.

5.2.3 Resistance of tungsten micro-heater

The micro-heater is made in tungsten so it is important to know how the resistance changes in function of the temperature.

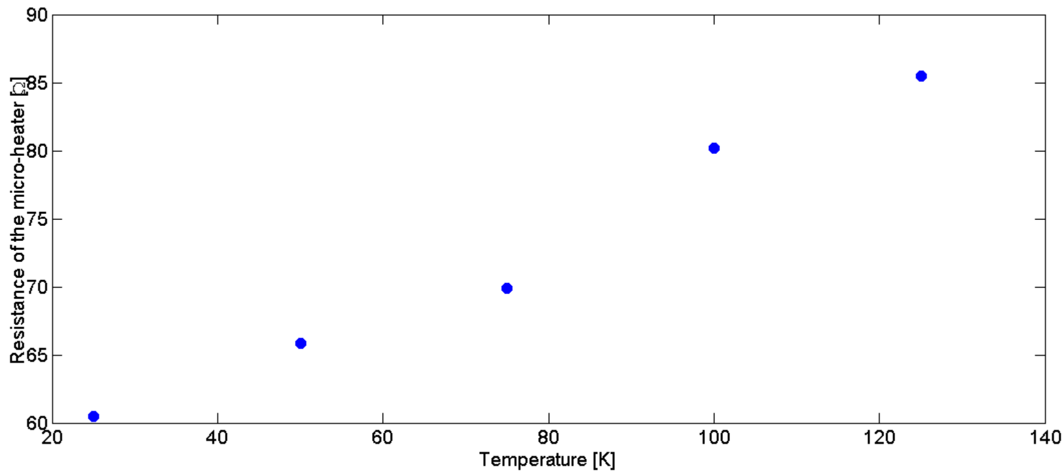

Figure 5.5: Resistance of tungsten micro-heater as a function of temperature

On figure 5.5, we can see the evolution of the resitance of the tungsten micro-heater as a function of the temperature. With this reference curve, we are able to compute the temperature coefficient of resistance, α. This coefficient can be found with the equation for the heater resistance, R, given by the following relationship:

$$R = (R_0 - R_T)[1 + \alpha(T - T_0)] + R_T \Rightarrow \alpha = \left(\frac{R - R_T}{R_0 - R_T} - 1\right) \times \frac{1}{T - T_0} \qquad (5.3)$$

Where R_T is the track resistance and is equal to 13 Ω at 25°C. We can see that the resistance at 25°C is 60.4541 Ω and at 100°C, the value if the resistance is 80.1837 Ω. Therefore, by using equation (5.3), we find that the α coefficient is:

$$\alpha = 5.54\ mK^{-1}$$

5.2.4 Voltage in the micro-heater as a function of the temperature

Another reference curve which is important to know is the voltage on the micro-heater as a function of the temperature. Indeed, in a first time, by doing the measurements on a temperature sensor which is not thinned, it allows to know which voltage to apply to obtain the desired temperature. This curve can be seen on figure 5.6.

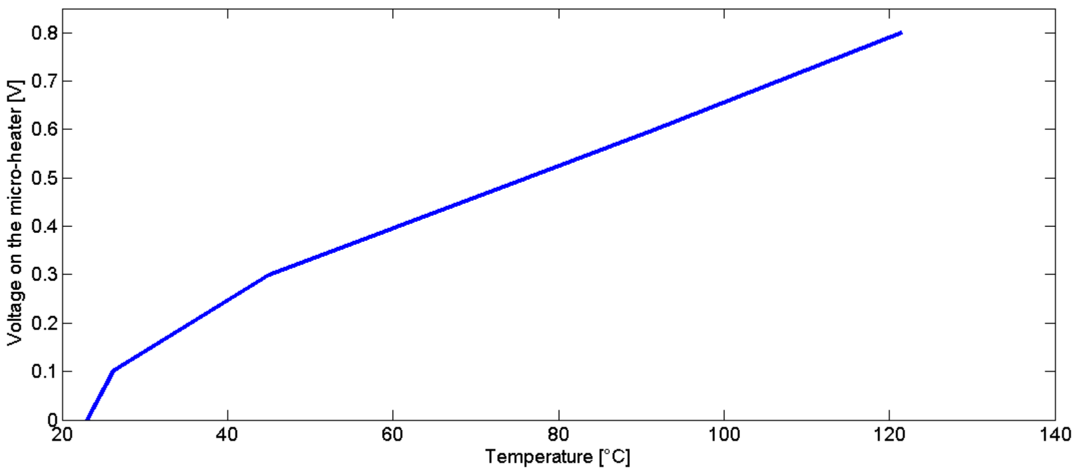

Figure 5.6: Voltage on the tungsten micro-heater as a function of the temperature

On figure 5.6, we can see that until a temperature of approximately 45 °C, the relationship between the voltage in the micro-heater and the temperature is quadratic and then it becomes linear. the total resistance of the system is given by:

$$R_{tot} = R_{contact} + R_{heater}$$

With the contact resistance being external of the membrane and the micro-heater resistance varying with the temperature. As a consequence, the voltage through the micro-heater is given by:

$$V = R_{tot} \times I$$

With I being the current through the micro-heater.
To find this curve, a voltage was applied on the micro-heater, then the diode was biased with a constant voltage of 0.8 V and its current was measured thanks to the equipment *Keithley K4200* and a test fixture. Finally by using the reference curve on figure 5.3, we were able to determine the temperature.

5.3 Static measurements

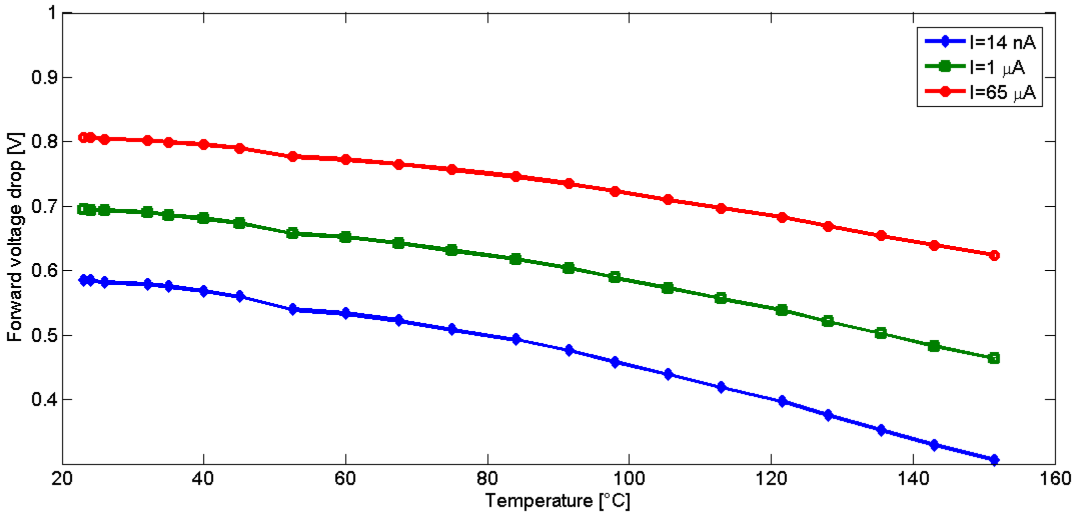

Figure 5.7: Forward voltage drop in the diode when a constant current, 14 nA, 1 μA or 65 μA, is applied and the temperature is applied on the micro-heater

On figure 5.7, we can see the result of static measurements for various constant current in the central diode. A voltage was applied on the micro-heater and converted into a temperature thanks to the curve shown on figure 5.6. It can be seen that the curves obtained with the measurements corresponds to the one shown on figure 1.7 in chapter 1. This figure confirms the good working of the tested device.

5.4 Pulsed measurements

After having obtained the result of static measurements, we are interested in obtaining the result of pulsed measurements. Indeed, in a first time, we would like to pulse the micro-heater to a known temperature and measure the temperature with the diode. In a second time, we would like to pulse the power MOSFET and measure the temperature with the diode.

5.4.1 Measurement of the temperature by heating the micro-heater inside of the temperature sensor

Setup of measurements

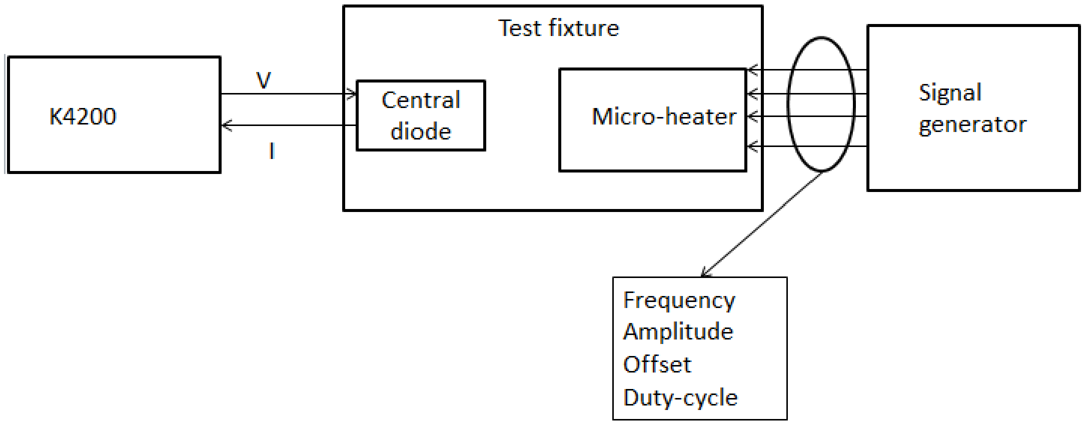

Figure 5.8: Setup for pulsed measurements when the embedded micro-heater of the die is heated

On figure 5.8, we can see the setup used with the equipment *Keithley K4200* and text fixture when doing measurements by heating the embedded micro-heater. The equipment *Keithley K4200* allows to do pulsed measurement controlled by a constant voltage. The diode is directly controlled by the K400, where we impose a constant voltage and we are measuring the variation of the current in function of the temperature of the micro-heater. In order to pulse the micro-heater, we use a pulse generator with a square signal and for which we can modify the value of the amplitude, frequency, offset and duty-cycle.The chip is inside a text fixture, which is a kind of bunker, to avoid the influence of external environment.

Result of a pulsed measurement

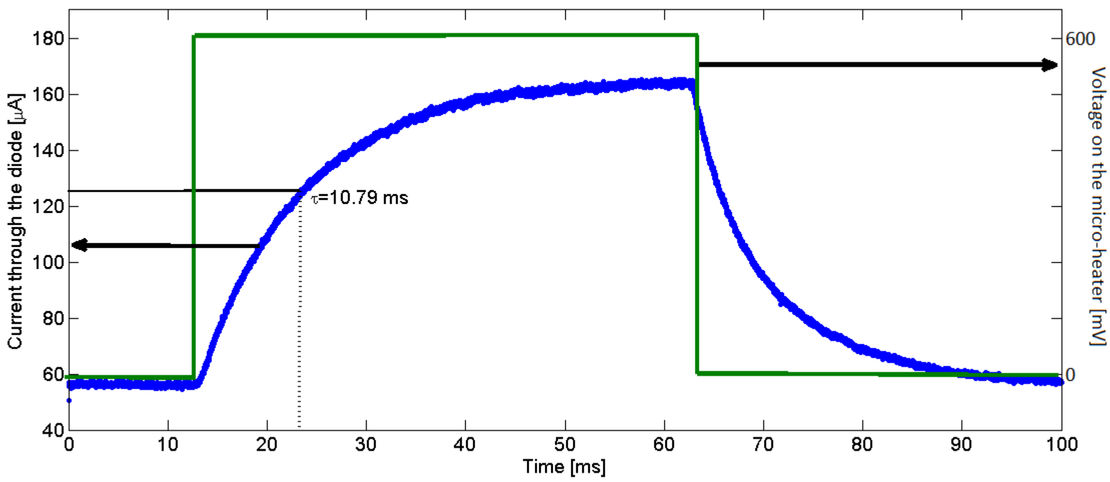

Figure 5.9: Result of a pulsed measurement when a an amplitude of 600 mV, corresponding approximately to 90 °C, is applied on the micro-heater with a frequency of 10 Hz and for a constant voltage on the diode of 800 mV

On figure 5.9, we can see the result of the measured current in the diode when a pulsed voltage is applied on the micro-heater. We can see that at approximately 12.58 ms, the high voltage is applied on the micro-heater and that the current in the diode follows the equation (5.2). The maximum value of the current is 164 μA and the minimum value is 56 μA. Therefore, the time constant, taken at 63 % of the final value, is given for the time when the current is equal to 124 μA and its value is 10.79 ms. For the best case of simulations obtained in section 2.4.2, the value of the time constant was 170 ms, which is 17 times greater than the one obtained with the measures. The only way to explain this difference is that thermal model of the package is not known. Indeed, when the package was not simulated, the wanted temperature was not reached but the time constant was 3.4 ms and normally, the time constant should not change with the step of temperature.
It also important to notice that the temperature applied to the micro-heater corresponds to a value of 90 °C, when looking on figure 5.6, but the one detected by the diode corresponds approximately to 58 °C, when looking on the reference curve of figure 5.3. This means that there is a difference of 30 °C between the real temperature applied on the micro-heater and the one detected by the diode.

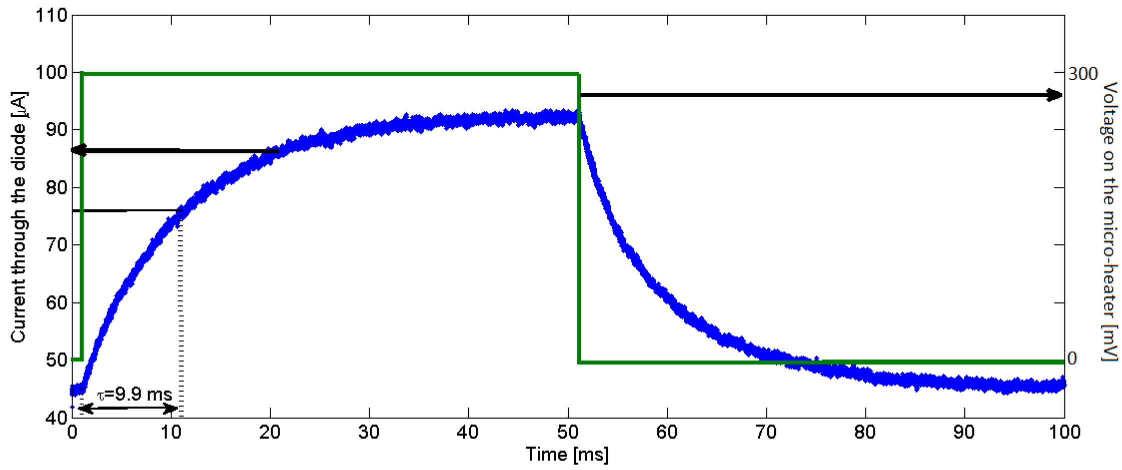

Figure 5.10: Result of a pulsed measurement when an amplitude of 300 mV, corresponding to 45 °C, is applied on the micro-heater with a frequency of 10 Hz and for a constant voltage on the diode of 800 mV

On figure 5.10, we can see the result of a pulsed measurement when a square signal with an amplitude of 300 mV is applied on the micro-heater. It can be seen that the obtained time constant is 9.9 ms. When a square signal with an amplitude of 600 mV is applied on the micro-heater, we obtain a time response of 10.79 ms. As a consequence, the error between the two time constants is less than 10 %, therefore, we can say that the step of temperature does not have an influence on the time response. The temperature detected by the diode is about 40 °C instead of 45 °C.

Influence of the bias voltage on the diode

The first parameter which can influence the obtained result is the bias voltage applied on the diode.

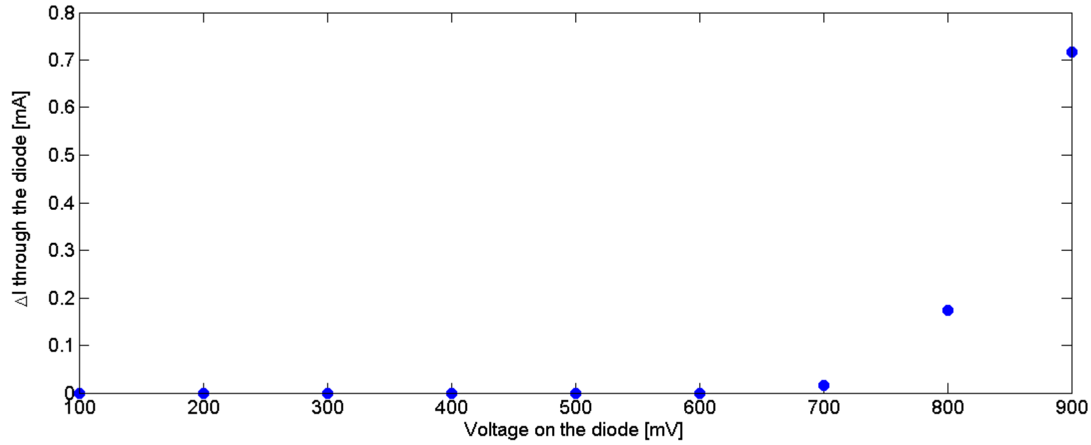

Figure 5.11: ΔI through the diode as a function of the bias voltage on the diode for a temperature from 25 °C to a temperature of 91.58 °C

On figure 5.11, we can see the influence of the bias of the diode on the central diode of *Die 1*. For a voltage lower than 650 mV, the current is zero regardless the applied temperature on the diode. As it was predicted by figure 5.3, the difference in the current of the diode is much important for higher voltage. We can analyse the sensitivity for these bias voltages.

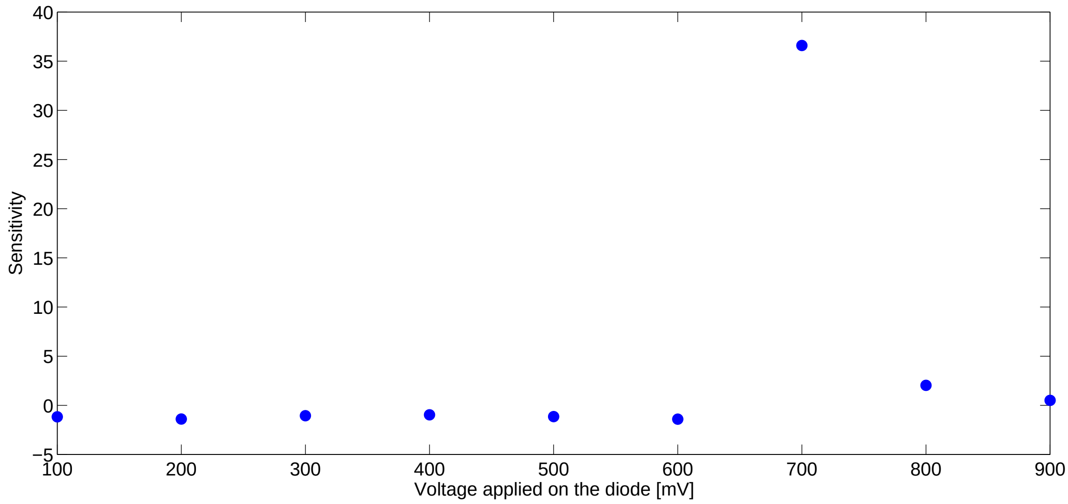

Figure 5.12: Sensitivity of the diode in function of the bias voltage

On figure 5.12, we can see the sensitivity of the diode as a function of the bias voltage. As it was predicted by figure 5.4, the sensitivity decreases with the rise of the bias voltage, when the ΔI, seen on figure 5.11, is higher than 0. But in the same time, the value of the current increases when the bias voltage rises. Therefore, it can not be confound with the noise.

Influence of the frequency of the square signal applied on the micro-heater

Another parameter which influences the value the current is the frequency of the square signal applied on the micro-heater. Indeed, in the ideal case, for each period, the micro-heater has enough time to cool down after being heated.

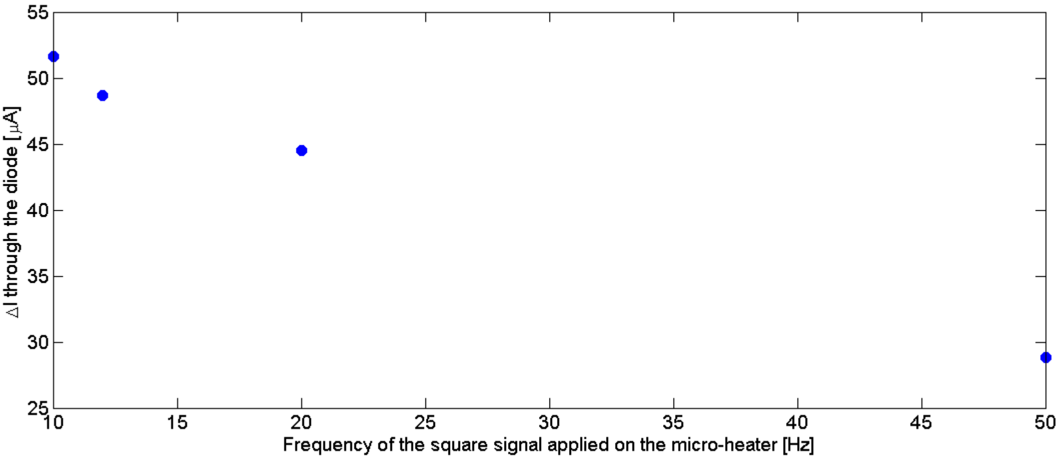

Figure 5.13: ΔI through the diode as a function of the frequency of the square signal applied on the micro-heater. The amplitude of the voltage on the micro-heater is 300 mV, corresponding approximately to 45 °C, and the voltage on the diode is 800 mV.

On figure 5.13, we can see the variation of the current through the diode when the temperature on the micro-heater goes from 25 °C to 45 °C in function of the frequency applied on the micro-heater. We can observe that when the frequency increases, the variation of the current decreases, this can be explained by the fact the micro-heater does not have enough time to be completely heated up to the maximum temperature and to completely cool down up to the ambient temperature. The important part is to detect the rise of the temperature. But if the frequency is too high, much greater than 50 Hz, the current through the diode will be almost constant and therefore, we will not be able to detect a rise of temperature.

5.4.2 Measurement of the temperature by heating a power MOSFET

Setup of measurements

This setup is similar to the one presented in 5.4.1, except that in this case we need to pulse the power MOSFET. To do this, we impose a constant voltage on the drain end and we pulse the gate end. As it can be seen in the datasheet of the n-channel power MOSFET used [34], the maximum threshold voltage for the gate is 4 V. Therefore, we will impose a square signal of 5 V amplitude on the gate end. For the drain end, we use a *DC Power Supply* which amplifies the input voltage, comprised between 0 et 5 V, up to 70 V [42]. In order to still have fast measurements, we have to use the equipment *Keithley K4200* and impose a constant voltage of 0.8 V on the diode.

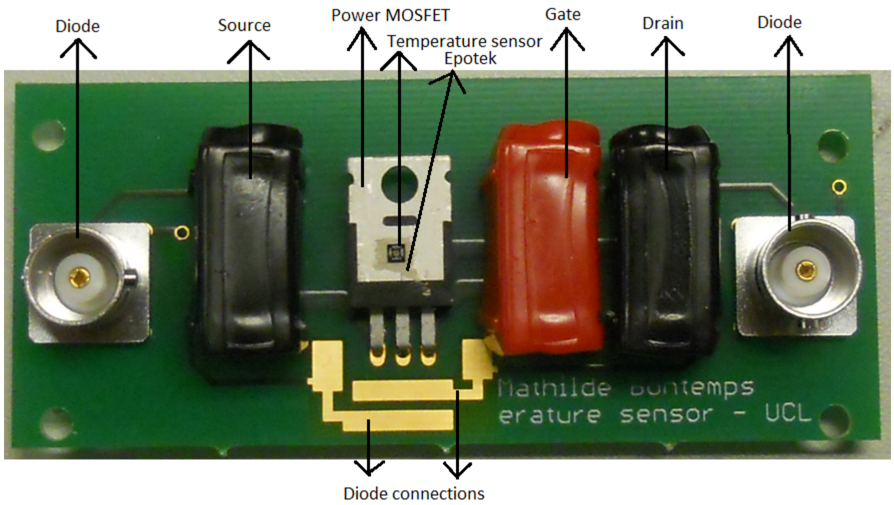

Figure 5.14: Design of a PCB to facilitate the measurements

On figure 5.14, we can see the design made in order to facilitate the measurement of the die transferred on the power MOSFET. We use three bananas sockets to impose the voltage on the three ends of the power MOSFET. The idea is to use the wirebonding between the pads of the diode and copper parts of the PCB and then measure the current through the diode thanks two coaxial cables.
For the thin die, the wirebonding does not work and the pads were broken because the die is too thin, 5 μm. Therefore, the idea was to use probes to directly measure the temperature on the pads. But when the power MOSFET heats up, the die expands and therefore the probes move with the pads and then when the power MOSFET cools down, the die tightens and as a consequence, the probes are not in contact with the pads anymore, so we are not able to measure correctly the temperature with this method. If we want to be sure that the probes stay in contact with the pads, we have to push on the probes but as the thickness is only 5 μm, the probes goes across the pads because the glue *epotek* was not enough dried. Therefore, we are not able to measure the time response of the diode when the power circuit is the heat source and the die is thinned down. A solution could be to use the monolithic integration presented in section 4.3, which means directly build the die on the power MOSFET.
For the non thinned die, we used the first technique with the wirebonding but at one time, the die heated too much, more than 400 °C, and the wirebonding breaks. As a consequence, we use the probes to put them on the pads and measure the current. Before doing any measurement, we have to be sure that there is a contact between the pads and the probes. With this method we obtain the results that can be seen on the following figure.

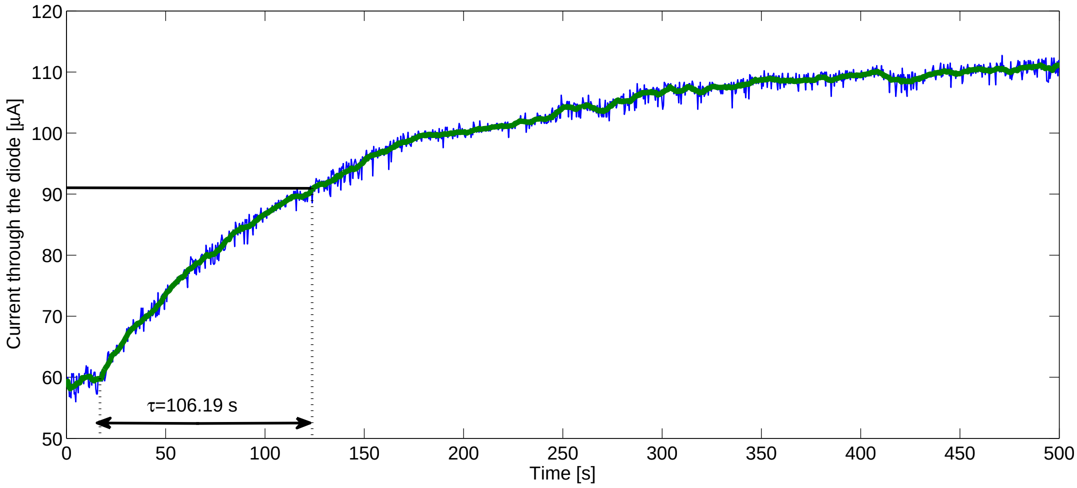

(a) Heating

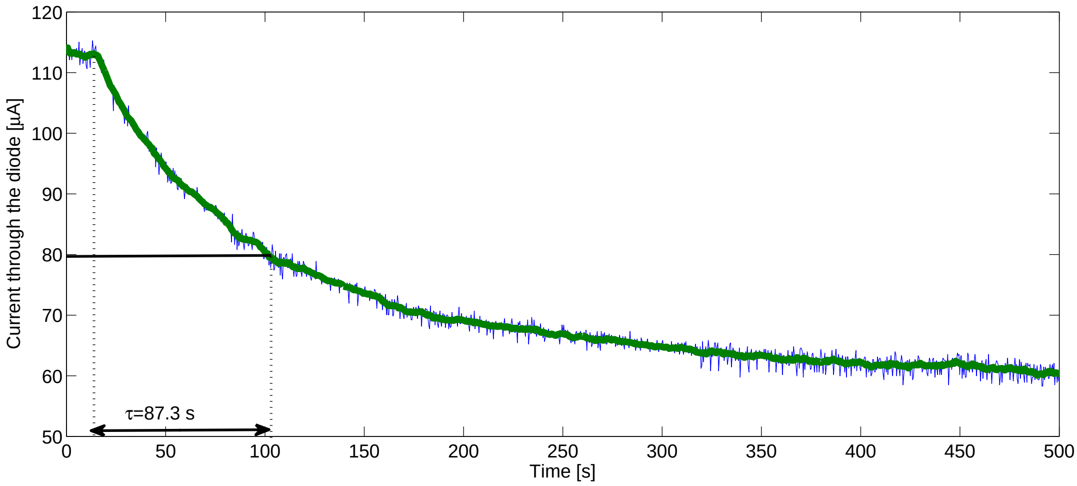

(b) Cooling

Figure 5.15: Heating and cooling of a non-thinned die glued on a power MOSFET

On figure 5.15, we can see the result of the measurements made with the K4200 equipment and using probes for a non-thinned die heated by a power MOSFET. By looking on figure 5.3, we can see that the minimum value of the current which is approximately 60 μA corresponds to the room temperature and the maximum value of the current which is about 110 μA corresponds to a temperature around 40 °C. On this figure, we can see that the time constant for the heating is 106.19 s and the one for the cooling is 87.3 s. To obtain this curve, a current of 2 A and a voltage of 0.4 V were applied between the source and drain and a voltage of 5 V was applied between the source and the gate. Therefore, the power delivered by the power transistor is 0.8 W.

The time constant obtained in section 3.3.5 is about 80 times smaller than the one obtained by the measurements. This can be explained by the fact that the distribution of the heat flux generated by the power MOSFET is not exactly known.

The last point is that the temperature of the power transistor is not exactly known. In a first time, a *Thermo Raytek* which is a thermometer without contact, was used to detect the temperature of the power circuit. But this device is not accurate and we were not able to obtain a consistent value for temperature. For example, the *Thermo Raytek* displays a value of 150 °C but the temperature detected by the diode was above 400 °C, because the package of the transistor melt. As the simulation for the combination of the die with substrate and the power MOSFET does not fit with the measurements, we are not able to predict the time constant when a thin die is used.

Conclusion

In this work, a thermodiode based fast temperature sensor designed at UCL is studied. In aerospace applications, this sensor can be used to detect a temperature rise in a power circuit and prevent overheating. The main goal is to determine the time response of the sensor which must be in the order of ms for the purpose of the application.

The time response of the sensor is measured experimentally using an embedded micro-heater or a power MOSFET as a heat source. In order to understand the impact of the physical parameters playing a role in the sensor response time, finite elements numerical simulations were carried out using Comsol ® and equivalent thermal circuit were studied with LTSpice.

The time response of the diode to a heat flow is studied in three different configurations. In the first one the embedded micro-heater is used as a power source. In the second and the third configurations, the sensor is glued on a power circuit. The difference is that in the third configuration the die is thinned down to remove the substrate in order to obtain a faster time response. The thinning process and die transfer to the power MOSFET is done at UCL.

When heated by the embedded micro-heater, the response of the diode is measured to be about 10 ms. Finite elements simulations give a time response of 170 ms. The package is found to be the determining factor influencing the time response. The lack of information of the physical properties of this package explains the difference between experimental results and numerical simulation.

The response time of the non-thinned die glued on the power circuit is 106 s as experimentally measured. The finite elements simulations and the thermal equivalent circuit where the power MOSFET is modelled as a simple heat source give a response time of respectively 23 s and 26 s. These results are comparable. When the detailed thermal model of the power MOSFET is inserted in the LTSpice equivalent thermal model, the response time drops to about 1 s. This is found to be due to an incorrect repartition of the heat generated by the power MOSFET between the sensor and the external ambient.

The thinned die glued on the power MOSFET is not experimentally measured. The thickness of the die, 5 μm, is too thin to perform wirebonding. Moreover the glue was not sufficiently dry to use probes despite an extra annealing time. The numerical simulations using Comsol ® results in a response time of 420 ms. The equivalent thermal model in LTspice modelling the power MOSFET as a heat source gives a value of 388 ms which deviates by 7% from the finite elements simulations. Modelling with the detailed power MOSFET thermal model results in a time response of 1 s. This value is extremely close from the value obtained for the non-thinned die, suggesting that the time constant is dominated by the power MOSFET rather than by the sensor.

The time constant measured for the non-thinned die is several orders of magnitude higher than expected. Indeed, for the final aerospace application a time constant in the order of a few ms is required. The value of the time constant for the thinned die cannot be extrapolated from the numerical simulations due to large difference between the experimental data and the simulations results. Nevertheless the main factors influencing the response time are identified. Determining their actual value for the studied device would allow to better fit the experimental results.

The next step of this work should be to measure the time response of the thinned die. In space, radiations can have a detrimental effect on the device and their impact should be studied.

Bibliography

[1] C-H. Park S-S. Lee B.T. Lim H.K. Bae W-G. Lee G-D. Kim, H-S. Lee. Silicon photonic temperature sensor employing a ring resonator manufactured using a standard CMOS process. *Optics express*, 2010.

[2] Y. Wang X. Dai D. Zhang, J. Wang. A fast response temperature sensor based on fiber bragg grating. *IOP publishing, measurement science and technology*, 2014.

[3] National Instruments. Fundamentals of Fiber Bragg Grating (FBG) optical sensing, Last consultation on 25/05/2017. `http://www.ni.com/white-paper/11821/en`.

[4] The leader in industrial I/O Acromag. Criteria for temperature sensor selection of t/c and rtd sensor types: the basics of temperature measurement using RTDs, part 2 of 3, 2011.

[5] Wikimedia commons. Thin film PRT, Last consultation on 28/05/2017. `https://commons.wikimedia.org/wiki/File:Thin_Film_PRT.png`.

[6] Electrical and Electronic Engineering BD. Contact - electrical thermometers, Last consultation on 28/05/2017. `http://69eeenews.blogspot.be/2013/11/contact-electrical-thermometers.html`.

[7] Innovative Sensor Technology. Platinum temperature sensors, Last consultation on 28/05/2017. `http://akizukidenshi.com/download/ds/ist/BTP_E1.0.pdf`.

[8] S. Amor; N. André; P. Gérard; F. Udrea; F. Tounsi; B. Mezghani; L. Francis; D. Flandre. Reliable characteristics and stabilization of on-membrane SOI MOSFET-based components heated up to 335°c. *Semiconductor Science and Technology*, 2016.

[9] S. Akhtar A. De Luca F. Udrea M. Mansoor, I. Haneef. Silicon diode temperature sensors-a review of applications. *Sensors ans actuators A: Physical*, 2015.

[10] J.W. Gardner F. Udrea, S. Santra. CMOS temperature sensors-concepts, state-of-the-art and prospects. *IEEE*, 2008.

[11] P.K. Guha S.Z. Ali I. Haneef F. Udrea, S. Santra. Ultra-high temperature (>300°c) suspended thermodiode in SOI CMOS technology. *Microelectronics journal*, 2010.

[12] S.Z. Ali I. Haneef F. Udrea J.W. Gardner S. Santra, P.K. Guha. SOI diode temperature sensor operated at ulra high temperatures - a critical analysis. *IEEE sensors conference*, 2008.

[13] M.S. Haque S.Z. Ali F. Udrea S. Santra, P.K. Guha. Si diode temperature sensor beyond 300°c. *IEEE*, 2007.

[14] D. Janvier D. Flandre. Compléments d'électricité. ELEC1755, 2014/2015.

[15] C.C.C. Lee F. Udrea W.I. Milne T. Iwaki J. Covington J.W. Gardner S. Maeng J. Park S.Z. Ali, P.K. Guha. High temperature SOI CMOS tungsten micro-heaters. *IEEE sensors conference*, 2006.

[16] U. Smith M. Rydberg. Long-term stability and electrical properties of compensation doped poly-Si IC resistors. *IEEE transactions on electron devices*, 2000.

[17] W.I. Milne J.W. Gardner S.Z. Ali, F. Udrea. Tungsten-based SOI microhotplates for smart gas sensors. *Journal of microelectromechanical systems*, 2008.

[18] Cambridge CMOS sensors Ltd. CCS4-17: Datasheet. *Cambridge*.

[19] K. Toshima M. Kimura. Thermistor-like pn junction temperature-sensor with variable sensitivity and its combination with a micro-air-bridge heater. *Sensors and actuators A*, 2003.

[20] E. Gatard. Analyse des phénomènes physiques dans les diodes p-i-n: Contribution à la modélisation électrothermique pour les applications de puissance RF et hyperfréquences, 2006.

[21] P. Bonnet. Capteurs - chaines de mesures. Université Lille1, sciences et technologies, Last consultation on 26/01/2017.

[22] Prof. Z.S. Spakovszky. 16.4 thermal resistance circuits. Thermodynamics and propulsion, Massachusetts Institute of Technology, 2007.

[23] P. Nance M. März. Thermal modeling of power-electronic systems. *Infineon Technologies AG, Munich*.

[24] M. Correvon. Chapitre 9. Modélisation thermique des composants de puissance. Institut d'automatisation industrielle, Haute Ecole Spécialisée de Suisse Occidentale.

[25] Haruna Tada. Chapter 3: Steady-state conduction. Mechanical Engineering Department *Tufts University*, Madford, 2002.

[26] The engineering toolbox. Air properties, Last consultation on 27/05/2017. `http://www.engineeringtoolbox.com/air-properties-d_156.html`.

[27] Comsol Multiphysics ®. Modeling natural and forced convection in COMSOL multiphysics ®, Last consultation on 27/05/2017. `https://www.comsol.com/blogs/modeling-natural-and-forced-convection-in-comsol-multiphysics/`.

[28] M. Ashby. *Materials selection in mechanical design, 5th edition*. Butterworth-Heinemann, 2016.

[29] COMSOL Multiphysics ®. *Reference manual*. COMSOL, May 2013.

[30] Vrej Barkhordarian. Power MOSFET basics, Last consultation on 16/04/2017. `http://www.infineon.com/dgdl/mosfet.pdf?fileId=5546d462533600a4015357444e913f4f`.

[31] M. Bekemans. Power electronics - components and technologies. LELEC 2660, 2015-2016.

[32] R.W. Erickson; D. Maksimovic. *Fundamentals of power electronics*. Springer science, 2001.

[33] Electrocnics cooling. How to select a heat sink, Last consultation on 07/06/2017. `http://www.electronics-cooling.com/1995/06/how-to-select-a-heat-sink/`.

[34] Infineon. IRF540NPbF, 2003. `http://www.farnell.com/datasheets/669916.pdf?_ga=2.61759657.428260260.1494689135-127339510.1494689109`.

[35] Alpha and Omega Semiconductor. Power MOSFET basics, Last consultation on 24/05/2017. `http://www.aosmd.com/res/application_notes/mosfets/Power_MOSFET_Basics.pdf`.

[36] Sajjad Haidar. Learn LTSpice, a tutorial, Last consultation on 23/05/2017. `http://learn-ltspice.weebly.com/thermal.html`.

[37] Infineon. Irf540npbf, Last consultation on 07/06/2017. http://www.infineon.com/cms/en/search.html#!term=IRF540NPBF&view=all.

[38] E. Ergun A. d'Auvernas. Characterization of thinned dies under bending for strain sensors and flexible electronics applications. ELEC2560, 2016/2017.

[39] A. Lecavalier des Etangs-Levallois. Report de technologie SOI-CMOS sur substrat flexible: une approche convergente vers les hautes fréquences et la stabilité des performances sous déformation mécanique, 2013.

[40] Y. Xu. Post-CMOS and post-MEMS compatible flexible skin technologies: a review. *IEEE sensors journal*, 2013.

[41] Cambridge CMOS sensors Ltd. CCS5-72-A: Datasheet. *Cambridge*.

[42] DELTA Elektronika BV. Sm 800 - series 800 w DC POWER SUPPLY, 2013. http://www.deltapowersupplies.com.

Rue Archimède, 1 bte L6.11.01, 1348 Louvain-la-Neuve **www.uclouvain.be/epl**